

ผลของการเติมผลึกเหลวโมเลกุลต่ำต่อการเป็นเนื้อเดียวกัน  
ของพอลิเมอร์ผสมซินดีโอแทกติกพอลิสไตรีน



นาย พิเชษฐ์ พงษ์ทรัพย์

สถาบันวิทยบริการ

จุฬาลงกรณ์มหาวิทยาลัย

วิทยานิพนธ์นี้เป็นส่วนหนึ่งของการศึกษาตามหลักสูตรปริญญาวิศวกรรมศาสตรมหาบัณฑิต

สาขาวิชาวิศวกรรมเคมี ภาควิชาวิศวกรรมเคมี

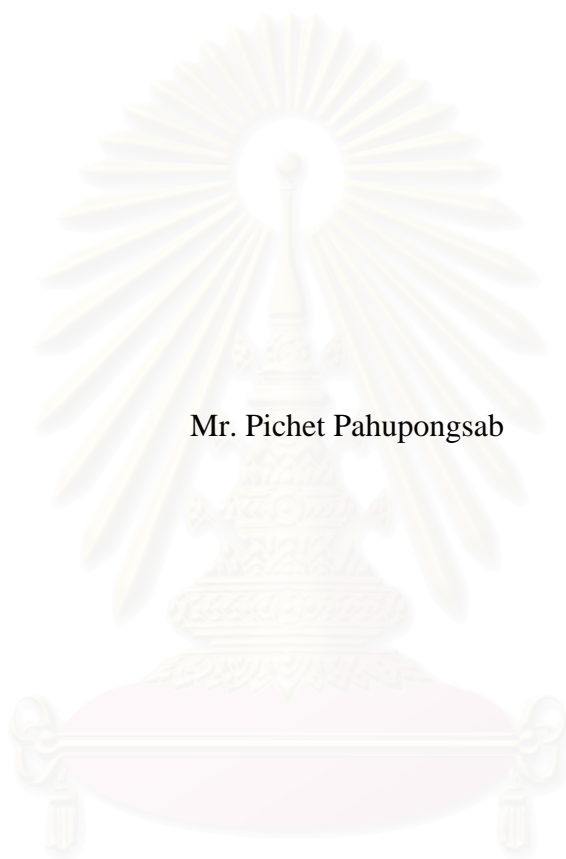
คณะวิศวกรรมศาสตร์ จุฬาลงกรณ์มหาวิทยาลัย

ปีการศึกษา 2547

ISBN 974-53-1382-3

ลิขสิทธิ์ของจุฬาลงกรณ์มหาวิทยาลัย

EFFECTS OF LOW MOLAR MASS LIQUID CRYSTAL ADDITION ON THE MISCIBILITY  
OF SYNDIOTACTIC POLYSTYRENE BLENDS



Mr. Pichet Pahupongsab

สถาบันวิทยบริการ  
จุฬาลงกรณ์มหาวิทยาลัย

A Thesis Submitted in Partial Fulfillment of the Requirements  
for the Degree of Master of Engineering in Chemical Engineering

Department of Chemical Engineering

Faculty of Engineering

Chulalongkorn University

Academic year 2004

ISBN 974-53-1382-3

Thesis Title                    EFFECTS OF LOW MOLAR MASS LIQUID CRYSTAL  
    ADDITION ON THE MISCIBILITY OF SYNDIOTACTIC  
    POLYSTYRENE BLENDS

By                                    Mr. Pichet Pahupongsab

Field of Study                    Chemical Engineering

Thesis Advisor                 Assistant Professor ML. Supakanok Thongyai, Ph.D.

---

Accepted by the Faculty of Engineering, Chulalongkorn University in  
Partial Fulfillment of the Requirements for the Master's Degree

.....Dean of the Faculty of Engineering  
(Professor Direk Lavansiri, Ph.D.)

THESIS COMMITTEE

..... Chairman  
(Associate Professor Suttichai Assabumrungrat, Ph.D.)

..... Thesis Advisor  
(Assistant Professor ML. Supakanok Thongyai, Ph.D.)

..... Member  
(Assistant Professor Seeroong Prichanont, Ph.D.)

..... Member  
(Joongjai Panpranot, Ph.D.)

พิเชษฐ พหุพงศ์ทรัพย์: ผลของการเติมผลึกเหลวมวลโมเลกุลต่ำต่อการเป็นเนื้อเดียวกันของพอลิเมอร์ผสมซินติโอแทกติกพอลิสไตรีน (EFFECTS OF LOW MOLAR MASS LIQUID CRYSTAL ADDITION ON THE MISCIBILITY OF SYNDIOTACTIC POLYSTYRENE BLENDS) อาจารย์ที่ปรึกษา: ผศ. ดร. มล. ศุภกนก ทองใหญ่, 134 หน้า, ISBN 974-53-1382-3

งานวิจัยนี้ มุ่งเน้นที่จะศึกษาเกี่ยวกับการผสมเข้ากันได้ของซินติโอแทกติกพอลิสไตรีน (SPS) กับพอลิเมอร์ตัวอื่น เช่น พอลิแอลฟาเมทิลสไตรีน (PaMS), พอลิเอทิลเมทาคริเลต (PEMA), พอลิบิวทิลเมทาคริเลต (PBMA), พอลิไซโคลเฮกซิลอะคริเลต (PCHA), พอลิไอโซพรีน (PIP) และ พอลิไวนิลเมทิลอีเธอร์ (PVME) โดยซินติโอแทกติกพอลิสไตรีนสังเคราะห์ด้วยตัวเร่งปฏิกิริยาเมทัลโลซีนและเมทิลอะลูมิเนียมออกเซนที่ปรับปรุงแล้วเป็นตัวเร่งปฏิกิริยาร่วม (MMAO) จากผลการทดลองพบว่า ซินติโอแทกติกพอลิสไตรีนสามารถผสมเข้ากันได้กับพอลิแอลฟาเมทิลสไตรีน, พอลิเอทิลเมทาคริเลต, พอลิบิวทิลเมทาคริเลต, พอลิไซโคลเฮกซิลอะคริเลต และ พอลิไอโซพรีน แต่ไม่สามารถผสมเข้ากันได้กับพอลิไวนิลเมทิลอีเธอร์ นอกจากนี้ยังศึกษาผลของการเติมไซโคลเฮกซิลไบฟีนิลไซโคลเฮกเซน (CBC-33) และ กลีเซอรอลมอนอสเตียเรต (GMS) ต่อสมบัติทางความร้อน และ ความเป็นผลึกของพอลิเมอร์ผสม จากผลการทดลองแสดงให้เห็นว่า ไซโคลเฮกซิลไบฟีนิลไซโคลเฮกเซน และ กลีเซอรอลมอนอสเตียเรต ทำให้อุณหภูมิหลอมเหลว ( $T_m$ ) ลดลงเล็กน้อย เนื่องจากสารทั้งสองไปลดความหนืดหลอมเหลวของพอลิเมอร์ผสม ทำให้ผลึกสามารถหลอมเหลวได้ง่ายขึ้น และก่อตัวเป็นผลึกได้ช้าลง ซึ่งสัมพันธ์กับอุณหภูมิการเกิดผลึก ( $T_c$ ) ที่มีแนวโน้มลดลงเช่นเดียวกัน

สถาบันวิทยบริการ  
จุฬาลงกรณ์มหาวิทยาลัย

ภาควิชา.....วิศวกรรมเคมี

ลายมือชื่อนิสิต.....

สาขาวิชา.....วิศวกรรมเคมี

ลายมือชื่ออาจารย์ที่ปรึกษา.....

ปีการศึกษา.....2547



# # 4670412021: MAJOR CHEMICAL ENGINEERING

KEY WORD: SYNDIOTACTIC POLYSTYRENE / POLYMER BLEND / LOW  
MOLAR MASS LIQUID CRYSTAL / LUBRICANT

PICHET PAHUPONGSAB: EFFECTS OF LOW MOLAR MASS LIQUID  
CRYSTAL ADDITION ON THE MISCIBILITY OF SYNDIOTACTIC  
POLYSTYRENE BLENDS. THESIS ADVISOR: ASST. PROF. ML.  
SUPAKANOK THONGYAI, Ph.D., 134 pp. ISBN 974-53-1382-3

This research is concerned with studying the miscibility of syndiotactic polystyrene (SPS) blend with several polymers such as poly( $\alpha$ -methyl styrene) (PaMS), poly(ethyl methacrylate) (PEMA), poly(*n*-butyl methacrylate) (PBMA), poly(cyclohexyl acrylate) (PCHA), poly(*cis*-isoprene) (PIP) and poly(vinyl methyl ether) (PVME). SPS synthesized by using metallocene catalyst and modified-methylaluminoxane (MMAO) as cocatalyst. From the experimental results, it was found that the SPS can be miscible with PaMS, PEMA, PBMA, PCHA and PIP but it can not be miscible with PVME. Furthermore, the study concerned with the effect of addition cyclohexylbiphenylcyclohexane (CBC-33) and glycerol monostearate (GMS) on thermal properties and the crystallinity of blended polymer. The results showed that CBC-33 and GMS can also slightly decrease melting temperature ( $T_m$ ) of the blends because they reduce melt viscosity of the blends, therefore the crystal of the blends will melt easier and form to crystalline slowly which correspond with depression of  $T_c$ .

สถาบันวิทยบริการ  
จุฬาลงกรณ์มหาวิทยาลัย

Department Chemical Engineering

Field of study Chemical Engineering

Academic Year 2004

Student's signature .....

Advisor's signature .....

## ACKNOWLEDGEMENTS

I would like to express my deeply gratitude to my advisor, Assistant Professor Dr. ML. Supakanok Thongyai, Ph.D. to his continuous guidance, enormous number of invaluable discussions, helpful suggestions, warm encouragement and patience to correct my writing. I am grateful to Associate Professor Suttichai Assabumrungrat, Ph.D., Assistant Professor Seeroong Prichanont, Ph.D. and Joongjai Panpranot, Ph.D. for serving as chairman and thesis committees, respectively, whose comments were constructively and especially helpful.

I cannot miss to thanks Dr. Nigel Clarke for his kind advice in this project and valuable guidance of this study.

Sincere thanks are made to Mekttec Manufacturing Corporation for using Differential Scanning Calorimetry (DSC), Polymer Engineering Research Laboratory (PEL), Chulalongkorn University for using digital hot-plate stirrer and Thai Petrochemical Industry Public Co., Ltd. (TPI) for using Gel Permeation Chromatography in this study.

Sincere thanks to all my friends and all members of the Center of Excellent on Catalysis & Catalytic Reaction Engineering (Petrochemical Engineering Research Laboratory), Department of Chemical Engineering, Chulalongkorn University for their assistance and friendly encouragement.

Finally, I would like to dedicate this thesis to my parents and my families, who generously supported and encouraged me through the year spent on this study.

# CONTENTS

	Page
ABSTRACT (IN THAI).....	iv
ABSTRACT (IN ENGLISH).....	v
ACKNOWLEDGEMENTS.....	vi
CONTENTS.....	vii
LIST OF FIGURES.....	xi
LIST OF TABLES.....	xvi
CHAPTERS	
I INTRODUCTION.....	1
1.1 The Objective of This Thesis.....	3
1.2 The Scope of This Thesis.....	3
II LITERATURE REVIEWS.....	5
2.1 Catalysts for Syndiotactic Polystyrene.....	5
2.1.1 Transition metal compounds.....	5
2.1.2 Half-titanocene compounds.....	7
2.1.3 Ansa-titanocene compounds.....	8
2.1.4 Zirconocene and ansa-zirconocene catalysts.....	9
2.1.5 Other Metal complexes.....	9
2.2 Cocatalyst.....	9
2.3 Polymer Blend.....	10
III THEORY.....	16
3.1 Catalytic Systems.....	16
3.1.1 Catalyst compounds.....	16
3.1.2 Aluminoxane.....	17
3.2 Syndiotactic Polystyrene.....	18
3.3 Polymer Tacticity of Polystyrene.....	20
3.4 Polymer Morphology.....	21
3.4.1 The Amorphous State.....	21
3.4.2 Glass Transition Temperature.....	22
3.4.3 The Crystalline Polymer.....	23

	Page
3.5 Melting Phenomena.....	24
3.6 Thermal Properties.....	25
3.7 Structure of Crystalline Polymers.....	26
3.8 Crystal Structure in Polymers.....	27
3.8.1 Crystallization from Dilute Solution.....	27
3.8.1.1 Polymer Single Crystals.....	27
3.8.1.2 The Folded Chain Model.....	30
3.8.1.3 The Switchboard Model.....	30
3.8.2 Crystallization from the Melt.....	31
3.8.2.1 Spherulitic Morphology.....	31
3.8.2.2 Mechanism of Spherulite Formation.....	33
3.8.2.3 Spherulites in Polymer Blends.....	33
3.8.2.4 Effect of Crystallinity on Glass Transition Temperature.....	33
3.9 Liquid Crystal.....	34
3.9.1 The History of Liquid Crystal.....	34
3.9.2 Introduction to Liquid Crystal.....	35
3.9.3 Main-Chain Polymer Liquid Crystals.....	36
3.9.4 Side Chain Polymer Liquid Crystals.....	38
3.9.5 Type of Liquid Crystal.....	40
3.9.6 Liquid Crystal Phases.....	41
3.9.7 Mesophasic Transition Temperature.....	43
3.9.8 Application of Liquid Crystals.....	44
3.9.9 Structural Considerations of Low Molecular Weight Liquid Crystal Systems.....	46
3.10 Terminology in polymer blending.....	50
3.11 Polymer blend.....	51
3.11.1 Melt Mixing.....	51
3.11.2 Solvent Casing.....	51
3.11.3 Freeze Drying.....	52
3.11.4 Emulsions.....	53

	Page
3.11.5 Reactive Blend .....	53
IV EXPERIMENT .....	54
4.1 Materials and Chemicals .....	54
4.1.1 Synthesis Part .....	54
4.1.2 Polymer Blend Part .....	56
4.2 Equipments .....	56
4.2.1 Equipment for handling air-sensitive compounds .....	56
4.2.2 Glass Reactor .....	59
4.2.3 Magnetic Stirrer and Hot Plate .....	59
4.2.4 Digital Hot Plate Stirrer .....	59
4.2.5 Cooling System .....	60
4.2.6 Syringe, Needle and Septum .....	60
4.3 Procedure .....	60
4.3.1 Catalyst Preparation .....	60
4.3.2 Styrene Monomer Preparation .....	60
4.3.3 Polymerization Procedure .....	61
4.3.4 Blend Preparation .....	61
4.4 Polymer Characterization .....	61
4.4.1 Soxhlet Extractor .....	61
4.4.2 Differential Scanning Calorimetry .....	62
4.4.3 Gel Permeation Chromatography .....	63
4.4.3 X-ray Diffraction .....	63
V RESULTS AND DISCUSSION .....	64
5.1 Polymerization of Styrene .....	64
5.2 Miscibility of Syndiotactic Polystyrene Blends .....	65
5.3 Effect of Additives on Thermal Properties of Polymer Blends .....	74
5.3.1 Glass transition temperature .....	74
5.3.2 Crystallization temperature .....	76
5.3.3 Melting temperature .....	77
5.4 Effect of Blending on Miscibility .....	79
5.5 Effect of Additives on Percent of Crystallinity .....	83

	Page
5.6 Effect of Blend on Crystal Formation.....	94
VI CONCLUSIONS AND SUGGESTIONS.....	95
6.1 Conclusions.....	95
6.2 Suggestions.....	97
REFERENCE.....	98
APPENDIX.....	102
VITA.....	134



สถาบันวิทยบริการ  
จุฬาลงกรณ์มหาวิทยาลัย

## LIST OF FIGURES

Figure	Page
3.1 Metallocene Compounds.....	16
3.2 Half-metallocene compounds.....	17
3.3 Plausible structure of methylaluminumoxane.....	18
3.4 Types of olefin polymer tacticity.....	20
3.5 Three different configurations of a mono-substituted polyethylene.....	23
3.6 The fringed micelle model.....	26
3.7 Electron micrograph of a single crystal of nylon-6 grown by precipitation from dilute glycerine solution.....	28
3.8 Optical micrograph showing corrugations in single crystal of linear polyethylene grown from a solution in perchloroethylene.....	29
3.9 Electron micrograph showing pleats in a crystal of linear polyethylene grown from a solution in perchloroethylene.....	29
3.10 Schematic view of a polyethylene single crystal exhibiting adjacent reentry.....	30
3.11 Switchboard Model.....	31
3.12 Model of spherulitic structure.....	32
3.13 The structure of MC-PLCs and SC-PLCs.....	35
3.14 The structure of MC-PLC.....	36
3.15 The structure of MC-PLC.....	37
3.16 The random orientation of monomers in the polymer chain.....	37
3.17 The irregularity of polymer substitute in polymer chain.....	38
3.18 120- degree kinks in the polymer chain.....	38
3.19 The structure of SC-PLCs.....	39
3.20 The spacer of methylene units and the mesogen of aromatic rings.....	39
3.21 The tangle conformation and orientation of the mesogens.....	40
3.22 The structure of smectic phase.....	42
3.23 The structure of nematic phase.....	42
3.24 The structure of cholesteric phase.....	43
3.25 The general structure of aromatic system.....	46
3.26 The general structure of alicyclic system.....	47
3.27 The structure of cholesteric system.....	48



Figure	Page
3.28 The structure of diskogens system.....	49
3.29 Classification of blended polymers.....	50
4.2.1(a) Glove box.....	56
4.2.1(b) Schlenk line.....	57
4.2.1(c) Schlenk tube.....	57
4.2.1(d) Inert gas supply system.....	58
4.2.1(e) Vacuum pump.....	58
4.2.2 Glass Reactor.....	59
4.4.1 Soxhlet extractor.....	62
5.1 Comparison of method in blending SPS/PaMS blends with Fox equation.....	79
5.2 Comparison of method in blending SPS/PEMA blends with Fox equation.....	79
5.3 Comparison of method in blending SPS/PBMA blends with Fox equation.....	80
5.4 Comparison of method in blending SPS/PCHA blends with Fox equation.....	80
5.5 Comparison of method in blending SPS/PIP blends with Fox equation.....	81
5.6 Curve of $s^2I(s)$ versus $s$ for polypropene [61].....	84
5.7 Nomogram of $K$ values as a function of $k$ and $s_p$ calculated for the chemical composition $(CH_2)_n$ and $s_0 = 0.1$ [61].....	85
5.8 X-ray diffraction pattern of amorphous SPS.....	85
5.9 The X-ray diffraction patterns for SPS/PaMS blends and their blend with additives at various compositions: (a) SPS/PaMS blends; (b) SPS/PaMS/LCC blends and (c) SPS/PaMS/GMS blends.....	86
5.10 The X-ray diffraction patterns for SPS/PEMA blends and their blend with additives at various compositions: (a) SPS/PEMA blends; (b) SPS/PEMA/LCC blends and (c) SPS/PEMA/GMS blends.....	87
5.11 The X-ray diffraction patterns for SPS/PBMA blends and their blend with additives at various compositions: (a) SPS/PBMA blends; (b) SPS/PBMA/LCC blends and (c) SPS/PBMA/GMS blends.....	88
5.12 The X-ray diffraction patterns for SPS/PCHA blends and their blend with additives at various compositions: (a) SPS/PCHA blends; (b) SPS/PCHA/LCC blends and (c) SPS/PCHA/GMS blends.....	89



Figure	Page
5.13 The X-ray diffraction patterns for SPS/PIP blends and their blend with additives at various compositions: (a) SPS/PIP blends; (b) SPS/PIP/LCC blends and (c) SPS/PIP/GMS blends.....	90
A.1 DSC curve of SPS.....	103
A.2 DSC curve of SPS blended with LCC.....	103
A.3 DSC curve of SPS blended with GMS.....	103
A.4 DSC curve of PaMS.....	104
A.5 DSC curve of PaMS blended with LCC.....	104
A.6 DSC curve of PaMS blended with GMS.....	104
A.7 DSC curve of SPS20/PaMS80 blends.....	105
A.8 DSC curve of SPS20/PaMS80/LCC blends.....	105
A.9 DSC curve of SPS20/PaMS80/GMS blends.....	105
A.10 DSC curve of SPS40/PaMS60 blends.....	106
A.11 DSC curve of SPS40/PaMS60/LCC blends.....	106
A.12 DSC curve of SPS40/PaMS60/GMS blends.....	106
A.13 DSC curve of SPS60/PaMS40 blends.....	107
A.14 DSC curve of SPS60/PaMS40/LCC blends.....	107
A.15 DSC curve of SPS60/PaMS40/GMS blends.....	107
A.16 DSC curve of SPS80/PaMS20 blends.....	108
A.17 DSC curve of SPS80/PaMS20/LCC blends.....	108
A.18 DSC curve of SPS80/PaMS20/GMS blends.....	108
A.19 DSC curve of PBMA.....	109
A.20 DSC curve of PBMA blended with LCC.....	109
A.21 DSC curve of PBMA blended with GMS.....	109
A.22 DSC curve of SPS20/PBMA80 blends.....	110
A.23 DSC curve of SPS20/PBMA80/LCC blends.....	110
A.24 DSC curve of SPS20/PBMA80/GMS blends.....	110
A.25 DSC curve of SPS40/PBMA60 blends.....	111
A.26 DSC curve of SPS40/PBMA60/LCC blends.....	111
A.27 DSC curve of SPS40/PBMA60/GMS blends.....	111
A.28 DSC curve of SPS60/PBMA40 blends.....	112
A.29 DSC curve of SPS60/PBMA40/LCC blends.....	112

Figure	Page
A.30 DSC curve of SPS60/PBMA40/GMS blends.....	112
A.31 DSC curve of SPS80/PBMA20 blends.....	113
A.32 DSC curve of SPS80/PBMA20/LCC blends.....	113
A.33 DSC curve of SPS80/PBMA20/GMS blends.....	113
A.34 DSC curve of PEMA.....	114
A.35 DSC curve of PEMA blended with LCC.....	114
A.36 DSC curve of PEMA blended with GMS.....	114
A.37 DSC curve of SPS20/PEMA80 blends.....	115
A.38 DSC curve of SPS20/PEMA80/LCC blends.....	115
A.39 DSC curve of SPS20/PEMA80/GMS blends.....	115
A.40 DSC curve of SPS40/PEMA60 blends.....	116
A.41 DSC curve of SPS40/PEMA60/LCC blends.....	116
A.42 DSC curve of SPS40/PEMA60/GMS blends.....	116
A.43 DSC curve of SPS60/PEMA40 blends.....	117
A.44 DSC curve of SPS60/PEMA40/LCC blends.....	117
A.45 DSC curve of SPS60/PEMA40/GMS blends.....	117
A.46 DSC curve of SPS80/PEMA20 blends.....	118
A.47 DSC curve of SPS80/PEMA20/LCC blends.....	118
A.48 DSC curve of SPS80/PEMA20/GMS blends.....	118
A.49 DSC curve of PCHA.....	119
A.50 DSC curve of PCHA blended with LCC.....	119
A.51 DSC curve of PCHA blended with GMS.....	119
A.52 DSC curve of SPS20/PCHA80 blends.....	120
A.53 DSC curve of SPS20/PCHA80/LCC blends.....	120
A.54 DSC curve of SPS20/PCHA80/GMS blends.....	120
A.55 DSC curve of SPS40/PCHA60 blends.....	121
A.56 DSC curve of SPS40/PCHA60/LCC blends.....	121
A.57 DSC curve of SPS40/PCHA60/GMS blends.....	121
A.58 DSC curve of SPS60/PCHA40 blends.....	122
A.59 DSC curve of SPS60/PCHA40/LCC blends.....	122
A.60 DSC curve of SPS60/PCHA40/GMS blends.....	122
A.61 DSC curve of SPS80/PCHA20 blends.....	123

Figure	Page
A.62 DSC curve of SPS80/PCHA20/LCC blends .....	123
A.63 DSC curve of SPS80/PCHA20/GMS blends .....	123
A.64 DSC curve of PIP .....	124
A.65 DSC curve of PIP blended with LCC .....	124
A.66 DSC curve of PIP blended with GMS .....	124
A.67 DSC curve of SPS20/PIP80 blends .....	125
A.68 DSC curve of SPS20/PIP80/LCC blends .....	125
A.69 DSC curve of SPS20/PIP80/GMS blends .....	125
A.70 DSC curve of SPS40/PIP60 blends .....	126
A.71 DSC curve of SPS40/PIP60/LCC blends .....	126
A.72 DSC curve of SPS40/PIP60/GMS blends .....	126
A.73 DSC curve of SPS60/PIP40 blends .....	127
A.74 DSC curve of SPS60/PIP40/LCC blends .....	127
A.75 DSC curve of SPS60/PIP40/GMS blends .....	127
A.76 DSC curve of SPS80/PIP20 blends .....	128
A.77 DSC curve of SPS80/PIP20/LCC blends .....	128
A.78 DSC curve of SPS80/PIP20/GMS blends .....	128
A.79 DSC curve of PVME .....	129
A.80 DSC curve of PVME blended with LCC .....	129
A.81 DSC curve of PVME blended with GMS .....	129
A.82 DSC curve of SPS20/PVME80 blends .....	130
A.83 DSC curve of SPS20/PVME80/LCC blends .....	130
A.84 DSC curve of SPS20/PVME80/GMS blends .....	130
A.85 DSC curve of SPS40/PVME60 blends .....	131
A.86 DSC curve of SPS40/PVME60/LCC blends .....	131
A.87 DSC curve of SPS40/PVME60/GMS blends .....	131
A.88 DSC curve of SPS60/PVME40 blends .....	132
A.89 DSC curve of SPS60/PVME40/LCC blends .....	132
A.90 DSC curve of SPS60/PVME40/GMS blends .....	132
A.91 DSC curve of SPS80/PVME20 blends .....	133
A.92 DSC curve of SPS80/PVME20/LCC blends .....	133
A.93 DSC curve of SPS80/PVME20/GMS blends .....	133

## LIST OF TABLES

Table	Page
2.1 Polymerization of styrene using various metal compounds with MAO .....	6
2.2 Catalyst activities of half-titanocenes containing trimethoxide .....	7
2.3 The effect of bite angle of Cp ligand on the catalyst performance .....	8
5.1 Polymerization of Styrene using Cp*TiCl <sub>3</sub> with MMAO <sup>a</sup> .....	64
5.2 Glass transition temperature (T <sub>g</sub> ), melting temperature (T <sub>m</sub> ), crystallization temperature (T <sub>c</sub> ) and melting enthalpy of SPS/PaMS blends .....	66
5.3 Glass transition temperature (T <sub>g</sub> ), melting temperature (T <sub>m</sub> ), crystallization temperature (T <sub>c</sub> ) and melting enthalpy of SPS/PaMS/LCC blends .....	67
5.4 Glass transition temperature (T <sub>g</sub> ), melting temperature (T <sub>m</sub> ), crystallization temperature (T <sub>c</sub> ) and melting enthalpy of SPS/PaMS/GMS blends .....	67
5.5 Glass transition temperature (T <sub>g</sub> ), melting temperature (T <sub>m</sub> ), crystallization temperature (T <sub>c</sub> ) and melting enthalpy of SPS/PEMA blends .....	68
5.6 Glass transition temperature (T <sub>g</sub> ), melting temperature (T <sub>m</sub> ), crystallization temperature (T <sub>c</sub> ) and melting enthalpy of SPS/PEMA/LCC blends .....	68
5.7 Glass transition temperature (T <sub>g</sub> ), melting temperature (T <sub>m</sub> ), crystallization temperature (T <sub>c</sub> ) and melting enthalpy of SPS/PEMA/GMS blends .....	69
5.8 Glass transition temperature (T <sub>g</sub> ), melting temperature (T <sub>m</sub> ), crystallization temperature (T <sub>c</sub> ) and melting enthalpy of SPS/PBMA blends .....	69
5.9 Glass transition temperature (T <sub>g</sub> ), melting temperature (T <sub>m</sub> ), crystallization temperature (T <sub>c</sub> ) and melting enthalpy of SPS/PBMA/LCC blends .....	70
5.10 Glass transition temperature (T <sub>g</sub> ), melting temperature (T <sub>m</sub> ), crystallization temperature (T <sub>c</sub> ) and melting enthalpy of SPS/PBMA/GMS blends .....	70
5.11 Glass transition temperature (T <sub>g</sub> ), melting temperature (T <sub>m</sub> ), crystallization temperature (T <sub>c</sub> ) and melting enthalpy of SPS/PCHA blends .....	71
5.12 Glass transition temperature (T <sub>g</sub> ), melting temperature (T <sub>m</sub> ), crystallization temperature (T <sub>c</sub> ) and melting enthalpy of SPS/PCHA/LCC blends .....	71
5.13 Glass transition temperature (T <sub>g</sub> ), melting temperature (T <sub>m</sub> ), crystallization temperature (T <sub>c</sub> ) and melting enthalpy of SPS/PCHA/GMS blends .....	72

Table	Page
5.14 Glass transition temperature ( $T_g$ ), melting temperature ( $T_m$ ), crystallization temperature ( $T_c$ ) and melting enthalpy of SPS/PIP blends.....	72
5.15 Glass transition temperature ( $T_g$ ), melting temperature ( $T_m$ ), crystallization temperature ( $T_c$ ) and melting enthalpy of SPS/PIP/LCC blends.....	73
5.16 Glass transition temperature ( $T_g$ ), melting temperature ( $T_m$ ), crystallization temperature ( $T_c$ ) and melting enthalpy of SPS/PIP/GMS blends.....	73
5.17 Glass transition temperature ( $T_g$ ), melting temperature ( $T_m$ ) and crystallization temperature ( $T_c$ ) of SPS/PVME blends.....	74
5.18 Melting temperature depression of their blends.....	78
5.19 Percentage of SPS in binary blends from calculation.....	82
5.20 %Crystallinity of SPS/PaMS, SPS/PaMS/GMS and SPS/PaMS/LCC blends at various compositions.....	91
5.21 %Crystallinity of SPS/PEMA, SPS/PEMA/GMS and SPS/PEMA/LCC blends at various compositions.....	92
5.22 %Crystallinity of SPS/PBMA, SPS/PBMA/GMS and SPS/PBMA/LCC blends at various compositions.....	92
5.23 %Crystallinity of SPS/PCHA, SPS/PCHA/GMS and SPS/PCHA/LCC blends at various compositions.....	93
5.24 %Crystallinity of SPS/PIP, SPS/PIP/GMS and SPS/PIP/LCC blends at various compositions.....	93



# CHAPTER I

## INTRODUCTION

Polymeric materials, which are well known under the common name 'Plastics', are very important and useful at present, because of their high properties per weight ratio, comparing to existing materials such as metals and woods. They are also used in many applications, for examples, household appliances, insulation and electronic equipment. These products required different properties of each polymer, which can be selected depending on each application.

Blending polymers is the technique to obtain the new properties of polymer from existing materials without synthesizing the new polymeric materials. Mixing two or more existing polymers may create the new properties of polymers. There were many ways to mix polymers together, such as by heat (melt-mixing), by using solvent (solution casting, freeze drying) and others. The results of blending polymers have many advantages; for example, blended polymers have lower cost than synthesis the new synthesized polymers, which have the same desired properties

Generally, polystyrene (PS) is one of the most important commodity polymers in the industry. Its applications range from high modulus, transparent grade to rubber modified, tough resins and blends with outstanding impact resistance and mechanical properties. Recently, coordination polymerization techniques were introduced for preparation of polystyrene, which has an entirely new range of possibilities and the feasibility to prepare a highly stereoregular, syndiotactic polystyrene (SPS) was demonstrated [1]. SPS prepared by coordination polymerization is a new semicrystalline thermoplastic material with high melting temperature (270 °C) and excellent chemical resistance. Also, SPS has been reported to show polymorphism according to crystallization conditions like as isotactic-polypropylene, isotactic-poly(butene), isotactic-poly(1-butene), and syndiotactic-poly(1-butene) [2–7]. However, because SPS has some economic disadvantages such as low strength [8], higher processing temperature [9], and efficiency of polymerization catalyst, it has

been restricted to a few applications. So, many researchers are still interested in blending with secondary polymer materials to reduce the product cost.

Some previous results have shown miscibility of polystyrene with several polymers, viz. Polyphenyleneether (PPE), polyvinylmethylether (PVME), poly-2-chlorostyrene (PCS), polymethylstyrene (PMS), polycarbonate of tetramethyl bisphenal-A (TMPC), polycyclohexyl acrylate (PCHA), polyethylmethacrylate (PEMA), polycyclohexyl methacrylate (PCHMA) and etc [10].

However, their excellent properties can become a cause of limitation in manufacturing processes especially the viscosity of melt polymers. To process the plastics requires many complicated operations because their processing and their manufacture consume high energy.

The processing properties of polymers can be improved by adding various additives, such as antioxidants, plasticizers and others. There are many additives to reduce melt viscosity of polymers for improving their processability, but those additives may cause many negative effects to their important properties, especially mechanical properties of final products.

Lubricant [11] is a substance that when added in small quantities, provides a considerable decrease in resistance to the movement of chains or segments of a polymer or at least partly amorphous structure. There are two kinds of lubricant that are internal lubricant and external lubricant. In general, if a lubricant appears to be effective in improving flow but does not have much effect on surface tension, it is considered internal lubricant. If it is found on the surface or on adjacent surfaces or if it modifies observables associated with the surface, it is considered external lubricant. If it behaves in one way under one set of conditions and in another way under a different set of circumstances, it is considered both an internal and external lubricant. These are referred to as balanced, combination or multifunctional lubricants.

Low molar mass liquid crystals were also found to improve processability of polymers. Patwardhan and co-workers reported that addition of low molar mass liquid

crystal to amorphous polymers could improve both processability and mechanical properties of the blends [12].

Following the above mentioned, this present work has investigated the effects of low molar mass liquid crystal (cyclohexylbiphenylcyclohexane: CBC-33) addition on the miscibilities of syndiotactic polystyrene blends with various polymers.

### 1.1 The Objectives of This Thesis

Study the miscibility of syndiotactic polystyrene, which synthesized by homogeneous half-metallocene catalyst system, blend with various polymers and the effect of two types of additives with syndiotactic polystyrene that influence on the crystallinity of the polymer blends by differential scanning calorimetry (DSC) and wide-angle X-ray diffraction (WAXD).

### 1.2 The Scope of This Thesis

1.2.1 Synthesize the high molecular weight SPS by using  $Cp^*TiCl_3/MMAO$  catalyst system.

1.2.2 Blend SPS with various polymers as follow:

Poly( $\alpha$ -methylstyrene), (PaMS)

Poly(ethyl methacrylate), (PEMA)

Poly(*n*-butyl methacrylate), (PBMA)

Poly(cyclohexyl acrylate), (PCHA)

Poly(*cis*-isoprene), (PIP)

Poly(vinyl methyl ether), (PVME)

1.2.3 Modify the blend with low molar mass liquid crystal (CBC-33) at the concentration of 1%(w/w) in comparison with GMS by melt mixing method.



1.2.4 Characterize SPS blends with or without additive by using differential scanning calorimetry (DSC), X-ray diffraction (XRD) and gel permeation chromatography (GPC) techniques.



สถาบันวิทยบริการ  
จุฬาลงกรณ์มหาวิทยาลัย

## CHAPTER II

### LITERATURE REVIEWS

#### 2.1 Catalysts for Syndiotactic Polystyrene

##### 2.1.1 Transition metal compounds

The syndiotacticity of SPS results from the homogeneous coordinative polymerization mechanism. Typically, Group 4 transition metal complexes are utilized with co-catalysts such as methylaluminoxane (MAO) or pentafluorophenyl borate derivatives. Initial evaluation reactions of various titanium compounds with MAO have been published [1,13-15].

The results shown in Table 2.1 indicate that titanium halide compounds (e.g.  $\text{TiCl}_4$ ,  $\text{TiBr}_4$ ,  $\text{CpTiCl}_3$ ,  $\text{Cp}^*\text{TiCl}_3$ ), and even titanium compounds lacking halogen atoms (e.g.  $\text{Ti}(\text{OEt})_4$ ,  $\text{Ti}(\text{OBu})_4$ ,  $\text{Ti}(\text{Net}_2)_4$ ,  $\text{Ti}(\eta^5\text{-C}_6\text{H}_6)_2$  and  $\text{CpTi}(\eta^5\text{-CH}_3\text{C}_6\text{H}_5)_2$ ) can produce SPS. Not only Ti(IV) but also Ti(III) compounds, such as  $\text{CpTi}(\eta^5\text{-C}_5\text{H}_5)\text{Cl}_2$ , give SPS.

Zambelli et al. [15] reported that Ti(II) (e.g.  $\text{Ti}(\eta^5\text{-C}_6\text{H}_6)_2$ ) also could produce SPS, but  $\text{Ti}(\text{bipy})_3$ , formally Ti(0), gave atactic PS. However, Ti(0) arene compounds can produce SPS.

สถาบันวิทยบริการ  
จุฬาลงกรณ์มหาวิทยาลัย

**Table 2.1** Polymerization of styrene using various metal compounds with MAO

Catalyst	[Al] mole	Conversion (wt%)	Stereospecificity
TiCl <sub>4</sub>	0.04	4.1	syndiotactic
TiBr <sub>4</sub>	0.04	2.1	syndiotactic
Ti(OCH <sub>3</sub> ) <sub>4</sub>	0.04	3.8	syndiotactic
Ti(OC <sub>2</sub> H <sub>5</sub> ) <sub>4</sub>	0.04	9.5	syndiotactic
Ti( $\eta^5$ -C <sub>5</sub> H <sub>5</sub> )Cl <sub>3</sub>	0.015	68.2	syndiotactic
	0.03	99.2	syndiotactic
Ti( $\eta^5$ -C <sub>5</sub> H <sub>5</sub> ) <sub>2</sub> Cl <sub>3</sub>	0.03	1.0	syndiotactic
Ti[( $\eta^5$ -C <sub>5</sub> (CH <sub>3</sub> ) <sub>5</sub> ) <sub>2</sub> Cl <sub>2</sub>	0.03	2.0	syndiotactic
Ti[( $\eta^5$ -C <sub>5</sub> (CH <sub>3</sub> ) <sub>2</sub> )ClH	0.03	8.8	syndiotactic
Ti( $\eta^5$ -C <sub>6</sub> H <sub>6</sub> ) <sub>2</sub>	0.025	5.4	syndiotactic
Ti( $\eta^5$ -CH <sub>3</sub> C <sub>6</sub> H <sub>5</sub> ) <sub>2</sub>	0.025	5.9	syndiotactic
Ti( $\eta^5$ -(CH <sub>3</sub> ) <sub>2</sub> C <sub>6</sub> H <sub>4</sub> ) <sub>2</sub>	0.025	5.7	syndiotactic
Ti( $\eta^5$ -(CH <sub>3</sub> ) <sub>3</sub> C <sub>6</sub> H <sub>3</sub> ) <sub>2</sub>	0.025	6.0	syndiotactic
Ti(acac) <sub>2</sub> Cl <sub>2</sub>	0.04	0.4	syndiotactic
Ti(Net <sub>2</sub> ) <sub>4</sub>	0.04	0.4	syndiotactic
ZrCl <sub>4</sub>	0.04	0.4	atactic
CpZrCl <sub>3</sub>	0.04	1.3	syndiotactic
Cp <sub>2</sub> ZrCl <sub>2</sub>	0.04	1.3	atactic
Cp <sub>2</sub> HfCl <sub>2</sub>	0.04	0.7	atactic
Cp <sub>2</sub> VCl <sub>2</sub>	0.04	0.7	atactic
Nb(OEt) <sub>5</sub>	0.04	0.2	atactic
Ta(OEt) <sub>5</sub>	0.04	0.1	atactic
Cr(acac) <sub>3</sub>	0.01	1.8*	atactic
Co(acac) <sub>3</sub>	0.01	1.8*	atactic
Ni(acac) <sub>2</sub>	0.01	80.8*	atactic

Polymerization conditions [15]; metal compounds  $5 \times 10^{-5}$  mole, styrene 23 cm<sup>3</sup>, toluene 100 cm<sup>3</sup>, at 50°C for 2 h.

\*As above condition, except metal compounds  $2.5 \times 10^{-5}$  mole, styrene 50 cm<sup>3</sup>.

### 2.1.2 Half-titanocene compounds

The catalytic activity was found to vary accordingly to ligands on the titanium. Among the SPS producing catalysts, titanocenes with one cyclopentadienyl ligand yield the highest activity for SPS. The polymerization activities of half-titanocene compounds containing trimethoxide have been reported as shown in Table 2.2.

**Table 2.2** Catalyst activities of half-titanocenes containing trimethoxide

Compound	Activity (kg SPS/gTi)
CpTi(OMe) <sub>3</sub>	10
(Me <sub>3</sub> Si) <sub>2</sub> CpTi(OMe) <sub>3</sub>	25
Me <sub>4</sub> CpTi(OMe) <sub>3</sub>	130
(Me <sub>3</sub> Si)Me <sub>4</sub> CpTi(OMe) <sub>3</sub>	135
Cp*Ti(OMe) <sub>3</sub>	200
EtMe <sub>4</sub> CpTi(OMe) <sub>3</sub>	210







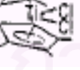
The data indicate that substituents on the cyclopentadienyl ligands which are electron releasing generally yield higher polymerization activities. This result suggests stabilization of the active site by electron releasing substituents. The polymerization activity in the presence of Cp\*TiR<sub>3</sub> compounds (R is alkoxide or chloride ligand) is as follows, in order of decreasing catalytic activity: Cp\*Ti(OMe)<sub>3</sub> > Cp\*Ti(OPh)<sub>3</sub> > Cp\*Ti(OC<sub>6</sub>H<sub>4</sub>CH<sub>3</sub>)<sub>3</sub> > Cp\*TiCl<sub>3</sub> > Cp\*Ti(O<sup>*t*</sup>Bu)<sub>3</sub> > Cp\*Ti(O<sup>*i*</sup>C<sub>3</sub>H<sub>4</sub>F<sub>6</sub>)<sub>3</sub>. The chloride ligand and the electron withdrawing alkoxide decrease the conversion as does the bulky *tert*-butoxide ligand. The methoxide, *iso*-propoxide, phenoxide and *p*-methylphenoxide are all similar in terms of conversion. Recently, Kaminsky showed that the catalytic activity of CpTiF<sub>3</sub> is better than CpTiCl<sub>3</sub> [16].

Ready et al. [17] observed that indenyltitanium trichloride, IndTiCl<sub>3</sub>, is a significantly more active catalyst than CpTiCl<sub>3</sub>. However, Tomotsu et al. compared the two catalysts and found that the catalytic activity of IndTiCl<sub>3</sub> is lower than that of CpTiCl<sub>3</sub> [18]. Difference in polymerization conditions may account for the observed differences in catalytic performance. Furthermore, Chien et al. [19] investigated the influence of aromatic substituents on indenyl ligands. The results suggested that benzindene has stabilized the active catalytic species more than that of the phenyl substitution on the C-5 ring for the indenyl ligand.

### 2.1.3 Ansa-titanocene compounds

The polymerization activities for several ansa-titanocene complexes have been reported by Tomotsu et al.[20]. The data indicate that the polymerization activity as well as syndiospecificity increase by decreasing the bite-angle, the angle of the Cp centroid-Ti-Cp centroid. Catalytic activity decreased in the following order:  $\text{CH}_2\text{Cp}_2\text{TiCl}_2 > \text{SiMe}_2\text{Cp}_2\text{Ti}_2 > \text{Me}_2\text{SiCp}_2\text{TiCl}_2 > (\text{Cp}^*)_2\text{TiCl}_2 > \text{Cp}_2\text{TiCl}_2$  (Table 2.3). The activities of ansa-titanocene complexes are less than those of monocyclopentadienyl complexes.

**Table 2.3** The effect of bite angle of Cp ligand on the catalyst performance

	Bite Angle (°)	Activity (g/g-Ti/Hr)	SPS/total PS (%)	Tacticity (rrrr%)
	131	21	11	94
	137	57	73	94
	121	573	96	99
	121	1037	98	99
	128	669	98	99
	128	957	98	99
	131	38	11	95

Condition:  $[\text{Al}]/[\text{Ti}] = 40$ ,  $[\text{Ti}] = 10 \text{ mM}$ , at  $15^\circ\text{C}$

### 2.1.4 Zirconocene and ansa-zirconocene catalysts

Zirconocenes produce isotactic polypropylene and atactic polystyrene while titanocenes produce atactic polypropylene and syndiotactic polystyrene.

The ansa-zirconocenes compounds show lower activity and lower stereospecificity than the corresponding ansa-titanocenes. These results are consistent

with the suggestion that the catalyst center and the mechanism of syndiospecific polymerization of styrene may be different from those of olefin polymerization in the formation of an active catalyst by the reaction with MAO. In comparison with the Ti compounds, the Zr compounds show lower activity and lower stereospecificity, which could arise from less electrophilic and larger ionic radius of zirconium in comparison with titanium.

### 2.1.5 Other Metal complexes

Yang et al. [21] examined rare earth coordination catalysts. Nd(naph)<sub>3</sub>/Al(*i*-Bu)<sub>3</sub> catalyst system was found to produce syndiotactic-rich polystyrene. They proposed that the catalytically active species might be an ionic complex, because the addition of CCl<sub>4</sub> increased the catalytic activity.

On the other hand, there are an increasing number of investigations on heterogeneous supported metallocene catalysts. These catalyst systems can also reduce amount of MAO used.

## 2.2 Cocatalyst

MAO is an important cocatalyst which activates the group 4 metallocenes in homogeneous Ziegler-Natta polymerization. Before the discovery of MAO, the homogeneous Ziegler-Natta catalyst Cp<sub>2</sub>TiCl<sub>2</sub>, activated with alkylaluminium, yielded atactic polystyrene with low catalytic activity. The use of MAO instead of alkylaluminium raised the catalytic activity by several orders of magnitude. MAO is routinely used for the synthesis of syndiotactic polystyrene [20].

Many researchers are trying to clarify the structure and roles of MAO. The role of MAO for syndiotactic polymerization of styrene was also examined by Miyashita [22]. MAO of different molecular weights were made by the distillation of normal MAO. Further more the effects of molecular weight of MAO on the catalytic activity are examined. They found that Me(Al(Me)O)<sub>15</sub>AlMe<sub>2</sub> showed the highest activity and a large amount of MAO was required. They also examined the molar electric conductivity of the reacted compound between titanocene and MAO. It was 0.006 S cm<sup>2</sup>/mol in toluene and it was concluded that the active site for polymerization must have the structure of zwitterionic Ti cation center.



MAO is known to contain trimethylaluminum (TMA) both in a form coordinated to MAO and as free TMA. Tomotsu et al. [20] examined the effects of TMA in MAO. They found it decreases the catalytic activity for SPS production.

### 2.3 Polymer Blend

Combination of different polymers into multiphase systems represents a very attractive route towards new materials. It is also an efficient way to improve some deficient properties of common plastics [23,24].

Due to its performances, syndiotactic polystyrene (SPS) has been widely viewed as an emerging class of engineering thermoplastics [13]. However, because SPS has some economic disadvantages such as low strength [8], higher processing temperature [9]. So, many researchers are still interested in blending with secondary polymer materials to reduce the product cost.

Widmaier, J.M. and Mignard G. [1987] [25] investigated the blends of polystyrene of molecular weights from 4000 to 80000 g/mol with poly( $\alpha$ -methylstyrene) of molecular weights from 55000 to 300000 g/mol were made by freeze-drying from benzene solutions. Glass transition temperature measurements by differential scanning calorimetry indicate that the miscibility behavior of the polymers is very sensitive to change of molecular weights. A decrease of polystyrene chain length changes a two-phase system into a miscible or partially miscible blend. Broadening of the transition region and temperature shifts suggest that the polystyrene dissolves more in the poly( $\alpha$ -methylstyrene) phase than does the poly( $\alpha$ -methylstyrene) in the polystyrene phase.

Cimmino and co-workers [26,27] investigated by means of solid-state NMR and DSC the dependence of miscibility on composition and temperature in SPS/PVME blends. The blends, prepared by casting a solution from *o*-dichlorobenzene at 130°C, are found to be immiscible for PVME > 20 wt%, in contrast with the miscibility found for APS/PVME blends. In fact, DSC experiments show two  $T_g$  values corresponding to an SPS-rich phase (83:17 wt%) and a PVME-rich phase (13:87 wt%). The lack of miscibility is also confirmed by the absence, in  $^{13}\text{C}$  NMR solid-state experiments, of cross-polarization from SPS protons to PVME methoxy carbons [27].

Later, Mandal and Woo [28] demonstrated that this system is miscible, and exhibits a behavior equivalent to APS/PVME blends. The previously found immiscibility is due to the relatively low value of the lower critical solution temperature, which a phase separation in 50:50 wt% blends was already induced at temperature of ca 120°C. In fact, OM, SEM and DSC, applied to blends (70:30 and 50:50 wt%) prepared by casting film from 1-2 % solution of chloronaphthalene at about 120°C, or by precipitation from the same solution with *n*-heptane, show a substantial homogeneity. However, OM measurements, performed at various temperatures on a series of samples, show a cloud point at ca 120°C and above, indicating the onset of segregation. At higher temperature, DSC shows two  $T_g$ s at -30°C (attributed to PVME) and at 95°C (attributed to SPS), shifted with respect to the pure compounds and corresponding to two partially miscible phases, one rich in PVME and the other rich in SPS. Under slow cooling the process appears to be reversible.

For SPS/PPE blends, DSC and DMTA measurements give a single  $T_g$  value [29-32], intermediate between those of the components and dependent on composition. The  $T_g$  values of SPS and PPE being very different from each other (98 and 220°C, respectively), this result constitutes an unambiguous proof of blend miscibility within the whole composition range.

The same techniques cannot be applied to the case of APS/SPS blends, as the two components have similar  $T_g$  values (less than 10°C difference). A higher resolution of close  $T_g$  values can be derived from the isothermal heat capacity curves, measured in the vicinity of  $T_g$  by modulated DSC [33]. Furthermore, SPS and APS, when annealed separately below  $T_g$ , exhibit in both DSC and modulated DSC distinct endothermic transitions owing to the enthalpy recovery [33,34]. Both methods, when applied to the SPS/APS blends, give a single temperature for all compositions in agreement with the presence of a miscibility between the components.

Choi et al. [30] investigated the toughening effect of rubber in SPS/PPE blends obtained via reactive extrusion. Whereas the impact strength of SPS/PPE blends has a value immediate with respect to the two components, the addition of a reactive polystyrene containing 5 wt% of oxazoline comonomer and MA-SEBS (SEBS grafted with maleic anhydride) as impact modifiers produces a synergic effect on toughening.



Polymeric blends of melt processable polymers and liquid crystalline compounds have been studied in many researches. This review covers liquid crystalline (LC) blends containing low molecular weight liquid crystal. The main reason of blending low molecular weight liquid crystal blends is to improving the melt viscosity of the blends.

Buckley, A. Conciatori, A.B. and Calundann, G.W. [35] investigated the blends of low molecular weight liquid crystalline compound with either polyolefin or polyester. The low molecular weight liquid crystalline compound (LCC) used have molecular weight less than about 1,000 g/mole. The LCC used came from the group consisting of N,N'-bis(p-methoxybenzylidene)-alpha,alpha]-bi-p-toluidine, p-methoxycinnamic acid, N,N]-bis(4-octyloxybenzylidene)-p-phenylenediamine. The concentration of low molecular weight liquid crystalline used is present in an amount of from about 0.5 to 5 % by weight and the melt viscosity of the blend was determined by a capillary rheometer. The melt viscosity of low molecular weight liquid crystalline blends reduced by as much as 25 to 30% compared with the pure matrix polymers.

Siegmann, A., Dagan, A., and Kenig, S. [36] prepared the polymer blends of liquid crystalline aromatic copolyester (based on 6-hydroxy-2-naphthanoic acid (HNA) and phydroxybenzoic acid) and an amorphous polyamide (PA) by melted mixing method. The rheological behavior of the blends was very different from pure component and viscosity of blends significantly changed. Only 5 % by weight of LCP in the blend could reduce the viscosity 20-25 times. The tensile mechanical behavior of the blends was very similar to that of polymeric matrix. The blend of two phase morphologies was found to be affected by the LCP compositions. The LCP phase changed gradually with increasing LCP content form ellipsoidal particles to rod-like and fibrillar structure.

Tariq M. Malik, Pierre J. Carreau and Nathalie Chapleau [37] investigated the mechanical and rheological properties of blends of a thermotropic liquid crystalline polyester with a polycarbonate. The blends are fibrillar in character and exhibit great hardness and toughness due to high degree of molecular orientation, which develops during the melt blending and processing steps. Increases of the Young modulus by 100 percent are observed for blends containing only 10 percent of liquid crystalline polymer (LCP). Time-dependent behavior of the blends was investigated by performing solid state relaxation measurements and the relaxation modulus was also

found to increase with the addition of LCP. The effect is relatively small in the glassy zone of viscoelastic response, but increases through the transition and viscous flow regions. The melt viscosity of the polycarbonate is slightly shear thinning whereas that of the unblended LCP increases rapidly with decreasing shear rate at low shear rate. This suggests the presence of yield stresses as confirmed by measurements on the Rheometrics RSR in the stress sweep mode. The melt viscosity of the blends was found to be similar to that of the unblended polycarbonate, but more shear thinning and less viscous. Preliminary results of scanning electron microscopy (SEM) showed the extended filaments of LCP are composed of fibers and fibrils oriented parallel to the tensile axis. Micrographs of blend containing 2.5, 5 and 10 percent LCP show homogeneous dispersion of the fibers in the PC matrix. These micrographs also suggest very good wetting and adhesion between the fibers and matrix. For the 25/75 percent LCP/PC blend, large voids and heterogeneities appear showing very poor wetting and lack of adhesion between the two polymers; they show as well lack of dispersion of fibers in the PC matrix. These void and poor dispersion properties at the higher LCP content.

Lin, Y.C., Lee, H.W. and Winter, H.H. [38] studied the miscibility and viscoelastic properties of blends of a segmented block copolyester that had the average molecular weight 11,500 g/mole and poly(ethylene terephthalate) that had the average molecular weight 50,000 g/mole . They found that addition of a small quantity of LCP has a dramatic effect on rheology. For example, an addition of 2wt% LCP reduces the viscosity by about 60%. This effect is most pronounced for PET of higher molar masses. The melt viscosity decreases exponentially with the LCP content in the range of composition where the blends are miscible. But there was no significant further reduction of viscosity when the LCP content exceeds 50wt%. The addition of LCP also changes the distribution of the relaxation times of PET and broadens the zero shear viscosity regimes.

Anchana Chuenchaokit [39] studied the effects of thermotropic liquid crystals on properties of polycarbonates. The low molecular weight liquid crystals were cyclohexylbiphenylcyclohexanes groups that had average molecular weight about 400 g/mole. The blends were prepared by melt mixing at 0.25, 0.5 and 1% by weight of liquid crystals. The shear viscosity of pure PC and their blends were investigated using a capillary rheometer and the glass transition temperatures were measured by Differential Scanning Calorimeter (DSC). Experimental results showed that the viscosity of the blends with only small weight fraction (1%) of low molecular weight

liquid crystal is about 90 percent lower than that of the pure polycarbonates. DSC thermograms also show the decreasing in the glass transition temperatures of PC.

Suraphan Powanusorn [40] prepared the blends of low molecular weight liquid crystal and nylon-6, polyethylene, polypropylene, polycarbonate and polyacetal. The low molecular weight liquid crystals had average molecular weight about 400 g/mole. Melt mixing was the preparation method for blending liquid crystal and base polymers together at 0.1, 0.2, 0.4% by weight of liquid crystal. The rheological, thermal and mechanical properties of the blends are investigated in order to compare with the base polymer that absence of liquid crystal. The results show that liquid crystal may improve the processability of the base polymer by reducing the melt viscosity while the liquid crystal did not affect the thermal and mechanical properties of the base polymer. The melt viscosity of the blends is about 20 to 80 percent lower than that of the base polymer depended on type of polymers at the some shear rate.

Noppawan Motong [41] studied effects of mixing and processing on the viscosity of polycarbonate blends with low molar mass thermotropic liquid crystals, cyclohexylbiphenylcyclohexane. Stirring melt mix was utilized in the first step blending of PC and CBC-33 with content at 0.1, 0.2, 0.4, 0.8 and 1.0 % by weight. Viscosity of the resulting blends were investigated and compared with the base PC. The result showed that 0.2 % by weight of CBC-33 is the suitable concentration because at higher concentration the effects of CBC-33 on the viscosity were less significant.

S. Wacharawichanant et al. [42] investigated the effects on molecular motion in melt mixed poly(styreneco-acrylonitrile) (SAN) containing 25% by weight of acrylonitrile (AN) and poly(methyl methacrylate) (PMMA) (20/80 wt%) blends after adding two low molar mass liquid crystals (CBC33 and CBC53) and two lubricants (GMS and zinc stearate) by using light scattering techniques. The samples were assessed in terms of the apparent diffusion coefficient ( $D_{app}$ ) obtained from observation of phase separation in the blends. The early stages of phase separation as observed by light scattering were dominated by diffusion processes and approximately conformed to the Cahn–Hilliard linearised theory. The major effect of liquid crystal (LC) was to increase the molecular mobility of the blends. The LC generally increased the Cahn–Hilliard apparent diffusion coefficient,  $D_{app}$ , of the blend when added with concentrations as low as 0.2 wt%. GMS and zinc stearate can also improve the mobility of the blend but to a lesser extent and the effect does not

increase at higher concentration. On the other hand, the more LC added, the higher the mobility.



สถาบันวิทยบริการ  
จุฬาลงกรณ์มหาวิทยาลัย

## CHAPTER III

### THEORY

#### 3.1 Catalytic System

##### 3.1.1 Catalyst Compounds

Metallocene [43] are a class of compounds in which cyclopentadienyl or substituted cyclopentadienyl ligands are  $\pi$ -bonded to the metal atom. Examples of metallocene compounds are shown in Figure 3.1.



**Figure 3.1** Metallocene Compounds [44]

These compounds are becoming an important class of catalyst for the synthesis of organic molecules and polymers. These compounds also have good potential to act as catalysts or catalyst precursors for a number of organic reactions. The discovery of Group 4 metallocene-aluminoxane systems as catalyst for polymerization reactions has opened up a new frontier in the area of organometallic chemistry and polymer synthesis.

A metallocene catalyst system comprises a metallocene and a cocatalyst, which could be MAO or a borate or borane. The polymerization of monoolefins by metallocenes in comparison to conventional Ziegler-Natta systems offers a versatile possibility to polymer synthesis. The broader flexibility of electronic and steric

variations in the cyclopentadienyl (Cp) type ligands allows the design of catalyst system. Such modifications govern the polyinsertion reaction leading to regio- and stereoregular polyolefins.

Metallocene having a single Cp group include bridged and unbridged compounds. Two Cp groups are not required to generate chiral complexes. Monocyclopentadienyl titanium derivatives combined with MAO, afford very efficient catalysts which promote polymerization of styrene to highly syndiotactic polymers. The structures of half-metallocene compounds are shown in Figure 3.2

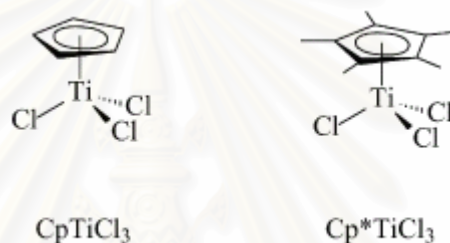


**Figure 3.2** Half-metallocene compounds [45]

### 3.1.2 Aluminoxane

Aluminoxanes are synthesized by controlled hydrolysis of aluminium alkyls [46,47]. Simple synthetic routes to methylaluminoxane are not available due to the high reactivity of trimethylaluminum (TMA) with water. Many inorganic hydrated compounds are used as a source of water for preparing aluminoxane from alkyl aluminum [48]. Hydrating compounds such as  $\text{CuSO}_4 \cdot 5\text{H}_2\text{O}$  and  $\text{Al}_2(\text{SO}_4)_3 \cdot 6\text{H}_2\text{O}$  are employed.

Various physicochemical data, such as compositional analysis, molecular weight determination, mass spectral technique, X-ray powder diffraction, infrared, and NMR spectroscopies, are used for the characterization of aluminoxanes [49]. In spite of these measurements, the structures of the alkyl aluminoxane are not unambiguously known. Methylaluminoxane (MAO) is considered to be the oligomeric (cyclic or linear) mixture of  $-\text{AlMeO}-$  units containing possibly cluster



like or supramolecular aggregates. In metallocene-based catalytic systems, MAO appears to have a combination of the following functions:

1. Aluminoxane alkylates the metallocene compound and scavenges the impurity.
2. Aluminoxane interacts with metallocene to generate cationic metallocene alkyl species.

The aluminoxane not only produces the cations but also stabilizes them. Thus, MAO must be a non-coordinating counteranion in order not to compete with an olefin monomer for coordinating to the active transition metal cation and also be chemically stable in order not to react with the very active metallocene catalyst.

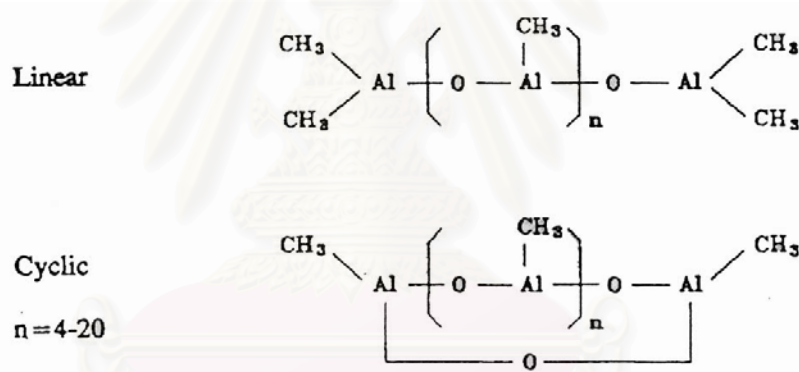


**Figure 3.3** Plausible structure of methylaluminoxane [50]

### 3.2 Syndiotactic Polystyrene

Syndiotactic polystyrene (SPS) is a semicrystalline polymer synthesized from styrene monomer using a single-site catalyst, such as metallocene. First synthesized in 1985 by Idemitsu Kosan Co. Ltd. (Tokyo, Japan), the material has been under joint product and process development by Idemitsu and Dow Plastics (Midland, MI) since 1988. Because of its semicrystalline nature, SPS products exhibit performance attributes that are significantly different from those of amorphous styrenic materials.

These properties include a high melting point, good chemical and moisture resistance, and a high degree of dimensional stability.

SPS can be differentiated from conventional styrenic polymers on the basis of molecular structure. Atactic, or general-purpose, polystyrene is produced with random stereochemistry, resulting in nonspecific placement of the cyclic aromatic portion of the molecule. In contrast, isotactic and syndiotactic polystyrene are made using stereo-specific catalysis techniques that result in highly ordered molecular structures.

Some typical and mechanical properties of SPS are reported below; some reported values, e.g. the melting temperature, can slightly for polymers synthesized with different catalysts, owing to the different content of steric effects [51].

Density	1050 kg/m <sup>3</sup>
Glass transition temperature (T <sub>g</sub> )	~100°C [7]
Melting temperature (T <sub>m</sub> )	270°C [3]
Izod impact strength (notched)	2 kJ/m <sup>2</sup> (ASTM D 256-A)
Tensile strength	41 Mpa (ASTM D 638)
Tensile modulus	3.4 GPA (ASTM D 638)
Elongation at break	1% (ASTM D 638)
Flexural modulus	3 GPa (ASTM D 790-1)
Flexural strength	75 GPa (ASTM D 790-1)
Dielectric constant, 23°C, 1 MHz	2.6 (IEC 250)

Whereas atactic polystyrene is as amorphous polymer with a T<sub>g</sub> of 100°C, syndiotactic polystyrene is semicrystalline with a T<sub>g</sub> similar to atactic polystyrene and a T<sub>m</sub> in the range 255-275°C. The crystallization rate of syndiotactic polystyrene is comparable to that of poly(ethylene terephthalate). SPS exhibits a polymorphic crystalline behavior which is relevant for blend properties.



### 3.3 Polymer Tacticity of Polystyrene

Stereoregularity arises because of order in the spatial structure of polymer chains. If the backbone of a polymer chain is drawn in a flat zigzag form in the plane of the paper, the patterns can be shown in Figure 3.4 and can be easily envisaged in the case of monosubstituted vinyl units. It should be noted that in (a) all the substituent R groups lie uniformly on the same side of the zigzag plane. Natta called this structure isotactic. In (b) the substituent R groups occupy positions alternatively above and below the backbone plane. Such a structure is termed syndiotactic. In (c) there is no regular arrangement of the substituent R groups and this structure is called atactic.

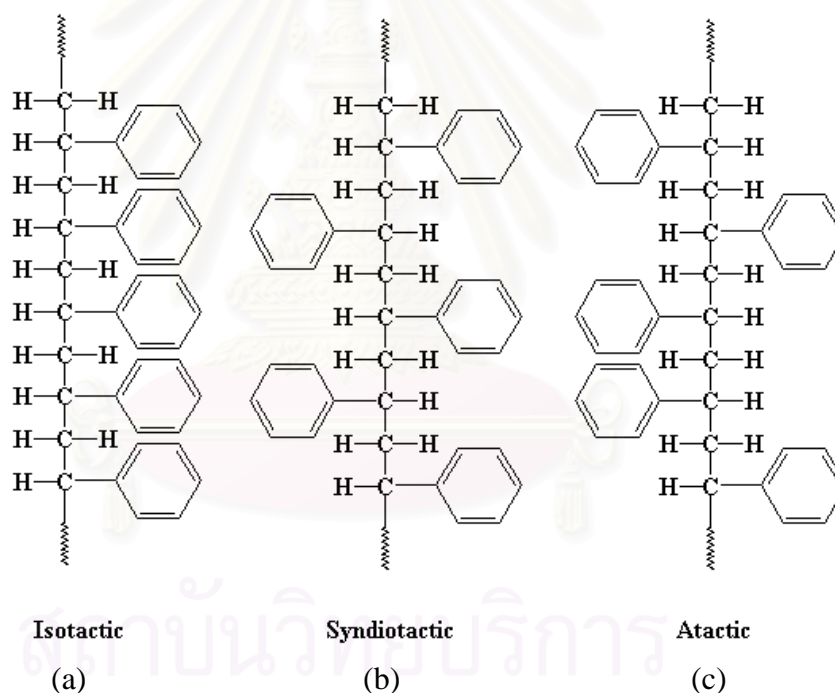


**Figure 3.4** Types of olefin polymer tacticity [43]

The regularity or lack of regularity in polymers affects their properties by way of large differences in their abilities to crystallize. Atactic polymers are amorphous (noncrystalline), soft (tacky) material with little or no physical strength. The corresponding isotactic and syndiotactic polymers are usually obtained as highly crystalline materials. The ordered structures are capable of packing into a crystal

lattice, while the unordered structures are not. Crystallinity leads to high physical strength and increased solvent and chemical resistance as well as differences in other properties that depend on crystallinity.

### **3.4 Polymer Morphology**

Generally, there are two morphologies of polymers, amorphous and crystalline. The former is a physical state characterized by almost complete lack of order among the molecules. The crystalline refers to the situation where polymer molecules are oriented or aligned. Because polymers for all practical purposes never achieve 100 % crystallinity, it is more practical to categorize their morphologies as amorphous and semicrystalline.

#### **3.4.1 The Amorphous State**

Some polymers do not crystallize at all. Therefore they remain in an amorphous state throughout the solidification. The amorphous state is characteristic of those polymers in the solid state that, for reasons of structure, exhibit no tendency toward crystallinity. In the amorphous state, the polymer resembles as a glass. We can imagine the amorphous state of polymers like a bowl of cooked spaghetti. The major difference between the solid and liquid amorphous states is that with the former, molecular motion is restricted to very short-range vibrations and rotations, whereas in the molten state there is considerable segmental motion or conformational freedom arising from rotation about chemical bonds. The molten state has been likened on a molecular scale to a can of worms, all intertwined and wriggling about, except that the average worm would be extremely long relative to its cross-sectional area. When an amorphous polymer achieves a certain degree of rotational freedom, it can be deformed. If there is sufficient freedom, the polymer flows then the molecules begin to move past one another. At low temperatures amorphous polymers are glassy, hard and brittle. As the temperature is raised, they go through the glass-rubber transition characterized by the glass transition temperature ( $T_g$ ).

### 3.4.2 Glass Transition Temperature

One of the most important characteristics of the amorphous state is the behavior of a polymer during its transition from solid to liquid. If an amorphous glass is heated, the kinetic energy of the molecules increases. Motion is still restricted, however, to short-range vibrations and rotations so long as the polymer retains its glasslike structure. As temperature is increased further, there comes  $x_0$  a point where a decided change takes place, the polymer loses its glasslike properties and assumes those more commonly identified with a rubber. The temperature at which this takes place is called the glass transition temperature. If heating is continued, the polymer will eventually lose its elastomeric properties and melt to a flowable liquid. The glass transition temperature is defined as the temperature at which the polymer softens because of the onset of long-range coordinated molecular motion. The amorphous parts of semicrystalline polymers also experience glass transition at a certain  $T_g$ .

The importance of the glass transition temperature cannot be overemphasized. It is one of the fundamental characteristics as it relates to polymer properties and processing. The transition is accompanied by more long-range molecular motion, greater rotational freedom and consequently more segmental motion of the chains. It is estimated that between 20 and 50 chain atoms are involved in this segmental movement at the  $T_g$ . Clearly for this increased motion to take place, the space between the atoms (the free volume) must increase, which gives rise to an increase in the specific volume. The temperature at which this change in specific volume takes place, usually observed by dilatometry (volume measurement), may be used as a measure of  $T_g$ . Other changes of a macroscopic nature occur at the glass transition. There is an enthalpy change, which may be measured by calorimetry. The modulus or stiffness, decreases appreciably, the decrease readily detected by mechanical measurements. Refractive index and thermal conductivity change.

### 3.4.3 The Crystalline Polymer

Polymers crystallized in the bulk state are never totally crystalline, a consequence of their long chain nature and subsequent entanglements. The melting temperature ( $T_m$ ) of the polymer, is always higher than the glass transition temperature,  $T_g$ . Thus the polymer may be either hard and rigid or flexible. For example, ordinary polyethylene that has a  $T_g$  of about  $-80\text{ }^\circ\text{C}$  and a melting temperature of about  $139\text{ }^\circ\text{C}$ . At room temperature it forms a leathery product as a result. Factors that control the  $T_m$  include polarity, hydrogen bonding and packing capability.

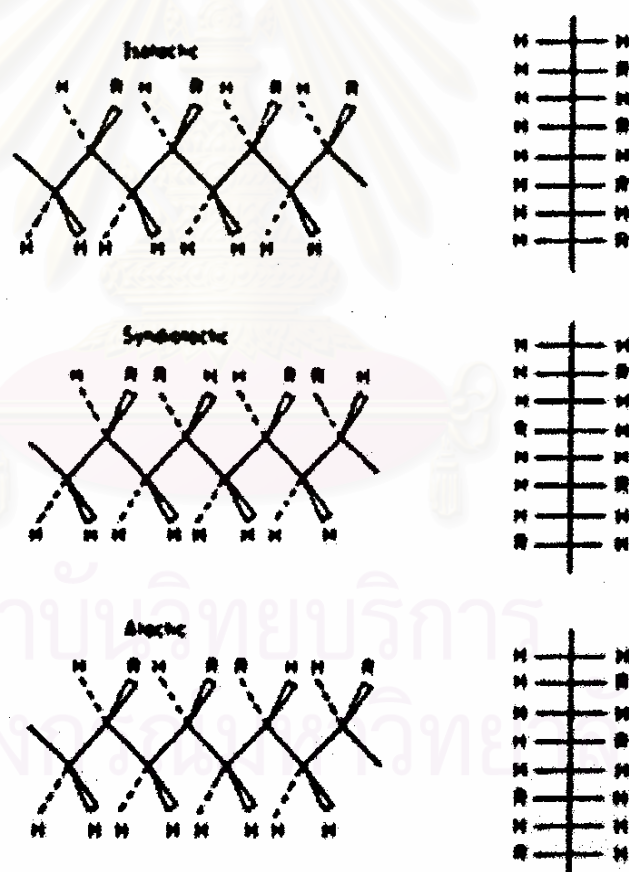


**Figure 3.5** Three different configurations of a mono-substituted polyethylene [52]

The development of crystallinity in polymers depends on the regularity of structure in the polymer, the tacticity of the polymer. The different possible spatial arrangements are called the tacticity of the polymer. If the R groups on successive pseudochiral carbons all have the same configuration, the polymer is called isotactic. When the pseudochiral centers alternate in configuration from one repeating unit to the next, the polymer is called syndiotactic. If the pseudochiral centers do not have any particular order, but in fact are statistical arrangements, the polymer is said to be atactic.

Thus isotactic and syndiotactic structures are both crystallizable, because of their regularity along the chain but their unit cells and melting temperatures are not the same. On the other hand, atactic polymers are usually completely amorphous unless the side group is so small or so polar as to permit some crystallinity.

Nonregularity of structure first decreases the melting temperature and finally prevents crystallinity. Mers of incorrect tacticity tend to destroy crystallinity. Thus statistical copolymers are generally amorphous. Blends of isotactic and atactic polymers show reduced crystallinity, with only the isotactic portion crystallizing. Furthermore, the long chain nature and the subsequent entanglements prevent total crystallization.

Crystalline polymers constitute many of the plastics and fibers of commerce. Polyethylene is used in films to cover dry-cleaned clothes and as water and solvent containers. Polypropylene makes a highly extensible rope, finding particularly important applications in the marine industry. Polyamides and polyesters are used as both plastics and fibers. Their use in clothing is world famous, cellulose, mentioned above, is used in clothing in both its native state and its regenerated state.

### **3.5 Melting Phenomena**

The melting of polymers may be observed by any of several experiments. For linear or branched polymer, the melting causes the samples to become liquid and flows. First of all, simple liquid behavior may not be immediately apparent because of

the polymer has high viscosity. If the polymer is cross-linked, it may not flow at all. It must also be noted that amorphous polymers soften at their glass transition temperature, which is emphatically not a melting temperature. If the sample does not contain colorants, it is usually hazy in the crystalline state because of the difference in refractive index between the amorphous and crystalline portions. On melting, the sample becomes clear or more transparent.

Ideally, the melting temperature, should give a discontinuity in the volume, with a concomitant sharp melting point. In fact, because of the very small size of the crystallites in bulk crystallized polymers, most polymers melt over a range of several degrees. The melting temperature is usually taken as the temperature at which the last trace of crystallinity disappears. This is the temperature at which the largest and/or most perfect crystals are melting.

### **3.6 Thermal Properties**

The existence of a polymeric system as a rigid glassy liquid, a mobile liquid, a microcrystalline solid or a liquid crystalline mesophase depends on the temperature and the chemical structure of the polymer. Changes from a microcrystalline state to a liquid crystalline or isotropic liquid state take place at the equilibrium melting temperature.

$T_m$  and  $T_g$  of crystallizable polymers vary widely with a change in the chemical structure. The presence of amide and aromatic groups in the chain raise  $T_m$  and  $T_g$ . The morphology of a thermoplastic crystallizable homopolymer at a particular usage temperature depends on  $T_m$ , which is in turn dependent on the intermolecular forces. If the usage temperature is greater than  $T_m$  for a crystallizable polymer, only a rubbery liquid morphology will be realized. At temperatures below  $T_m$  but above  $T_g$  such a material will be partially crystalline, when crystallized quiescently, with rubbery interlayers. Below  $T_g$ , the interlayers between crystalline will be glassy.



In various kind of the polymers, the melting points refer to the melting of crystal form with the highest  $T_m$ . Changes from one form to another at easily attained temperatures and pressures can be reversible or involve melting of one form and crystallization of the other.

Some polymers with few chain irregularities, although intrinsically crystallizable, can be easily super cooled, without appreciable crystallizable, into a glassy amorphous state upon rapid cooling from the melt to a temperature below  $T_g$ . Polymers showing this type of behavior usually contain rings in the main of side chains. Examples are poly (ethylene terephthalate) and various polymers that form liquid crystalline mesophases. These supercooled materials can be crystallized by heating to a temperature where the polymer is below  $T_m$  but above  $T_g$ . Sufficient time for the various portions of the chains to adopt the conformation necessary for crystallization is then supplied.

### 3.7 Structure of Crystalline Polymers

Very early studies on bulk materials showed that some polymers were partly crystalline. X-ray line broadening indicated that the crystals were either very imperfect or very small. Because of the known high molecular weight, the polymer chain was calculated to be even longer than the crystallites. Hence it was reasoned that they passed in and out of many crystallites and many unit cells. These findings led to the fringed micelle model.

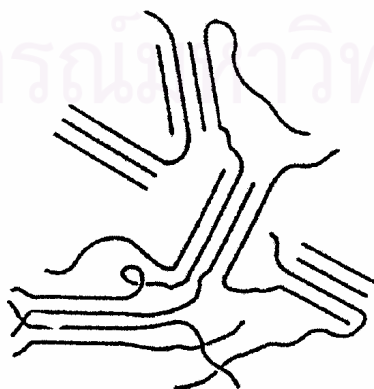


**Figure 3.6** The fringed micelle model [52]

According to the fringed micelle model, the crystallites are about  $100 \text{ \AA}$  long. The disordered regions separating the crystallites are amorphous. The chains wander from the amorphous region through a crystallite and back into the amorphous region. The chains are long enough to pass through several crystallites, binding them together.

The fringed micelle model was used with great success to explain a wide range of behaviour in semicrystalline plastics and also in fibers. The amorphous regions, if glassy, yielded a stiff plastic. However, if they were above  $T_g$ , then they were rubbery and were held together by the hard crystallites. This model explains the leathery behaviour of ordinary polyethylene plastics. The greater tensile strength of polyethylene over that of low molecular weight hydrocarbon waxes was attributed to amorphous chains wandering from crystallite to crystallite, holding them together by primary bonds. However, the exact stiffness of the plastic was related to the degree of crystallinity or fraction of the polymer that was crystallized.

### **3.8 Crystal Structure in Polymers**

#### **3.8.1 Crystallization from Dilute Solution**

##### **3.8.1.1 Polymer Single Crystals**

Although the formation of single crystals of polymers was observed during polymerization many years ago, such crystals could not be produced from polymer solution because of molecular entanglement. In several laboratories, the phenomenon of growth has been reported for so many polymers, including polyethylene, polypropylene and other poly( $\alpha$ -olefins), that it appears to be quite general and universal.

All the structures described as polymer single crystals have the same general appearance, being composed of thin, flat platelets (lamellae) about  $100 \text{ \AA}$  thick and often many micrometers in lateral dimensions. They are usually thickened by the

spiral growth of additional lamellae from screw dislocations. A typical lamellae crystal is shown in Figure 3.7



**Figure 3.7** Electron micrograph of a single crystal of nylon-6 grown by precipitation from dilute glycerine solution [52]

The size, shape and regularity of the crystals depend on their growth conditions, such as solvent, temperature and growth rate being important. The thickness of the lamellae depends on crystallization temperature ( $T_c$ ) and any subsequent annealing treatment. Electron-diffraction measurements indicated that the polymer chains are oriented very nearly normal to the plane of the lamellae. Since the molecules in the polymers are at least  $1000 \text{ \AA}$  long and the lamellae are only about  $100 \text{ \AA}$  thick, the only reasonable description is that the chains are folded, for example, the molecules of polyethylene can fold in such a way that only about five chain carbon atoms are involved in the fold itself.

Many single crystals of essentially linear polyethylene show secondary structural features, including corrugations as shown in Figure 3.8 and pleats as shown in Figure 3.9.



**Figure 3.8** Optical micrograph showing corrugations in single crystal of linear polyethylene grown from a solution in perchloroethylene [52]



**Figure 3.9** Electron micrograph showing pleats in a crystal of linear polyethylene grown from a solution in perchloroethylene [52]

Both these features result from the fact that many crystals of polyethylene grow in the form of hollow pyramids. When solvent is removed during the preparation of the crystals for microscopy, surface-tension forces cause the pyramids to collapse.



### 3.8.1.2 The Folded Chain Model

This led to the folded chain model, shown in Figure 3.10

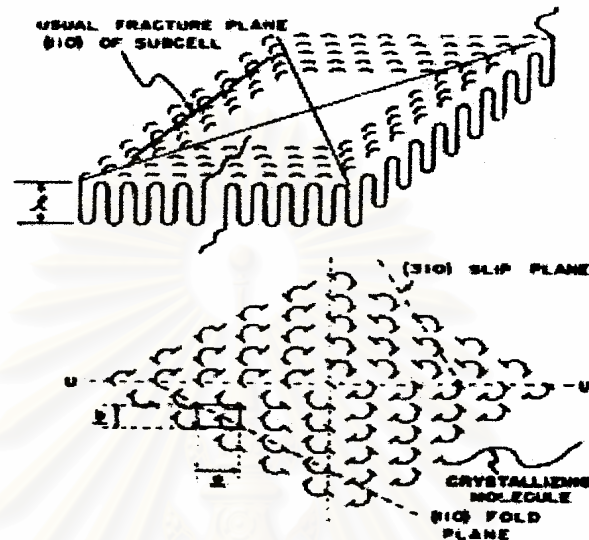


**Figure 3.10** Schematic view of a polyethylene single crystal exhibiting adjacent reentry [52]

Ideally, the molecules fold back and forth with hairpin turns building a lamellar structure by regular folding. The chain folding is perpendicular to the plane of the lamellar. While adjacent reentry has been generally confirmed by small-angle neutron scattering and infrared studies for single crystals. For many polymers, the single crystals are not simple flat structures. The crystals often occur in the form of hollow pyramids, which collapse on drying. If the polymer solution is slightly more concentrated, or if the crystallization rate is increased, the polymers will crystallize in the form of various twins, spirals and dendritic structures, which are multilayered.

### 3.8.1.3 The Switchboard Model

In the switchboard model, the chains do not have a reentry into the lamellae by regular folding, but rather reentry more or less randomly. Both the perfectly folded chain and switchboard models represent limiting cases. Real system may combine elements of both.

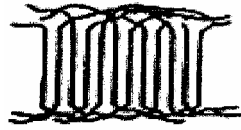


**Figure 3.11** Switchboard Model [52]

## **3.8.2 Crystallization from the Melt**

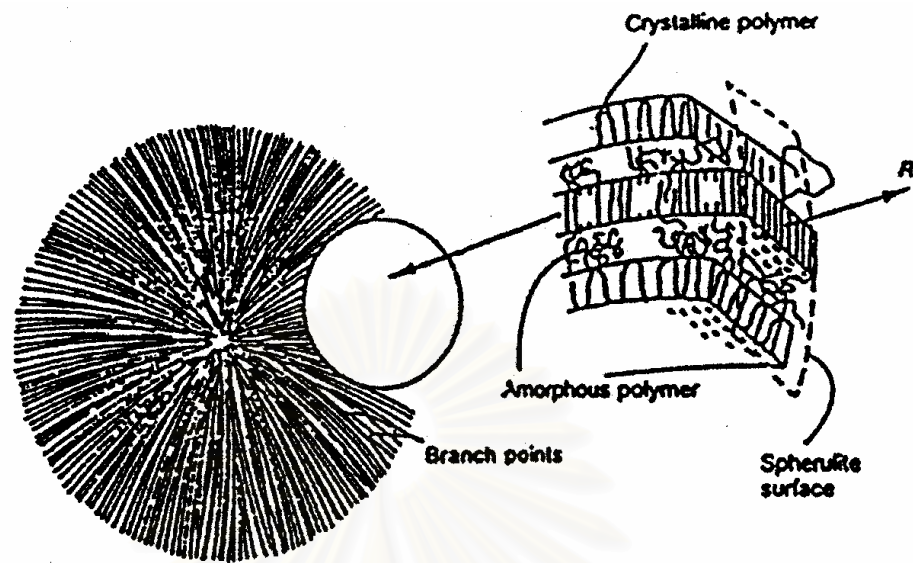
### **3.8.2.1 Spherulitic Morphology**

When polymer samples are crystallized from the bulk of an unstained melt, the most obvious of the observed structures are the spherulites. Spherulites are sphere-shaped crystalline structures that form in the bulk. Usually the spherulites are really spherical in shape only during the initial stages of crystallization. During the latter stages of crystallization, the spherulites impinge on their neighbors. When the spherulites are nucleated simultaneously, the boundaries between them are straight. However, when the spherulites have been nucleated at different times, they are different in size when impinging on one another, and their boundaries form hyperbolas. Finally, the spherulites form structures that pervade the entire mass of the material.

Electron microscopy examination of the spherulitic structure shows that the spherulites are composed of individual lamellar crystalline plates. The lamellar structures sometimes resemble staircases, being composed of nearly parallel lamellae of equal thickness.

These patterns arise from the spherulitic structure of the polymer, which is optically anisotropic, with the radial and tangential refractive indices being different. A model of the spherulite structure is illustrated in Figure 3.12





The chain direction in the bulk crystallized lamellae is perpendicular to the broad plane of the structure, just like the dilute solution crystallized material. The spherulite lamellae also contain low-angle branch points, where new lamellar structures are initiated. The new lamellae tend to keep the spacing between the crystallites constant. While the lamellar structures in the spherulites are the analogue of the single crystals. In between the lamellar structures lies amorphous material. This portion is rich in components such as atactic polymers, low molecular weight material or impurities of various kinds.

The individual lamellae in the spherulites are bonded together by tie molecules, which lie partly in one crystallite and partly in another. Sometimes these tie molecules are actually in the form of what are called intercrystalline links, which are long, threadlike crystalline structures. These intercrystalline links are thought to be important in the development of the great toughness characteristic of semicrystalline polymers. They serve to tie the entire structure together by crystalline regions and/or primary chain bonds.

### 3.8.2.2 Mechanism of Spherulite Formation

On cooling from the melt, the first structure that forms is the single crystal. These rapidly degenerate into sheaf like structures during the early stages of the growth of polymer spherulites. These sheaf like structures have been variously called axialites or hedrites. These transitional, multilayered structures represent an intermediate stage in the formation of spherulites.

### 3.8.2.3 Spherulites in Polymer Blends

There are two cases to be considered. Either the two polymers composing the blend may be miscible and form one phase in the melt or they are immiscible and form two phase. If the glass transition of the non-crystallizing component is lower than that of the crystallizing component (i.e., its melt viscosity will be lower, other things being equal), then the spherulites will actually grow faster, although the system is diluted. The crystallization behavior is quite different if the two polymers are immiscible in the melt. On spherulite formation, the droplets, which are non-crystallizing, become ordered within the growing arms of the crystallizing component.

### 3.8.2.4 Effect of Crystallinity on Glass Transition Temperature

Semicrystalline polymers such as polyethylene or polypropylene types also exhibit glass transitions, though only in the amorphous portions of these polymers. The  $T_g$  is often increased in temperature by the molecular-motion restricting crystallites. Sometimes  $T_g$  appears to be masked, especially for high crystalline polymers.

Many semicrystalline polymers appear to possess two glass temperatures (1) a lower one,  $T_g$  (L), which refers to the completely amorphous state and which should be used in all correlations with chemical structure and (2) an upper value,  $T_g$  (U), which occurs in the semicrystalline material and varies with extent of crystallinity and morphology.

## 3.9 Liquid Crystal

### 3.9.1 The History of Liquid Crystal [53]

The discovery of liquid crystals has been approximately occurred 150 years ago, although its significance was not fully realized until over a hundred years later. Around the middle of the last century, Virchow, Mettenheimer and Valentin found from their research that the nerve fiber formed a fluid substance when left in water that exhibited a strange behavior when it was viewed by polarized light. They did not realize this as a different phase, but they are attributed with the first observation of liquid crystal. Later, in 1877, Otto Lehmann used a polarizing microscope with hot stage to investigate the phase transitions of various substances. He found that one substance would change from a clear liquid to a cloudy liquid before crystallizing but thought that this was simply an imperfect phase transition from liquid to crystalline. In 1888 Reinitzer conducted similar experiments and was the first to suggest that cloudy fluid was a new phase of matter. He has consequently been given the credit for the discovery of the liquid crystalline phase. Up till 1890 all the investigated liquid crystalline substances had been naturally occurred and it was the first synthetic liquid crystal, pazoxyanisole, was produced by Gatterman and Ritschke. Subsequently, more liquid crystals were synthesized and it is now possible to produce liquid crystals with specific predetermined material properties.

In the beginning of this century George Freidel conducted many experiments on liquid crystals and firstly explained the orienting effect when applied electric fields in the presence of defects in liquid crystals. In 1922, he proposed a classification of liquid crystals based upon the different molecular orderings of each substance. It was between 1922 and the World War II that Oseen and Zocher developed a mathematical basis for the study of liquid crystals. After the war started, many scientists believed that the important features of liquid crystals had completely been discovered and it was not until the 1950's that work by Brown in America, Chistiakoff in the Soviet Union and Gray and Frank in England led to a revival of interest in liquid crystals. Maier and Saupe formulated a microscopic theory of liquid crystals, Frank and later Leslie and Ericksen developed continuum theories for static and dynamic systems and

in 1968 scientists from Radio Corporation of America first demonstrated a liquid crystal display. The interest in liquid crystals has grown ever since.

### 3.9.2 Introduction to Liquid Crystal [54]

Polymer liquid crystals (PLCs) are a class of materials that combine the properties of polymers with those of liquid crystals. These hybrids show the same mesophases characteristic of ordinary liquid crystals, while still retained the useful and versatile properties of polymers.

Difference from normally flexible polymers, characteristics of the display liquid crystals have rod-like or disk-like elements called mesogens incorporated into their chains. The placement of the mesogens plays a large role in determining the type of PLC that is formed. Main-chain polymer liquid crystals or MC-PLCs are formed when the mesogens are themselves part of the main chain of a polymer. Conversely, side chain polymer liquid crystals or SC-PLCs are formed when the mesogens are connected as side chains to the polymer by a flexible bridge called the spacer.

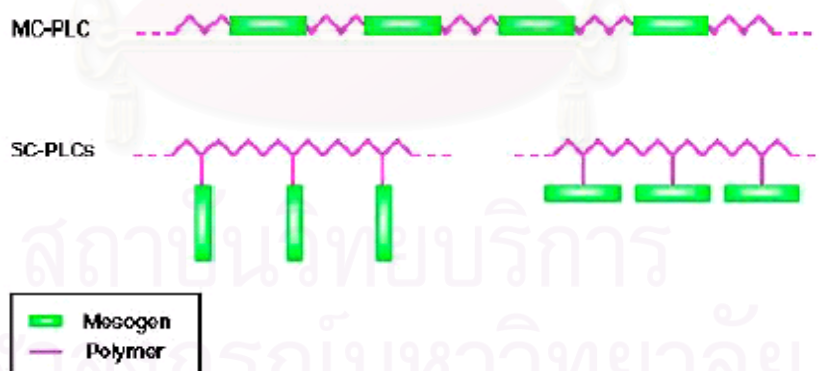


**Figure 3.13** The structure of MC-PLCs and SC-PLCs. [54]

### 3.9.3 Main-Chain Polymer Liquid Crystals

Main chain polymer liquid crystals are formed when rigid elements are incorporated into the backbone of normally flexible polymers, these interact usually occur through a condensation reaction. These stiff regions along the chain allow the polymer to orient in a manner similar to ordinary liquid crystals, and thus display liquid crystal characteristics. There are two distinct groups of MC-PLCs, differentiated by the manner in which the stiff regions are formed. The first group of main chain polymer liquid crystals is characterized by stiff, rod-like monomers. These monomers are typically made up of several aromatic rings, which provide the necessary size. The following figure shows an example of this kind of MC-PLC.

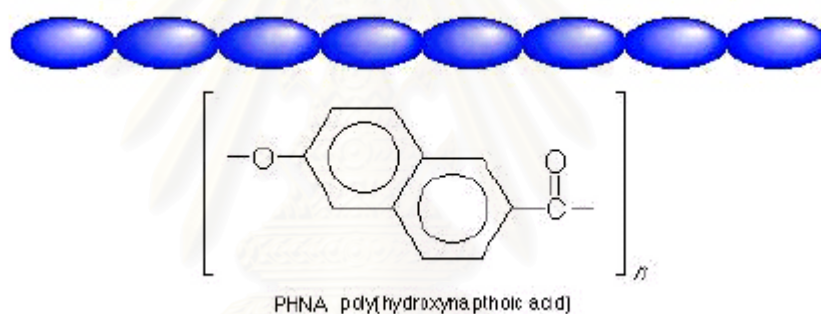


**Figure 3.14** The structure of MC-PLC. [54]

The second and more prevalent group of main chain polymer liquid crystals is different because it incorporates a mesogen directly into the chain. The mesogen acts just like the stiff areas in the first group. Generally, the mesogenic units are made up of two or more aromatic rings which provide the necessary restriction on movement that allow the polymer to display liquid crystal properties. The stiffness is necessary for liquid crystallinity results from restrictions on rotation caused by steric hindrance and resonance this gives the polymer its stiffness. Otherwise, the molecules are not rod-like enough to display the characteristics of liquid crystals. This group is different from the first in that the mesogens are separated or "decoupled" by a flexible bridge called a spacer. Decoupling of the mesogens provides for independent movement of the molecules which facilitates proper alignment. The following is a figure of this



type of main chain polymer liquid crystal. Notice the flexible spacer (methylene groups) and the stiff mesogen (aromatic ring and double bonds).

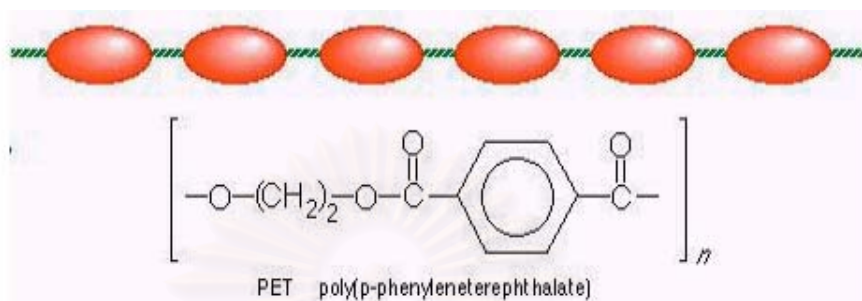


**Figure 3.15** The structure of MC-PLC. [54]

It is difficult to create polymer liquid crystals that show mesogenic behavior over temperature ranges which are convenient to work with. In fact, many times the temperature of the liquid crystalline behavior is actually above the point where the polymer begins to decompose. This problem can be avoided in one or more of the following ways. The first method of lowering polymer melting temperatures involves the arrangement of the monomers in the chain. If the molecules are put together in random orientation (head-to-tail, head-to-head, etc.), interactions between successive chains are minimized. This allows for a lower melting temperature.



**Figure 3.16** The random orientation of monomers in the polymer chain. [54]

Another method to bring the temperature down to a useful range involves copolymerization. If a random copolymer can be created, the regularity of the chains is greatly reduced. This will help to minimize the interactions between the chains by breaking up the symmetry, which in turn will lower polymer melting temperature. The following figure shows how the irregularity of polymer substitute can lead to decreased interactions.



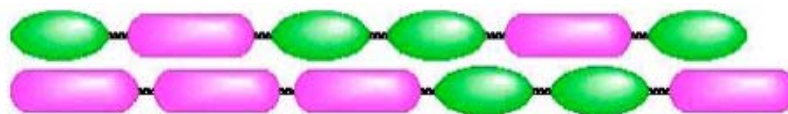


**Figure 3.17** The irregularity of polymer substitute in polymer chain. [54]

Finally, defects can be introduced into the chain structure which lower the polymer melting temperature. This method creates 120-degree "kinks" in the chain which disrupt the ability for neighboring polymers to line up. Unfortunately, this also decreases the effective persistence length so too many kinks can destroy any liquid crystal behavior.



**Figure 3.18** 120- degree kinks in the polymer chain. [54]

#### 3.9.4 Side Chain Polymer Liquid Crystals

It has been demonstrated that main chain polymer liquid crystals often cannot show mesogenic behavior over a wide temperature range. Side chain polymer liquid crystals are able to expand this scale. These materials are formed when mesogenic units are attached to the polymer as side chains which interact through a addition reaction.

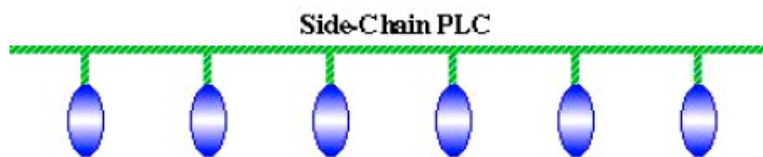


**Figure 3.19** The structure of SC-PLCs. [54]

Side chain polymer liquid crystals have three major structural components: the backbone, the spacer, and the mesogen. The versatility of SC-PLCs arises because these structures can be varied in a number of ways.

The backbone of a side chain polymer liquid crystal is the element that the side chains are attached to. The structure of the backbone can be very important in determining if the polymer shows liquid crystal behavior. Polymers with rigid backbones typically have high glass transition temperatures, and thus liquid crystal behavior is often difficult to observe. In order to lower this temperature, the polymer backbone can be made more flexible.

Perhaps the most important part of a side chain polymer liquid crystal is the mesogen. It is the alignment of these groups that causes the liquid crystal behavior. Usually, the mesogen is made up of a rigid core of two or more aromatic rings joined together by a functional group. The following figure is a typical repeating unit in a side chain polymer liquid crystal. Notice the spacer of methylene units and the mesogen of aromatic rings.

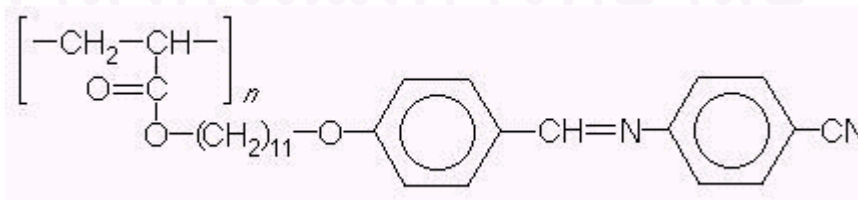


**Figure 3.20** The spacer of methylene units and the mesogen of aromatic rings. [54]

Like their main chain counterparts, mesogens attached as side groups on the backbone of side chain polymer liquid crystals are able to orient because the spacer allows for independent movement. Notice in the following figure that even though the polymer may be in a tangled conformation, orientation of the mesogen is still possible because of the decoupling action of the spacer.



**Figure 3.21** The tangle conformation and orientation of the mesogens. [54]

The structure of the spacer is an important determining factor in side chain polymer liquid crystals. Generally, the spacer consists of two to four methylene ( $\text{CH}_2$ ) groups attached together in a line. Accordingly, the spacer length has a profound effect on the temperature and type of phase transitions. Usually, the glass transition temperature decreases with increasing spacer length. Short spacers lead to nematic phases, while longer spacers lead to smectic phases.

### 3.9.5 Type of Liquid Crystal [55]

Liquid crystals can be classified into two main categories:

1. Thermotropic liquid crystals
2. Lyotropic liquid crystals

These two types of liquid crystals are distinguished by the mechanisms that drive their selforganization, but they are also similar in many ways.

Thermotropic liquid crystals are occurred in most liquid crystals, and they are defined by the fact that the transitions to the liquid crystalline state are induced

thermally. That is, one can arrive at the liquid crystalline state by raising the temperature of a solid and/or lowering the temperature of a liquid. Thermotropic liquid crystals can be classified into two types:

1. Enantiotropic liquid crystals, which can be changed into the liquid crystal state from either lowering the temperature of a liquid or raising of the temperature of a solid.
2. Monotropic liquid crystals, which can only be changed into the liquid crystal state from either an increase in the temperature of a solid or a decrease in the temperature of a liquid, but not both.

In general, thermotropic mesophases occur because of anisotropic dispersion forces between the molecules and because of packing interactions.

Lyotropic liquid crystal transitions occur with the influence of solvents, not by a change in temperature. Lyotropic mesophases occur as a result of solvent-induced aggregation of the constituent mesogens into micellar structures. Lyotropic mesogens are typically amphiphilic, meaning that they are composed of both lyophilic (solvent-attracting) and lyophobic (solvent-repelling) parts. This causes them to form into micellar structures in the presence of a solvent, since the lyophobic ends will stay together as the lyophilic ends extend outward toward the solution. As the concentration of the solution is increased and the solution is cooled, the micelles increase in size and eventually coalesce. This separates the newly formed liquid crystalline state from the solvent.

### **3.9.6 Liquid Crystal Phases**

Friedel was able to distinguish clearly three different types of mesophase :

1. Smectic phase
2. Nematic phase
3. Cholesteric phase

Smectic phase begin from the word smectic that is derived from the Greek word “soap”, ironically the slippery substance found out the bottom of a soap dish is actually a type of smectic liquid crystal. The smectic phase is the most ordered state, where all the mesogens are arranged in a parallel and lateral order. Although this state is rare and is only observed for thermotropic polymers. In this phase the liquid crystal is turbid and the viscosity is rather high.



**Figure 3.22** The structure of smectic phase. [53]

Nematic phase, the molecules having no positional order but tend to point in the same direction characterize this phase. It is observed that the mesogens are arranged in parallel order but do not have lateral order. Also aromatic polyamides (aramid) form a nematic order when mixed in a heavy concentration of solution. In this phase the liquid crystal is turbid but the viscosity is decrease, the molecules can move because it is mobile state.

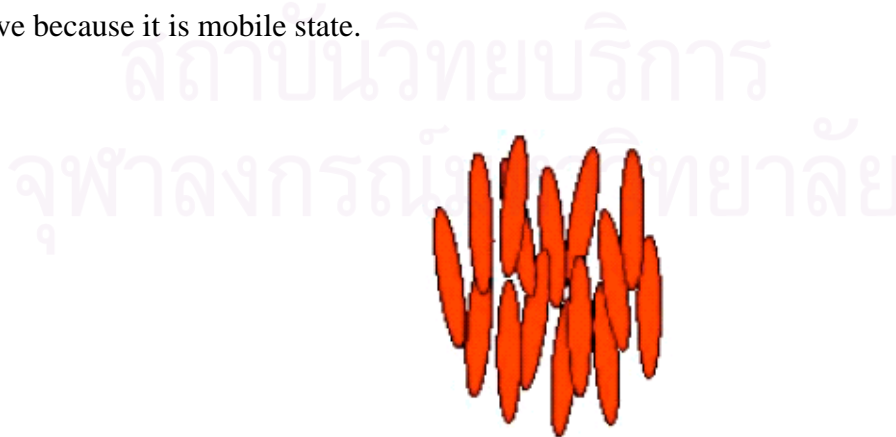


**Figure 3.23** The structure of nematic phase. [53]

Cholesteric phase occurs when the mesogens are arranged parallel to each other, but the directions vary from one layer to the next. In this phase the liquid crystal is turbid but the viscosity is decrease, the molecules can move because it is mobile state, exhibiting some unique optical characteristics, quite different form those of the smectic and nematic phases. The majority of compounds exhibiting this type of mesophase are derived from cholesterol or other sterol systems.



**Figure 3.24** The structure of cholesteric phase. [53]

### 3.9.7 Mesophasic Transition Temperature [56]

The various transitions that liquid crystal undergo as the temperature increases from the most ordered to the least ordered states, can be shown

Crystal → Smectic → Nematic → Isotropic

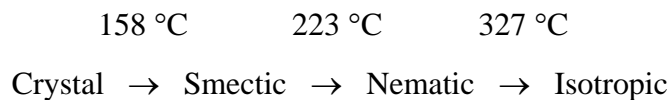
The temperature that a liquid crystal change from crystal to the smectic phase is called “crystalline melting temperature”.

The temperature that liquid crystal change from smectic phase to nematic phase is called “S-N transition temperature”.

The temperature that liquid crystal change from nematic phase to isotropic liquid is called “clearing temperature”.



The example of mesophasic transition temperature of low molecular weight liquid crystal used in this study (CBC-33) is shown below.



### 3.9.8 Applications of Liquid Crystals [54]

Liquid crystal technology has had a major effects in many areas of science and engineering, as well as device technology. Applications for this special kind of material are still being discovered and continued to provide effective solutions to many different problems.

1. Liquid crystal displays (LCD) is the most common application of liquid crystal technology. This field has grown into a multi-billion dollar industry, and many significant scientific and engineering discoveries have been made.
2. Liquid crystal thermometers demonstrated earlier, chiral nematic (cholesteric) liquid crystals reflect light with a wavelength equal to the pitch. Because the pitch is dependent upon temperature, the color reflected also is dependent upon temperature. Liquid crystals make it possible to accurately gauge temperature just by looking at the color of the thermometer. By mixing different compounds, a device for practically any temperature range can be built.
3. Optical imaging is an application of liquid crystals that is only now being explored, is optical imaging and recording. In this technology, a liquid crystal cell is placed between two layers of photoconductor. Light is applied to the photoconductor, which increases the material's conductivity. This causes an electric field to develop in the liquid crystal corresponding to the intensity of the light. The electric pattern can be transmitted by an electrode, which enables the image to be recorded. This technology is still

being developed and is one of the most promising areas of liquid crystal research.

4. High-strength fibers is an application of polymer liquid crystals that has been successfully developed for industry, is the area of high strength fibers. Kevlar, which is used to make such things as helmets and bullet-proof vests, is just one example of the use of polymer liquid crystals in applications calling for strong, light weight materials. Ordinary polymers have never been able to demonstrate the stiffness necessary to compete against traditional materials like steel. It has been observed that polymers with long straight chains are significantly stronger than their tangled counterparts. Main chain liquid crystal polymers are well-suited to ordering processes. For example, the polymer can be oriented in the desired liquid crystal phase and then quenched to create a highly ordered, strong solid. As these technologies continue to develop, an increasing variety of new materials with strong and light-weight properties will become available.
5. Other applications of liquid crystal have a multitude of other uses. They are used for nondestructive mechanical testing of materials under stress. This technique is also used for the visualization of RF (radio frequency) waves in wave guides. They are used in medical applications where, for example, transient pressure transmitted by a walking foot on the ground is measured. Low molar mass (LMM) liquid crystals have applications including erasable optical disks, full color "electronic slides" for computer-aided drawing (CAD), and light modulators for color electronic imaging.

### 3.9.9 Structural Considerations of Low Molecular Weight Liquid Crystal Systems [57]

#### 1. Aromatic Systems

Looking back to the period before the 1970s, the great majority of liquid crystal materials were aromatic in character and of general structure

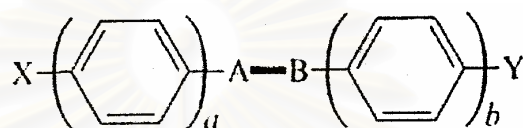


**Figure 3.25** The general structure of aromatic system. [57]

Where

1. X and Y represent a range of terminal substituents such as alkyl, alkoxy and cyano.
2. A-B represents a linking unit in the core structure, e.g., -CH=N-, -N=N-, N=NO-, -CO.O-
3. *a* and *b* have small integral values.

It was quickly realized that any substituent X or Y that does not broaden the molecule too much is superior to an H at the end of the molecule, and that groups such as cyano and alkoxy are more favorable than others such as alkyl or halogen in promoting high  $T_{N-I}$  values. At typical nematic terminal group efficiency order is  $CN > OCH_3 > NO_2 > Cl > Br > N(CH_3)_2 > CH_3 > H$ . The nature of the central linkage is also of great importance and linking units containing multiple bonds that maintain the rigidity and linearity of the molecules are most satisfactory in preserving high  $T_{N-I}$  values. Thus in simply systems in figure 3.25 with *a* and *b* = 1, the  $CH_2-CH_2$  flexible unit is a poor one and gives rise to vary weak or nonexistent nematic tendencies. The ester function contains no multiple bonds in the chain of atoms actually linking the rings, but conjugative interactions within the ester function and with the rings lead to some double bond character and a stiffer structure than might be expected. Esters are in fact fairly planar systems and quite strongly nematogenic. A typical central group

nematic efficiency order is  $trans\text{-CH=CH} > \text{N=NO} > \text{CH=NO} > \text{C=C} > \text{N=N} > \text{CO.O} > \text{none}$ .

## 2. Alicyclic Systems

The fairly low  $T_{\text{N-I}}$  values of the cyanobiphenyls gave little scope for structure modification by lateral substitution of the molecules, although this was possible in the case of the related terphenyl systems, used as high  $T_{\text{N-I}}$  additives.

The first major development of the biphenyl class of mesogen came therefore with the preparation of the cyclohexane analogs of structure in figure 3.26 where  $a$  may be 1 in the cyclohexane ring compounds.

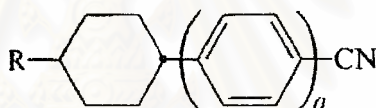


**Figure 3.26** The general structure of alicyclic system. [57]

However, the cyclohexane ring compounds also had higher  $T_{\text{N-I}}$  values than the biphenyl analogs, e.g.,  $\text{R}=\text{C}_5\text{H}_{11}$  have  $T_{\text{N-I}}$  values of biphenyl 35 °C but  $T_{\text{N-I}}$  values of cyclohexane ring 55 °C. This disadvantageous effect of the cyclohexane ring at high temperatures may be due to the flexibility of the ring and its ability to adopt skewed or twisted conformations that are higher in energy and less conducive to nematic order. With regard to polymers, the advantages or disadvantages of using cyclohexane ring would also depend on  $T_{\text{N-I}}$  values. However, there are other features of using cyclohexane rings that may be important. The viscosity of low molecular weight liquid crystal systems is lowered e.g., in cyanobiphenyl analogs that  $\text{R}=\text{C}_5\text{H}_{11}$  the viscosity at 20 °C in nematic phase 32 cP but in cyclohexane rings analogs have the viscosity at 20 °C in nematic phase 21 cP.

### 3. Cholesteric Systems

Since the cholesteric phase is a spontaneously twisted analog of the nematic phase, it is not surprising that molecular structural changes affect the transition temperatures of cholesteric and nematic phases in the same way. Consequently, the above generalizations about structure change in relation to  $T_{N-I}$  values apply to  $T_{Ch-I}$  values.

Only the pitch of the twist and its sense need therefore be considered additionally. Twist sense is very sensitive to structure change and for cholesterogens derived from sterols such as cholesterol. However, for commercially useful cholesterogens we do not usually want to have the presence of a bulky and often UV-sensitive steryl skeleton, and most of the important low molecular weight materials are simply chiral analogs of nematogens, the chirality being introduced by having a chiral center in a terminally situated alkyl or alkoxy group.

Turning therefore to twisting power, this decreases as the chiral center is moved away from the ring system, i.e., as  $n$  is increased in a structure such as figure 3.27. Practically speaking, the best value of  $n$  to use is 1. This achieves a good tightness of the pitch without involving the very great reduction in  $T_{N-I}$  values that arises with  $n=0$ .

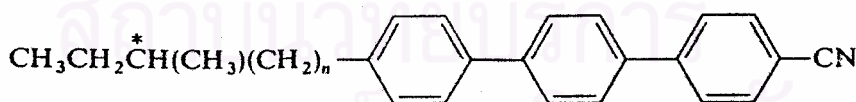


**Figure 3.27** The structure of cholesteric system. [57]

#### 4. Smectic Systems

In low molecular weight liquid crystal systems of commercial interest one usually wished to avoid smectic properties. This is not always the case, however, for latent smectic properties can be valuable for increasing the sensitivity of the color response of cholesteric phase to temperature.

Although correlated smectic phases can be envisaged for liquid crystal main chain polymers, these structures would be so akin to solids that it is doubtful, if like correlated low molecular weight smectics, these would be of commercial interest. With liquid crystal side chain polymers it is hard to envisage long range correlation of the smectic ordering of the side chain groups that would not be interfered with by the polymer backbone.

#### 5. Diskogens

Diskogens has centered recently around compounds consisting of flat, disk-shaped molecules that can pack together to form flexible columns. These columns then constitute a diskotic liquid crystal phase, quite distinct from smectic or nematic liquid crystal phases, and having a negative sign of the optic axis.

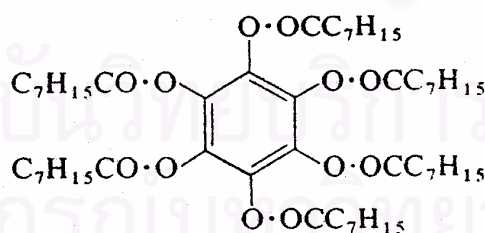


**Figure 3.28** The structure of diskogens system. [57]

The relevance of such diskotic phases to polymer systems, liquid crystal main chain, or liquid crystal side chain polymers is hard to judge. Presumably a fairly straight polymer backbone with a sufficient density of lateral functions radiating



outward could constitute a columnar structure, but whether this approximates closely enough to a stacking of individual disk-shaped molecules can not easily be judged.

### 3.10 Terminology in polymer blending

Blended polymers can show miscibility, partial miscibility or complete immiscibility. The first thermoplastic polyblends comprised polymers that were at least partially miscible, for example PVC/ABS and PPE/HIPS are miscible and in fact the most important blends comprise immiscible polymers, for example rubber toughened engineering plastics, where it is necessary for controlled phase separation to occur.

Total miscibility between polymers rarely occurs, partial miscibility and immiscibility are the usual cases. Several types of blended polymer systems was shown in Figure 3.29

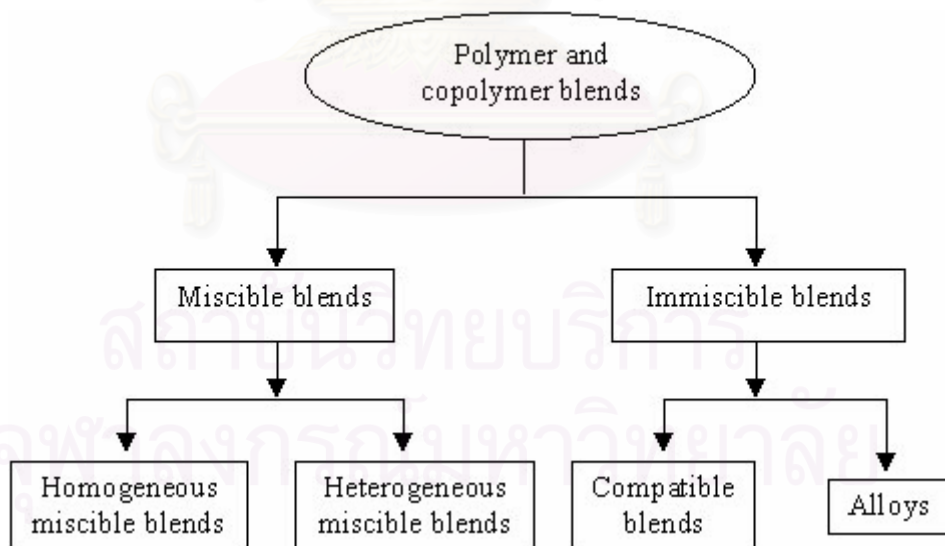


**Figure 3.29** Classification of blended polymers.

### **3.11. Polymer blend [58]**

Polymer blends are the mixtures of at least two or more polymers. The mixing of two or more existing polymers may obtain the new properties of the blend. By using these techniques the designed properties can be explored without synthesizing the new polymer which have the designed properties. The results of blending polymers have many advantages, for example, lower cost than synthesizing the desired properties of new polymer. The new properties can be under control.

#### **3.11.1 Melt Mixing**

Melt mixing of thermoplastics polymer is performed by mixing the polymers in the molten state under shear in various mixing equipment. This method is popular in preparation of polymer blends on the large commercial scale because of its simplicity, speed of mixing and the advantage of being free from foreign components (e.g. solvent) in the resulted blends. A number of devices are available for laboratory-scale mixing such as brabender mixer, electrically-heated two-roll mill, extruder, rotational rheometer.

The advantages of this method are the most similar to the industrial practice. The commercial compounding or adding additives into base polymers are applied by melt mixing. So the investigations of polymer blends by melt mixing method are the most practical methods in industrial applications.

#### **3.11.2 Solvent Casting**

This method group is performed by dissolving polymers in the same solvent. The solution is then cast on a glass plate into thin films and the removal of solvent from the films is performed by evaporating the solvent out at ambient or elevated temperature. Solvent casting is the simplest mixing method available and is widely practiced in academic studies, usually when the experiments need very small quantities of polymers.

The most severe problem with solvent casting is the influence of the solvent on the resulted product especially the shift of the phase diagram. In spite of the fact that the most of the solvent can be removed from a cast film, the nature of the film depends strongly on the types of solvents and casting condition.

To remove traces of solvents from the casting polymer films, the condition of high temperature is invariably needed, and protection of the polymer in case of degradation is essential. The inert gas or lower down the pressure (vacuum) typically used. In the vacuum conditions, the vapor pressure can be reduced and thus allows the solvents to evaporate more easily. However, too fast evaporation rate of solvent will result in the bubble in the final films produced.

### **3.11.3 Freeze Drying**

In the freeze drying processes, the solution of the two polymers is quenched down immediately to a very low temperature and the solution is frozen. Solvent is then removed from the frozen solution by sublimation at a very low temperature. Dilute solutions must be used and the solution volume must have as large surface area as possible for good heat transfer.

An advantage of this method is that the resulted blend will be independent of the solvent, if the single phase solution is freezed rapidly enough. However, there are many limitations of this method. Freeze drying method seems to work best with solvents having high symmetry, i.e. benzene, naphthalene, etc. The powdery from of the blend after solvent removal is usually not very useful and further shaping must be performed. While not complex, freeze drying does require a good vacuum system for low – boiling solvents and it is not a fast blending method. After solvent removal, the blend is in the powdery form, which usually needs further shaping. The advantage of this method is the simplicity. However, this method needs a good fume trap, vacuum line for the sublimation solvent and it takes to complete the sublimation process.

#### 3.11.4 Emulsions

The advantages of the emulsion polymer mixing are the easy handling and all the other advantages as the solvent casting. The mixing or casting of the film requires neither expensive equipment nor high temperature. However, emulsions of polymers are an advance technique and not always applicable to all monomers.

#### 3.11.5 Reactive Blend

Co-crosslinking and interpenetrating polymer networks (IPN) formations are the special methods for forming blends. The idea of these methods is to enforce degree of miscibility by reactions between the polymer chains. Other methods involve the polymerization of a monomer in the presence of a polymer and the introduction of interface graft copolymer onto the polymer chains.

## CHAPTER IV

### EXPERIMENT

In this chapter, the materials and chemicals, equipments, polymerization procedure, characterization instruments and sample preparations will be explained.

#### 4.1 Materials and Chemicals

##### 4.1.1 Synthesis Part

1. Styrene monomer purchased from Fluka Chemie A.G., Switzerland was distilled from sodium under vacuum just before use.
2. Trichloro(pentamethyl cyclopentadienyl) titanium (IV) ( $\text{Cp}^*\text{TiCl}_3$ , 97.0%) was purchased from Aldrich chemical Company, Inc.
3. Modified methylaluminumoxane (MMAO) 1.831 M in toluene was donated from Tosoh Akso, Japan.
4. Toluene commercial grade was donated from Exxon Chemical Ltd., Thailand. This solvent was dried over dehydrated  $\text{CaCl}_2$  and distilled over sodium/benzophenone under argon atmosphere before use.
5. Argon gas (Ultra high purity grade, 99.999 %) was purchased from Thai Industrial Gas Co., Ltd. (TIG) and further purified by passing through columns packed with copper catalyst, NaOH,  $\text{P}_2\text{O}_5$  and molecular sieve 4A to remove traces of oxygen and moisture.
6. Benzophenone (purity 99.0%) was obtained from Fluka Chemie A.G. Switzerland.
7. Calcium chloride (Dehydrated) was manufactured from Fluka Chemie A.G. Switzerland.
8. Hydrochloric acid (Fuming 36.7%) was supplied from Sigma.
9. Methanol (Commercial grade) was purchased from SR lab.
10. Sodium (lump in kerosene, 99.0%) was supplied from Aldrich chemical Company, Inc.

11. Methyl ethyl ketone (MEK) purchased from Carlo Erba, Italy was used without further treatment.

#### 4.1.2 Polymer Blend Part

1. Cyclohexylbiphenylcyclohexane (CBC-33) purchased from Merck Co., Ltd., Germany was used as received.
2. Glycerol monostearate (GMS) obtained from Rikevita Ltd., Malaysia was used as received.
3. Poly(n-butyl methacrylate), (PBMA) was purchased from Scientific Polymer Products, Inc.
4. Poly( $\alpha$ -methyl styrene), (P $\alpha$ MS) was purchased from Scientific Polymer Products, Inc.
5. Poly(cyclohexyl acrylate), (PCHA) was purchased from Scientific Polymer Products, Inc.
6. Poly(cyclohexyl methacrylate), (PCHMA) was purchased from Scientific Polymer Products, Inc.
7. Poly(vinyl methyl ether), (PVME) was purchased from Scientific Polymer Products, Inc.
8. Poly(cis-isoprene), (PIP) was purchased from Scientific Polymer Products, Inc.
9. Poly(ethyl methacrylate), (PEMA) was purchased from Scientific Polymer Products, Inc.



## 4.2 Equipments

### 4.2.1 Equipment for handling air-sensitive compounds

Since the most of reagents and catalysts were very sensitive to the oxygen and moisture therefore special techniques were taken in the handling of reagents and for loading the catalyst into the reactor. Such equipment utilized for this purpose are as follows:

(a) Glove box (Vacuum Atmospheres) with oxygen and moisture analyzer for transferring solid reagents under inert atmosphere and for storing air-sensitive reagents. The oxygen and moisture levels are normally below 2 ppm inside the glove box. The glove box is shown in Figure 4.2.1(a).

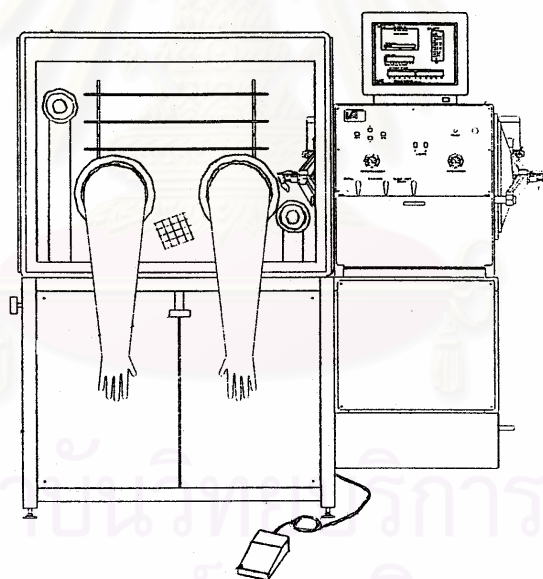


**Figure 4.2.1(a)** Glove box

(b) Schlenk line included of vacuum line connected to vacuum pump and argon line for purging when reagents are transferred. The schlenk line was shown in Figure 4.2.1(b).

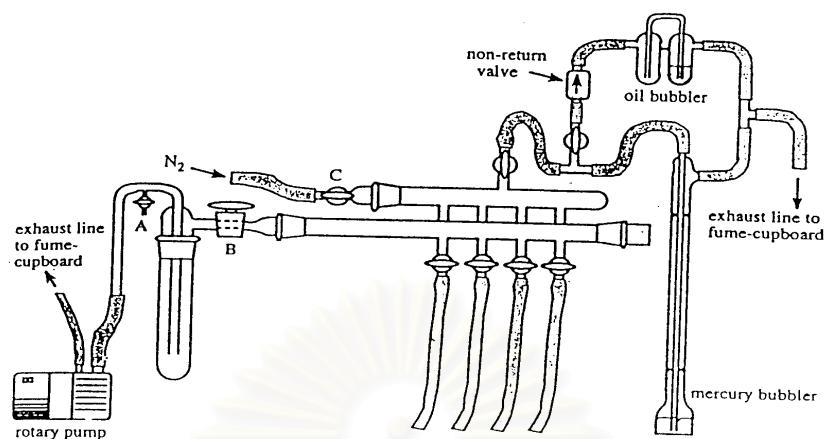


**Figure 4.2.1(b)** Schlenk line

c) Schlenk tube for keeping reagents under argon atmosphere outside the glove box. It was used accompanied with the Schlenk line. Schlenk tube is a tube with a ground joint and side arm which was three way glass valve as shown in Figure 4.2.1(c).

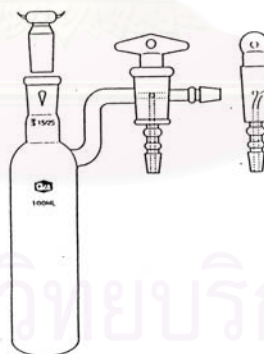


**Figure 4.2.1(c)** Schlenk tube

(d) The inert gas (argon) was pass through columns of oxygen trap (BASF catalyst, R3-11G), moisture trap (molecular sieve), sodium hydroxide (NaOH) and phosphorus pentaoxide ( $P_2O_5$ ) for purifying ultra high purity argon before use in Schlenk line and solvent distillation column. The inert gas supply system is shown in Figure 4.2.1(d).

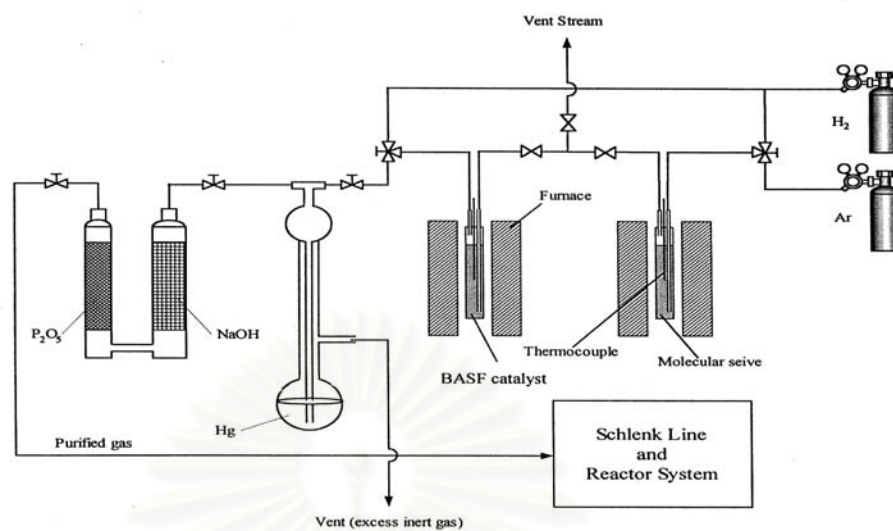


**Figure 4.2.1(d)** Inert gas supply system

(e) The vacuum pump model 195 from Labconco Corporation was used. A pressure of  $10^{-1}$  to  $10^{-3}$  mmHg was adequate for the vacuum supply to the vacuum line in the Schlenk line. The vacuum pump is shown in Figure 4.2.1(e).

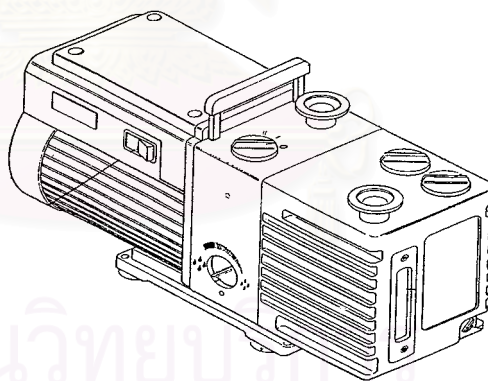


**Figure 4.2.1(e)** Vacuum pump

### 4.2.2 Glass Reactor

The polymerization reactor was a 250 ml. three-neck flask. The reactor was equipped with several fittings for injecting the chemicals and purging with argon gas. The Glass Reactor is shown in Figure 4.2.2.

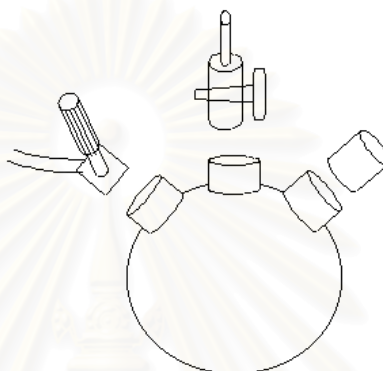


**Figure 4.2.2** Glass Reactor

### 4.2.3 Magnetic Stirrer and Hot Plate

The magnetic stirrer and hot plate model RCT basic from IKA Labortechnik were used.

### 4.2.4 Digital Hot Plate Stirrer

A Cole-Parmer digital hot plate stirrer was used for blending the polymers. The hot plate stirrer is programmable. All functions can be set from digital panel and display their status on LCD. The plate temperature, stirrer speed and time are controllable.

#### 4.2.5 Cooling System

The cooling system was in the solvent distillation in order to condense the freshly evaporated solvent.

#### 4.2.6 Syringe, Needle and Septum

The syringe was used in the experiment had a volume of 50 and 10 ml and the needle were No. 17 and 20, respectively. The septum was a silicone rod. It was used to prevent the surrounding air from entering into glass bottle by blocking at the needle end. The solvent, catalyst, cocatalyst and monomer were transferred to a glass reactor by using needles.

### 4.3 Procedures

All operations were performed under argon atmosphere by using Schlenk line and glove box.

#### 4.3.1 Catalyst Preparation

$\text{Cp}^*\text{TiCl}_3$  approximately 0.014 g was stirred in 35 ml of toluene under argon atmosphere until dissolved.

#### 4.3.2 Styrene Monomer Preparation

Styrene monomer (chemical reagent grade) was washed with 5% aqueous sodium hydroxide (NaOH) solution and distilled water, then distilled under reduced pressure.

### 4.3.3 Polymerization Procedure

Polymerization of styrene was carried out in a 250 cm<sup>3</sup> glass reactor equipped with a magnetic stirring by introducing 46 ml. of toluene, 32 ml. of Cp\*TiCl<sub>3</sub> dissolved in toluene, 13.6 ml. of MMAO and 28.4 ml. of styrene at the desired temperature of 25 °C under argon atmosphere. The total volume of the polymerization mixture was 120 ml. The addition of styrene was taken as the start of the polymerization reaction. After the desired reaction time was passed, reaction was terminated by addition methanol and 10% HCl in methanol followed. The resulting precipitated polymer was washed several times with methanol and dried at room temperature. The polymer was extracted with refluxing methyl ethyl ketone (MEK) for 12 h in order to determine the SPS portion of the polymer obtained.

### 4.3.4 Blend Preparation

The blends were made by melt mixing at 310°C by hand on the digital controllable hotplate with various compositions. All the samples were kept at 300°C for five minutes and immediately quenched to 200°C for twenty minutes before further experiments at room temperature.

## 4.4 Polymer Characterization

### 4.4.1 Soxhlet Extractor

Soxhlet extractor was used for syndiotactic content determination. (Figure 4.4.1) The obtain polystyrene was extracted with boiling methyl ethyl ketone (MEK) or 2-butanone to give syndiotactic (insoluble) and atactic (soluble) polystyrene. A % syndiotactic index (% S.I.) is computed from

$$\% \text{ S.I.} = (\text{Insoluble Weight of PS} / \text{Total Weight of PS}) \times 100$$



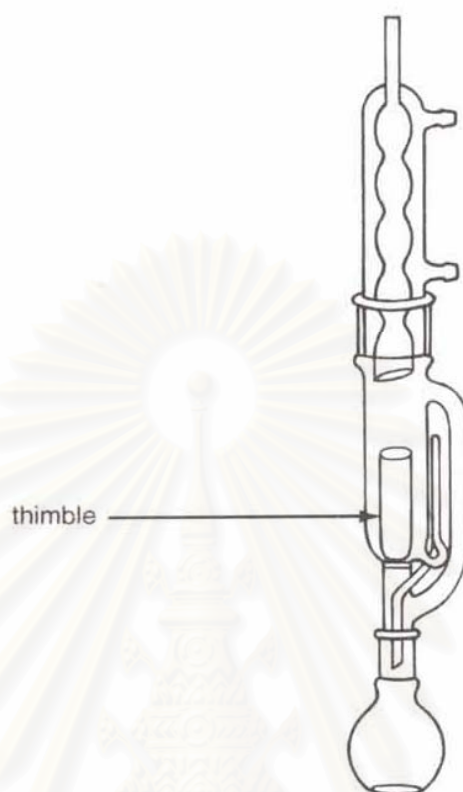


**Figure 4.4.1** Soxhlet Extractor

#### 4.4.2 Differential Scanning Calorimetry (DSC)

The melting temperature and glass transition temperature of the polymers were determined with a Perkin-Elmer DSC-Diamond. The analyses were performed at the heating rate of 20°C/min in the temperature range 50 to 300°C. The heating cycle was run twice. In the first scan, samples were heated up and then cooled down to 50°C. In the second scan, samples were reheated at the same rate. Both the results of the first and second scan were reported. Percent crystallinity was computed from enthalpies of melting by Equation (a), using the reliable value of Wunderlich.

$$\chi (\%) = (\Delta H_m / \Delta H_m^\circ) \times 100 \quad (a)$$

#### 4.4.3 Gel Permeation Chromatography (GPC)

One of the most widely used methods for the determination of molecular weight (Mw) and molecular weight distribution (MWD) was gel permeation chromatography (GPC). Samples were prepared accurately at a concentration of approximately 0.5-1.0 mg/ml in the mobile phase and dissolved by using the PL-SP 260 at a temperature of 150 °C for approximately hours. The dissolved sampled were transferred into PL-GPC 220. GPC were performed at Thai Petrochemical Industry Public Co., Ltd.

#### 4.4.4 X-ray diffraction (XRD)

XRD was performed to determine the bulk crystalline phase of samples. It was conducted using a SIEMENS D-5000 X-ray diffractometer with  $\text{CuK}\alpha$  ( $\lambda=1.54439$  °A). The spectra were scanned at a rate of 0.04 degree/second in the range  $2\theta = 10-40$  degree.

## CHAPTER V

### RESULTS AND DISCUSSION

In this research, the blends of syndiotactic polystyrene (SPS) with several types of amorphous polymers, such as poly( $\alpha$ -methyl styrene), poly (ethyl methacrylate), poly(*n*-butyl methacrylate), poly(cyclohexyl acrylate), poly(*cis*-isoprene) and poly(vinyl methyl ether) were be explored. This chapter provides information about polymerization of styrene, miscibility of SPS with various polymers, thermal properties and crystal structure of these polymers and their blends with low molar mass liquid crystal (CBC-33) and commercial lubricant (GMS) are investigated.

#### 5.1 Polymerization of Styrene

The results of polymerization of styrene using Pentamethylcyclopentadienyl titanium trichloride ( $\text{Cp}^*\text{TiCl}_3$ ) with modified-methylaluminoxane (MMAO) as cocatalyst are given in Table 5.1.

**Table 5.1** Polymerization of Styrene using  $\text{Cp}^*\text{TiCl}_3$  with MMAO<sup>a</sup>

% Yield <sup>b</sup>	72.67 wt %
Catalytic Activity	5,084.67 g PS/mmole Ti-hr
% Syndiotactic Index	93.38 %
$M_w^c$	1,943,500 g/mole
$M_n^c$	592,300 g/mole
Molecular weight distribution (MWD) <sup>c</sup>	3.3
$T_g^d$	97.90 °C
$T_m^d$	271.41 °C

<sup>a</sup>Conditions:  $[\text{Cp}^*\text{TiCl}_3] = 3.68 \times 10^{-4}$  M,  $[\text{MMAO}] = 1.83$  M,  $[\text{Styrene}] = 2.06$ , Al/Ti = 563, 25 °C

<sup>b</sup>Calculated from (weight of synthesized polymer/weight of monomer)×100

<sup>c</sup>Obtained from GPC and MWD was calculated from  $M_w/M_n$

<sup>d</sup>Obtained from DSC

## 5.2 Miscibility of Syndiotactic Polystyrene Blends

There are six systems of blends between syndiotactic polystyrene (SPS) and several polymers:

System 1: SPS and poly( $\alpha$ -methyl styrene), (PaMS)

System 2: SPS and poly (ethyl methacrylate), (PEMA)

System 3: SPS and poly(*n*-butyl methacrylate), (PBMA)

System 4: SPS and poly(cyclohexyl acrylate), (PCHA)

System 5: SPS and poly(*cis*-isoprene), (PIP)

System 6: SPS and poly(vinyl methyl ether), (PVME)

The glass transition temperature is a characteristic of the amorphous part of polymers. At  $T_g$ , a dramatic change occurs in the local movement of molecule level of polymer chain from glassy state to rubbery state, which this changes almost all of the physical and mechanical properties of polymer [59].

The glass transition temperature ( $T_g$ ), crystallization temperature ( $T_c$ ) and melting temperature ( $T_m$ ) of polymers were evaluated by the differential scanning calorimetry (DSC) between 50 °C to 300 °C at ramping rate of 20 °C/min. The heating cycle was run twice. Before the first scan, samples were melted at 300°C, quench to 200 °C for 10 minutes and then cooled to room temperature. Thus before the first scan, the polymer blends were preheated at the isothermal crystallization condition at 200°C. Before the second scan, the polymer blends were cooling down at the constant cooling rate of 20°C per minute from 300°C to 50°C. The crystallization temperatures,  $T_c$  were detected and recorded. The second scan, samples were reheated at rate 20 °C/min from 50°C to 300°C, both the results of the first and second scan were reported. From DSC curves, most of the first scan show two  $T_g$  because of blending by hand may result in not well-mixed in the molecular level but the samples were allow to melt and mix with out shear in the DSC of the first scan. So, the second scan show single  $T_g$  which shifts to a higher temperature with the SPS content. This result suggested the miscibility of the two components in the blends after they were

allowed to be completely mixed inside the DSC. Thus, in this research  $T_g2$  were chosen to represent the miscibility of the polymers. However, the mixing inside the DSC is purely free of shear rate the mixing condition is not as good as solvent casting especially in the small sample size.

The miscibility of binary blends is frequently ascertained by measurements of their  $T_g$ . Table 5.2 shown  $T_g$  of each composition of SPS/PaMS blend. It is observed that the  $T_g$  of pure SPS and PaMS is 97.90 and 87.33 °C, respectively. All the blends with different compositions exhibit single  $T_g$  which shifted to a higher temperatures in the same trend as the SPS content in the samples. This result may imply the miscibility of the two components in the blends under the DSC condition.

**Table 5.2** Glass transition temperature ( $T_g$ ), melting temperature ( $T_m$ ), crystallization temperature ( $T_c$ ) and melting enthalpy of SPS/PaMS blends

%SPS	$T_{g1.1}$ (°C)	$T_{g1.2}$ (°C)	$T_{g2}$ (°C)	$T_{m1}$ (°C)	$T_{m2.1}$ (°C)	$T_{m2.2}$ (°C)	$T_c$ (°C)	$\Delta H_m$ (J/g)
100	n.a.	98.18	97.90	269.99	271.41	264.06	242.66	25.73
80	78.29	96.54	94.03	266.06	266.34	n.a.	237.91	22.54
60	77.68	92.29	87.90	263.13	263.87	n.a.	233.35	20.33
40	76.32	92.45	86.95	260.85	261.05	n.a.	232.46	11.74
20	76.98	98.53	85.61	259.26	260.59	n.a.	230.78	10.90
0	87.33	n.a.	87.33	n.a.	n.a.	n.a.	n.a.	n.a.

n.a. = not available

$\Delta H_m$  can be referred to the amount of crystal in the samples. However, due to inaccurate calculation methods, the values showed here will not be further discussed.

**Table 5.3** Glass transition temperature ( $T_g$ ), melting temperature ( $T_m$ ), crystallization temperature ( $T_c$ ) and melting enthalpy of SPS/PaMS/LCC blends

%SPS	$T_{g1.1}$ (°C)	$T_{g1.2}$ (°C)	$T_{g2}$ (°C)	$T_{m1}$ (°C)	$T_{m2}$ (°C)	$T_{m2.2}$ (°C)	$T_c$ (°C)	$\Delta H_m$ (J/g)
100	n.a	97.84	97.73	269.13	270.57	262.51	239.06	23.91
80	78.39	94.83	93.59	266.85	267.12	n.a	239.47	21.62
60	78.12	93.59	88.48	264.95	265.63	n.a	235.92	20.10
40	77.79	95.09	87.74	263.65	263.61	n.a	235.38	19.14
20	77.94	96.74	84.81	263.45	263.54	n.a	234.11	15.68
0	89.81	n.a	89.81	n.a	n.a	n.a	n.a	n.a

n.a. = not available

**Table 5.4** Glass transition temperature ( $T_g$ ), melting temperature ( $T_m$ ), crystallization temperature ( $T_c$ ) and melting enthalpy of SPS/PaMS/GMS blends

%SPS	$T_{g1.1}$ (°C)	$T_{g1.2}$ (°C)	$T_{g2}$ (°C)	$T_{m1}$ (°C)	$T_{m2.1}$ (°C)	$T_{m2.2}$ (°C)	$T_c$ (°C)	$\Delta H_m$ (J/g)
100	n.a	99.66	99.25	270.62	271.01	263.30	240.64	24.60
80	79.44	94.82	93.26	267.82	268.57	n.a	236.41	22.94
60	78.36	92.12	88.25	265.25	265.60	n.a	232.46	20.57
40	79.53	94.89	87.36	263.18	262.90	n.a	229.66	16.54
20	77.69	95.69	86.04	260.76	261.87	n.a	225.71	11.49
0	89.89	n.a	89.89	n.a	n.a	n.a	n.a	n.a

n.a. = not available

Table 5.5 shown  $T_g$  of each composition of SPS/PEMA blend. It is observed that all the blends with different compositions exhibit single  $T_g$  which shifts to a higher temperature with the SPS content. This result may imply that the miscibility of the two components in the amorphous state of the blends.



**Table 5.5** Glass transition temperature ( $T_g$ ), melting temperature ( $T_m$ ), crystallization temperature ( $T_c$ ) and melting enthalpy of SPS/PEMA blends

%SPS	$T_{g1.1}$ (°C)	$T_{g1.2}$ (°C)	$T_{g2}$ (°C)	$T_{m1}$ (°C)	$T_{m2.1}$ (°C)	$T_{m2.2}$ (°C)	$T_c$ (°C)	$\Delta H_m$ (J/g)
100	n.a.	98.18	97.90	269.99	271.41	264.06	242.66	25.72
80	75.63	95.95	95.43	269.70	270.06	n.a.	239.44	23.64
60	91.29	91.29	91.17	269.54	269.22	n.a.	238.12	23.92
40	86.38	86.38	88.71	269.26	269.41	n.a.	238.19	20.51
20	62.24	92.12	80.70	267.66	267.61	n.a.	234.07	15.77
0	65.54	n.a.	65.54	n.a.	n.a.	n.a.	n.a.	n.a.

n.a. = not available

**Table 5.6** Glass transition temperature ( $T_g$ ), melting temperature ( $T_m$ ), crystallization temperature ( $T_c$ ) and melting enthalpy of SPS/PEMA/LCC blends

%SPS	$T_{g1.1}$ (°C)	$T_{g1.2}$ (°C)	$T_{g2}$ (°C)	$T_{m1}$ (°C)	$T_{m2.1}$ (°C)	$T_{m2.2}$ (°C)	$T_c$ (°C)	$\Delta H_m$ (J/g)
100	n.a.	98.26	97.88	269.13	270.57	262.51	239.06	23.91
80	69.39	95.32	95.18	268.55	268.58	n.a.	234.00	22.14
60	67.40	90.16	90.29	265.74	266.52	n.a.	232.40	19.38
40	66.78	66.78	87.42	266.76	267.15	n.a.	230.42	16.40
20	62.76	62.76	79.94	263.95	265.75	n.a.	223.43	7.60
0	52.94	n.a.	62.72	n.a.	n.a.	n.a.	n.a.	n.a.

n.a. = not available

**Table 5.7** Glass transition temperature ( $T_g$ ), melting temperature ( $T_m$ ), crystallization temperature ( $T_c$ ) and melting enthalpy of SPS/PEMA/GMS blends

%SPS	$T_{g1.1}$ (°C)	$T_{g1.2}$ (°C)	$T_{g2}$ (°C)	$T_{m1}$ (°C)	$T_{m2.1}$ (°C)	$T_{m2.2}$ (°C)	$T_c$ (°C)	$\Delta H_m$ (J/g)
100	n.a.	99.66	99.25	270.62	271.01	263.30	240.64	24.60
80	95.51	95.51	95.72	269.29	270.03	n.a.	239.29	22.28
60	67.55	95.28	90.06	266.87	268.02	n.a.	236.19	18.27
40	67.27	92.43	86.15	268.42	268.02	n.a.	233.15	17.91
20	60.07	86.94	80.57	266.15	266.92	n.a.	223.89	12.05
0	61.38	n.a.	58.82	n.a.	n.a.	n.a.	n.a.	n.a.

n.a. = not available

Table 5.8 shown  $T_g$  of each composition of SPS/PBMA blend. It is observed that all the blends with different compositions exhibit single  $T_g$  which shifts to a higher temperature with the SPS content. This result may imply that the miscibility of the two components in the amorphous state of the blends.

**Table 5.8** Glass transition temperature ( $T_g$ ), melting temperature ( $T_m$ ), crystallization temperature ( $T_c$ ) and melting enthalpy of SPS/PBMA blends

%SPS	$T_{g1.1}$ (°C)	$T_{g1.2}$ (°C)	$T_{g2}$ (°C)	$T_{m1}$ (°C)	$T_{m2.1}$ (°C)	$T_{m2.2}$ (°C)	$T_c$ (°C)	$\Delta H_m$ (J/g)
100	n.a.	98.18	97.90	269.99	271.41	264.06	242.66	25.72
80	79.21	96.13	94.81	269.48	270.24	n.a.	240.53	25.57
60	66.92	95.71	93.33	269.43	270.55	n.a.	238.37	23.19
40	77.14	96.80	89.36	268.13	268.89	n.a.	238.48	22.42
20	68.89	94.13	84.32	267.41	266.99	n.a.	234.39	21.14
0	31.85	n.a.	31.85	n.a.	n.a.	n.a.	n.a.	n.a.

n.a. = not available

**Table 5.9** Glass transition temperature ( $T_g$ ), melting temperature ( $T_m$ ), crystallization temperature ( $T_c$ ) and melting enthalpy of SPS/PBMA/LCC blends

%SPS	$T_{g1.1}$ (°C)	$T_{g1.2}$ (°C)	$T_{g2}$ (°C)	$T_{m1}$ (°C)	$T_{m2.1}$ (°C)	$T_{m2.2}$ (°C)	$T_c$ (°C)	$\Delta H_m$ (J/g)
100	n.a.	97.84	97.73	269.13	270.57	262.51	239.06	23.91
80	74.88	97.66	94.02	268.07	268.48	n.a.	238.07	24.20
60	70.74	93.89	91.69	267.22	267.34	n.a.	235.79	22.52
40	75.45	95.15	90.79	267.41	268.23	n.a.	235.65	21.83
20	72.51	93.99	85.30	266.98	267.40	n.a.	234.39	21.68
0	29.85	n.a.	29.85	n.a.	n.a.	n.a.	n.a.	n.a.

n.a. = not available

**Table 5.10** Glass transition temperature ( $T_g$ ), melting temperature ( $T_m$ ), crystallization temperature ( $T_c$ ) and melting enthalpy of SPS/PBMA/GMS blends

%SPS	$T_{g1.1}$ (°C)	$T_{g1.2}$ (°C)	$T_{g2}$ (°C)	$T_{m1}$ (°C)	$T_{m2.1}$ (°C)	$T_{m2.2}$ (°C)	$T_c$ (°C)	$\Delta H_m$ (J/g)
100	n.a.	99.66	99.25	270.62	271.01	263.30	240.64	24.60
80	74.85	95.93	93.98	267.29	267.70	n.a.	237.58	20.77
60	72.36	97.89	91.84	268.13	268.14	n.a.	236.75	20.93
40	69.73	91.32	89.51	266.94	266.97	n.a.	235.57	20.02
20	69.72	92.54	84.90	266.60	267.00	n.a.	234.82	19.85
0	29.88	n.a.	29.88	n.a.	n.a.	n.a.	n.a.	n.a.

n.a. = not available

Table 5.11 shown  $T_g$  of each composition of SPS/PCHA blend. It is observed that all the blends with different compositions exhibit single  $T_g$  which shifts to a higher temperature with the SPS content. This result may imply that the miscibility of the two components in the blends happened in the amorphous state.

**Table 5.11** Glass transition temperature ( $T_g$ ), melting temperature ( $T_m$ ), crystallization temperature ( $T_c$ ) and melting enthalpy of SPS/PCHA blends

%SPS	$T_{g1.1}$ (°C)	$T_{g1.2}$ (°C)	$T_{g2}$ (°C)	$T_{m1}$ (°C)	$T_{m2.1}$ (°C)	$T_{m2.2}$ (°C)	$T_c$ (°C)	$\Delta H_m$ (J/g)
100	n.a.	98.18	97.90	269.99	271.41	264.06	242.66	25.72
80	66.84	94.02	90.21	268.24	268.23	n.a.	234.80	18.53
60	51.86	95.33	87.80	268.63	268.22	n.a.	233.51	15.05
40	44.61	85.88	78.40	268.46	268.04	n.a.	229.28	14.20
20	53.5	91.92	57.86	266.98	266.51	n.a.	225.16	12.05
0	25.49	n.a.	25.49	n.a.	n.a.	n.a.	n.a.	n.a.

n.a. = not available

**Table 5.12** Glass transition temperature ( $T_g$ ), melting temperature ( $T_m$ ), crystallization temperature ( $T_c$ ) and melting enthalpy of SPS/PCHA/LCC blends

%SPS	$T_{g1.1}$ (°C)	$T_{g1.2}$ (°C)	$T_{g2}$ (°C)	$T_{m1}$ (°C)	$T_{m2.1}$ (°C)	$T_{m2.2}$ (°C)	$T_c$ (°C)	$\Delta H_m$ (J/g)
100	n.a.	97.84	97.73	269.13	270.57	262.51	239.06	23.91
80	64.76	92.49	87.09	264.14	265.38	n.a.	229.86	18.74
60	53.75	90.62	86.20	264.90	264.89	n.a.	229.77	15.52
40	49.22	98.84	80.61	266.58	265.76	n.a.	227.27	10.18
20	53.72	89.82	56.23	264.45	264.09	n.a.	225.54	6.46
0	26.46	n.a.	26.46	n.a.	n.a.	n.a.	n.a.	n.a.

n.a. = not available

**Table 5.13** Glass transition temperature ( $T_g$ ), melting temperature ( $T_m$ ), crystallization temperature ( $T_c$ ) and melting enthalpy of SPS/PCHA/GMS blends

%SPS	$T_{g1.1}$ (°C)	$T_{g1.2}$ (°C)	$T_{g2}$ (°C)	$T_{m1}$ (°C)	$T_{m2.1}$ (°C)	$T_{m2.2}$ (°C)	$T_c$ (°C)	$\Delta H_m$ (J/g)
100	n.a.	99.66	99.25	270.62	271.01	263.30	240.64	24.60
80	51.19	94.19	90.26	269.08	268.03	n.a.	233.13	17.54
60	49.27	93.44	88.77	268.62	267.37	n.a.	228.48	16.02
40	47.08	90.07	80.75	266.50	266.08	n.a.	225.14	11.60
20	50.49	90.44	58.57	266.93	267.05	n.a.	225.13	6.16
0	25.29	n.a.	25.29	n.a.	n.a.	n.a.	n.a.	n.a.

n.a. = not available

Table 5.14 shown  $T_g$  of each composition of SPS/PIP blend. It is observed that all the blends with different compositions exhibit single  $T_g$  which shifts to a higher temperature with the SPS content. This result may imply that the miscibility of the two components in the blends when they are in the amorphous state.

**Table 5.14** Glass transition temperature ( $T_g$ ), melting temperature ( $T_m$ ), crystallization temperature ( $T_c$ ) and melting enthalpy of SPS/PIP blends

%SPS	$T_{g1}$ (°C)	$T_{g2}$ (°C)	$T_{m1}$ (°C)	$T_{m2.1}$ (°C)	$T_{m2.2}$ (°C)	$T_c$ (°C)	$\Delta H_m$ (J/g)
100	98.18	97.90	269.99	271.41	264.06	242.66	25.72
80	64.12	86.61	267.85	268.86	n.a.	228.46	18.04
60	58.14	80.16	266.55	267.48	n.a.	223.09	15.22
40	44.25	65.96	264.57	266.69	n.a.	220.18	15.02
20	42.40	56.38	264.00	265.46	n.a.	219.75	14.06
0	-32.93	-32.93	n.a.	n.a.	n.a.	n.a.	n.a.

n.a. = not available

**Table 5.15** Glass transition temperature ( $T_g$ ), melting temperature ( $T_m$ ), crystallization temperature ( $T_c$ ) and melting enthalpy of SPS/PIP/LCC blends

%SPS	$T_{g1}$ (°C)	$T_{g2}$ (°C)	$T_{m1}$ (°C)	$T_{m2.1}$ (°C)	$T_{m2.2}$ (°C)	$T_c$ (°C)	$\Delta H_m$ (J/g)
100	98.26	97.88	269.13	270.57	262.51	239.06	23.91
80	64.90	87.12	265.94	266.39	n.a.	225.56	17.58
60	59.40	81.98	265.45	266.88	n.a.	221.20	15.74
40	44.42	69.77	263.04	265.42	n.a.	215.38	10.72
20	38.38	56.88	262.12	264.58	n.a.	213.50	9.68
0	-33.84	-33.87	n.a.	n.a.	n.a.	n.a.	n.a.

n.a. = not available

**Table 5.16** Glass transition temperature ( $T_g$ ), melting temperature ( $T_m$ ), crystallization temperature ( $T_c$ ) and melting enthalpy of SPS/PIP/GMS blends

%SPS	$T_{g1}$ (°C)	$T_{g2}$ (°C)	$T_{m1}$ (°C)	$T_{m2.1}$ (°C)	$T_{m2.2}$ (°C)	$T_c$ (°C)	$\Delta H_m$ (J/g)
100	99.66	99.25	270.62	271.01	263.30	240.64	24.60
80	61.64	90.07	265.89	266.87	n.a.	221.65	18.38
60	58.03	82.75	264.47	265.91	n.a.	221.68	15.59
40	49.9	66.50	264.93	265.42	n.a.	218.74	15.01
20	35.03	53.00	262.07	264.48	n.a.	217.33	5.31
0	-30.74	-30.74	n.a.	n.a.	n.a.	n.a.	n.a.

n.a. = not available



**Table 5.17** Glass transition temperature ( $T_g$ ), melting temperature ( $T_m$ ) and crystallization temperature ( $T_c$ ) of SPS/PVME blends

%SPS	$T_{g2.1}$ (°C)	$T_{g2.2}$ (°C)	$T_c$ (°C)	$T_m$ (°C)
100	n.a.	97.90	242.66	271.41
80	-15.70	97.23	237.38	269.26
60	-14.52	97.74	233.77	269.83
40	-19.33	91.83	234.83	268.76
20	-17.43	96.76	227.05	270.30
0	-26.68	n.a.	n.a.	n.a.

n.a. = not available

In Table 5.17, the thermal characteristics of SPS/PVME blends and pure polymers are shown. With increasing the PVME content, the crystallization temperature of blends decreased, but the melting temperatures did not shift. Their blends showed two  $T_g$  and both values are very close to the pure polymers. This result implies the immiscible of the two components in the blends. This might be because of the miscibility of SPS with PVME is sensitive to humidity in air which usually facilitate phase separate of polymer blends.

From these results, it was found that the SPS have tendency to be miscible with PaMS, PEMA, PBMA, PCHA and PIP by melt mixing method, but the phase separation were found in the systems of PVME blends.

### 5.3 Effect of Additives on Thermal Properties of Polymer Blends

#### 5.3.1 Glass Transition Temperature

In Table 5.3-5.4, the thermal characteristics of SPS/PaMS/LCC blends and SPS/PaMS/GMS blends are shown, respectively. From this Table,  $T_g$  of binary blends are in the same vicinity of their blends with CBC-33 and GMS. The difference

between  $T_g$  of binary blends and their blends with additives are less than  $1^\circ\text{C}$ , and cannot be distinguished from each other. These phenomena may be resulted from the too small (1.0% w/w) amount of additives in the matrix phase of the binary blends that are not enough to plasticize the blends to such an extent that the significant reducing in  $T_g$  of the blends can be observed.

In Table 5.6-5.7, the thermal characteristics of SPS/PEMA/LCC and SPS/PEMA/GMS blends are shown, respectively. From this Table,  $T_g$  of binary blends are in the same vicinity to their blends with CBC-33 and GMS. Thus, the additions of CBC-33 and GMS have not significantly affected  $T_g$  of binary blends as same as SPS/PaMS blends.

Table 5.9-5.10 showed thermal characteristics of SPS/PBMA/LCC and SPS/PBMA/GMS blends, respectively. From this Table,  $T_g$  of binary blends are in the same vicinity to their blends with CBC-33 and GMS. Thus, the additions of CBC-33 and GMS have not significantly affected  $T_g$  of binary blends.

Table 5.12-5.13 showed thermal characteristics of SPS/PCHA/LCC and SPS/PCHA/GMS blends, respectively. From this Table,  $T_g$  of binary blends are in the same vicinity as their blends with CBC-33 and GMS. Thus, the additions of CBC-33 and GMS have not significantly affected  $T_g$  of binary blends.

Table 5.15-5.16 showed thermal characteristics of SPS/PIP/LCC and SPS/PIP/GMS blends, respectively. From this Table,  $T_g$  of binary blends are in the same vicinity as their blends with CBC-33 and GMS. Thus, the additions of CBC-33 and GMS have not significantly affected  $T_g$  of binary blends.

Thus, the glass transition temperatures of all the blends with additives do not significantly change from additive less binary blends. This phenomenon proves that additives do not have direct plasticizing effects on glass transition temperature of pure binary blends.

### 5.3.2 Crystallization Temperature

From Table 5.2-5.4, when  $T_c$  of SPS/PaMS blends and their blends with additives were compared, it showed that addition of LCC have affected the increasing  $T_c$  of their blends at cooling rate of 20°C per minute in the amount of less than 3 °C apart from the pure blend. These differences were located in error limit of the DSC that is less than  $\pm 5$  °C apart from each other. But the addition of GMS have affected the decreasing  $T_c$  of their blends are less than 3 °C apart from the pure blend. These differences were not clearly changed while the concentration of the blend changed.

For SPS/PEMA blends, the addition of LCC affected the decreasing  $T_c$  of their blends about 4-11 °C from pure blend without LCC. The addition of GMS also affected the decreasing  $T_c$  of their blends about 2-10 °C. These temperature difference were significant and we can draw the conclusion that the additives tend to decrease  $T_c$  of SPS/PEMA blends.

For SPS/PBMA blends, the additions of LCC or GMS both have affected the decreasing  $T_c$  of their blends about 3 °C from the pure blend. Thus, the addition of LCC or GMS have small significant trended to decreasing  $T_c$  of SPS/PBMA blends.

For SPS/PCHA blends, the additions of LCC or GMS have affected the decreasing  $T_c$  of their blends about 2-5 °C from the pure blend. Thus, both additives have significant effect on decreasing  $T_c$  of SPS/PCHA blends.

For SPS/PIP blends, the addition of LCC or GMS have significantly affected the decreasing  $T_c$  of their blends about 2-7 °C from the pure blend. Thus, both additives have significant effect to decreasing  $T_c$  of SPS/PIP blends from the pure blend.

From these results, the effects of adding LCC or GMS resulted in the slightly decreasing  $T_c$  of polymer blends. Because LCC and GMS can reduce melt viscosity of the blends [42], the molecules of the polymers in the blend could move or separate

easily. Therefore the crystals have difficulty to form the crystalline, because the more mobile molecules tend to move out from the order (crystal). The crystalline temperature will decrease according to the mobility of the molecules when added the LCC or the GMS due to the easily mobile chain molecules.

### 5.3.3 Melting Temperature

The decreasing melting point of the crystal due to the addition of small molecule can be calculated from the equation below,

$$\ln x_B = \frac{\Delta H}{RT} \left( \frac{1}{T_m^*} - \frac{1}{T_{md}} \right)$$

where

$x_B$  = mole fraction of SPS

$T_m^*$  = pure melting temperature

$T_{md}$  = melting temperature depression

For polymer blends, melting temperature depression phenomenon that results from the lower of the blend Gibbs free energy can be show in Table 5.18. The melting temperature of binary blends and their blends with additives have slight tendency to lower the temperature from the pure component of the polymers. The CBC-33 and GMS addition were summarized the effects as they were slightly decreased melting temperature of their blends from the pure components. Because of molecular mobility enhancement from both CBC-33 and GMS [42], the crystal of the blends will melt easier. The molecules can slide depart from each other more easier, therefore crystal will melt more easier than the polymer blend without the additive. In every systems concerned in this thesis, the crystalline melting points when added the LCC or GMS will be lower than the pure polymer blend. From melting point depression phenomenon, the crystalline melting point will be lower. However the quantities of the crystalline melting point depression will partly come from the melting point depression and the contribution from the addition of the LCC. In this thesis, we can

conclude that the effects in lowering the crystalline melting point largely come from the contribution from the addition of the LCC more than the melting point depression. More over, the ease of the moving of the molecule will enhance the depression in the crystalline temperature ( $T_c$ ). The systems will have the difficulty to ally the molecule in the shape of the crystal from the fast mobility melt of the polymer blends.

**Table 5.18** Melting temperature depression of their blends

Samples	Melting Temperature Depression (°C)				
	100/0	80/20	60/40	40/60	20/80
SPS/PaMS	271.41	271.14	271.05	270.70	270.53
SPS/PaMS/LCC	270.57	270.27	270.19	270.12	269.95
SPS/PaMS/GMS	271.01	270.72	270.64	270.49	270.16
SPS/PEMA	271.41	271.29	271.24	270.17	271.02
SPS/PEMA/LCC	270.57	270.33	270.27	270.17	269.58
SPS/PEMA/GMS	271.01	270.76	270.68	270.64	270.38
SPS/PBMA	271.41	271.35	271.29	271.25	271.18
SPS/PBMA/LCC	270.57	270.57	270.57	270.57	270.57
SPS/PBMA/GMS	271.01	270.75	270.73	270.69	270.64
SPS/PCHA	271.41	271.31	271.22	271.14	270.99
SPS/PCHA/LCC	270.57	270.29	270.20	269.95	269.45
SPS/PCHA/GMS	271.01	270.70	270.65	270.46	269.82
SPS/PIP	271.41	271.38	271.33	271.28	271.20
SPS/PIP/LCC	270.57	270.27	270.21	270.00	269.84
SPS/PIP/GMS	271.01	270.72	270.64	270.59	269.66

#### 5.4 Effect of Blending on Miscibility

Method in blending polymers have effected to miscibility of polymer blend. In this part will compare method of blending between melt mixing and solvent casting. Information of blending by solvent casting comes from Ampaipun Sivavichchakij [60].

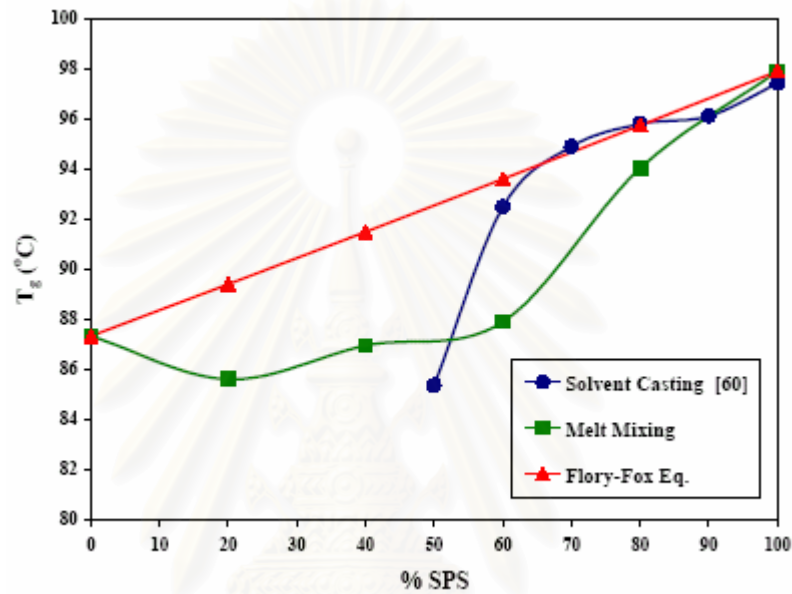


**Figure 5.1** Comparison of method in blending SPS/PaMS blends with Fox equation

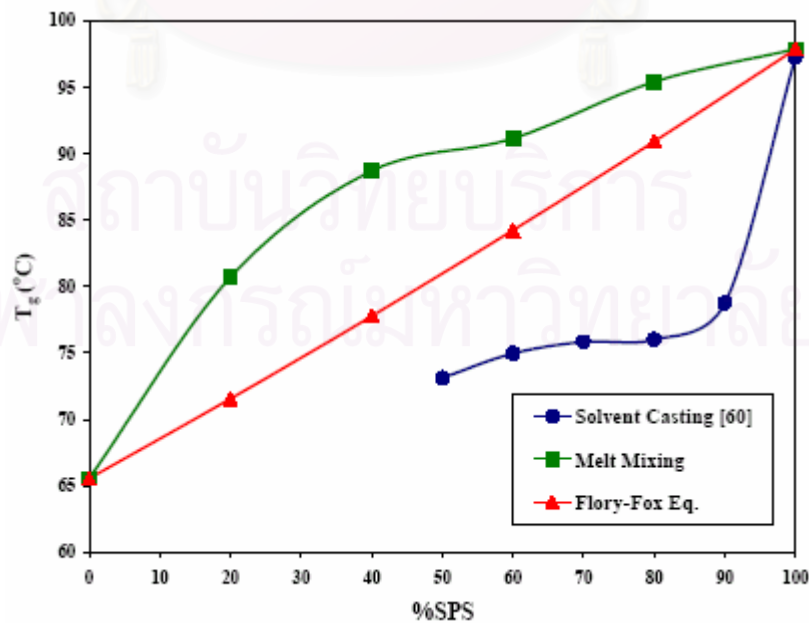


**Figure 5.2** Comparison of method in blending SPS/PEMA with Fox equation



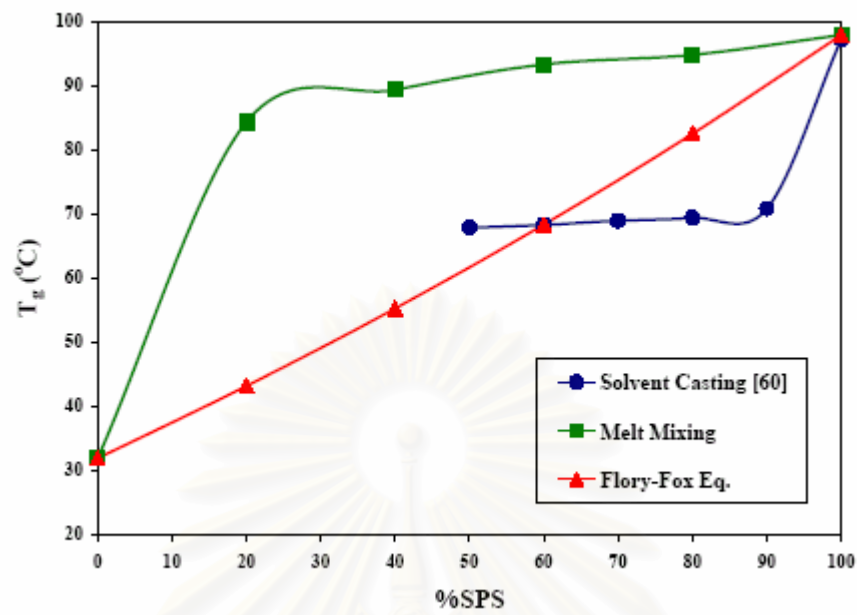


**Figure 5.3** Comparison of method in blending SPS/PBMA with Fox equation

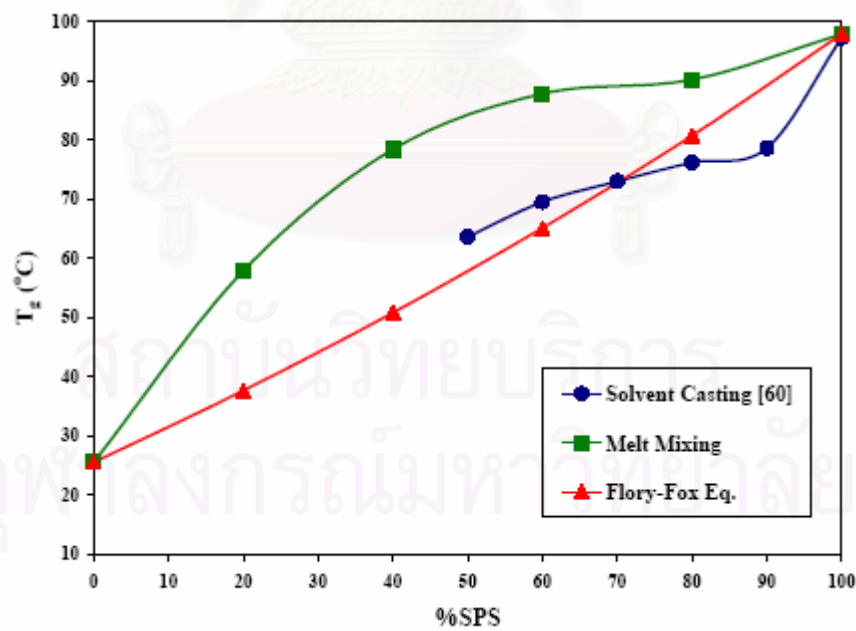


**Figure 5.4** Comparison of method in blending SPS/PCHA with Fox equation

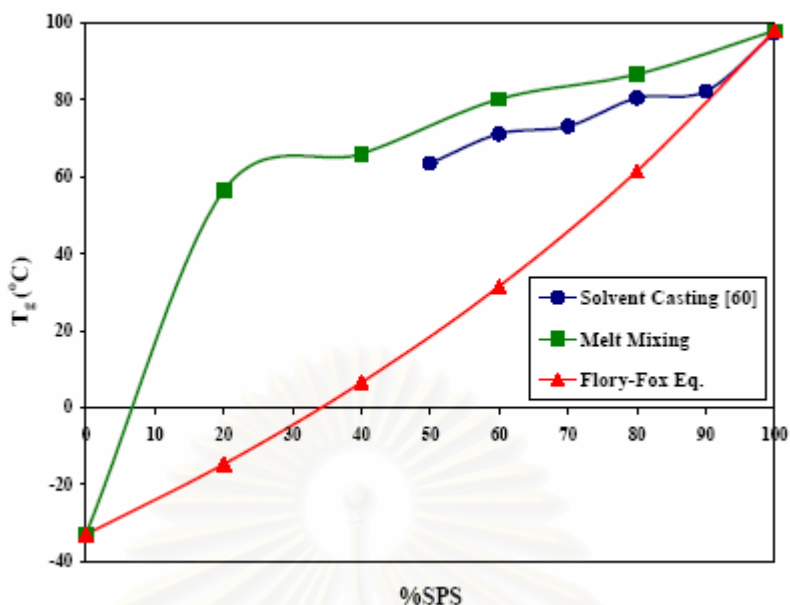


**Figure 5.5** Comparison of method in blending of SPS/PIP blends with Fox equation

The methods of blending in this thesis mostly come from the melt mixing method. In some of the first heating, two  $T_g$ s in the vicinity of the pure polymers could be observed which represented the phase separations in the blends. In the small amount of polymer, solvent casting may be the better method for blending the polymers. Some of the discrepancy of the melted mixing method can be shown in the above picture. Even after the melting at 300°C in the DSC, the different  $T_g$  in the melted mixing system from the solution casting system can be observed. The higher  $T_g$  in the case of the melt mixing methods could be resulted from the phase separation in the domain of the samples. More over, due to the inhomogeneous of the samples from melt mixing method, some of the samples may contain more solid part which represented the more SPS, so that the measured  $T_g$ s were more represented more SPS than the expected composition of the blend. This situation cannot be found in the case of the solution casting because all the liquid solution were homogeneous. However in the large scale of polymer mixing, the melted mixing will be the most appropriate methods because of the low cost of operation and the method do not require the further removal of the solvents. Never the less the data from both methods can be confirmed the results of each other which can be conclude in this thesis.

Normally the Flory-Fox equation can be utilize to predict the  $T_g$  of the polymer blend according to the follow equation.

$$\frac{1}{T_g} = \frac{W_1}{T_{g1}} + \frac{(1 - W_1)}{T_{g2}}$$

where

$T_g$  = glass transition temperature of polymer blends (Experiment)

1 and 2 = SPS and amorphous polymers respectively

$W_i$  = weight fraction of component i

From Flory-Fox equation, if the  $T_g$  of the blend (from DSC measurements) and both the pure  $T_g$  of the components are known, the weight fraction ( $W_1$ ) can be predicted from this equation. In this thesis, the prediction of the equation can be found as the Table 5.19.

**Table 5.19** Percentage of SPS in binary blends from calculation

% SPS (real)	% SPS from calculation ( $W_1 \times 100$ )				
	SPS/PaMS	SPS/PEMA	SPS/PBMA	SPS/PCHA	SPS/PIP
100	100.00	100.00	100.00	100.00	100.00
80	64.06	92.99	96.12	91.27	94.24
60	5.54	80.67	94.24	88.46	90.78
40	-3.70	73.42	89.12	77.12	82.71

From Table 5.19, SPS content predicted from Flory-Fox equation are largely different from % SPS from weight fraction. These might be because of the Flory-Fox equation is too simple to represent the real composition in the blend or the DSC samples that measure the  $T_g$  of the blend contain different SPS from weight fraction. The new model of  $T_g$  is needed and from these data, the DSC samples mostly contain SPS (predict value is higher than the weight value). The phase separation will remain in the second heating or the inhomogeneous sample can not be represent the melted mix value.

### 5.5 Effect of Additives on Percent of Crystallinity

The crystallinity is determined by measuring the integrated area of the crystalline reflections and the integrated of the non-crystalline background and comparing the two. In this research calculated percent of crystallinity from Ruland's Method [61].

The intensity of the x-rays scattered over all angles by a given assemblage of atoms is independent of their state of order or disorder. It follows that if the crystalline and amorphous scattering in the diffraction pattern can be separated from each other, the crystalline fraction is equal to the ratio of the integrated crystalline scattering to the total scattering, both crystalline and amorphous. In the ensuing treatment we shall adhere rather closely to the presentation given by Ruland. We designate the magnitude of reciprocal-lattice vector  $\rho_{hkl}$  by the symbol  $s$

$$s = \frac{2 \sin \theta}{\lambda} \quad (\text{Eq. 1})$$

The fraction of crystalline material in the specimen is given by

$$x_c = \frac{\int_{s_0}^{s_p} s^2 I_c ds}{\int_{s_0}^{s_p} s^2 I ds} \left( K(s_0, s_p, D, \bar{f}^2) \right) = \text{const.} \quad (\text{Eq. 2})$$

$I(s)$  = the intensity of coherent x-ray scatter from a specimen at the point  $s$  in reciprocal space.

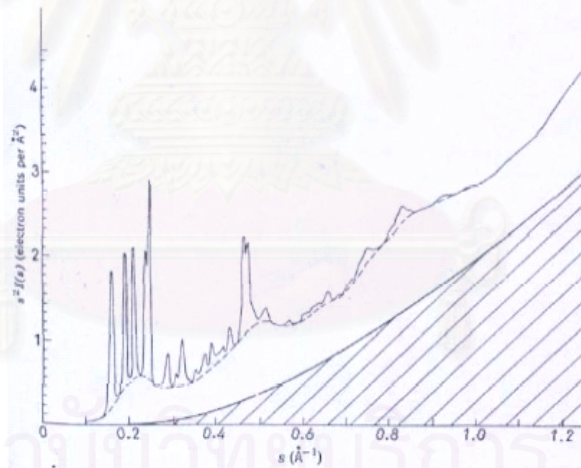
$I_c(s)$  = the part of the intensity at the same point that is concentrated in the crystalline peaks.

$\left( K(s_0, s_p, D, \bar{f}^2) \right)$  is lost from peaks and appears as diffuse scatter in the background as a result of atomic thermal vibrations and lattice imperfections.  $K$  can be found from the empirical chart and can be assume as a constant for each system.

However, Ruland found that calculated values of the coefficient

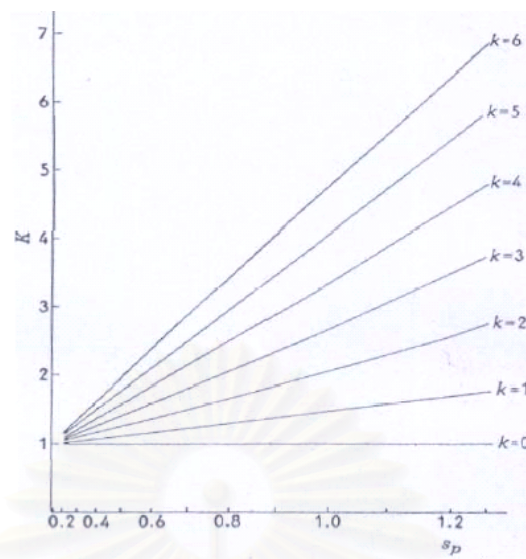
$$K = \frac{\int_{s_0}^{s_p} s^2 \bar{f}^2 ds}{\int_{s_0}^{s_p} s^2 \bar{f}^2 D ds} \quad (\text{Eq. 3})$$

Figure 5.6 shows the curve of  $s^2I(s)$  versus  $s$  of one of the polypropene. To determine  $x_c$  from the  $s^2I_c$  and  $s^2I$  curves of any specimen it is useful to prepare nomogram of  $K$  versus  $s_p$  for a range of values of the coefficient  $k$  in the lattice-imperfection factor  $D = \exp(-ks^2)$ . Such a nomogram, calculated by using (Eq. 3) for  $s_0 = 0.1$  and for  $\bar{f}^2$  corresponding to the chemical composition  $(\text{CH}_2)_n$ , is shown in Figure 5.7. It will be noticed that the curves of  $K$  versus  $s_p$  are nearly linear. For a given polypropene sample Ruland could read from this nomogram the optimal value of  $k$  to make  $x_c$  as nearly constant as possible irrespective of  $s_p$ .



**Figure 5.6** Curve of  $s^2I(s)$  versus  $s$  for polypropene [61].

From our angle of concern, the  $s_0$  and  $s_p$  is in the range of 0.1 to 0.3 which is quite narrow and in the left hand side limit of the chart. From Figure 5.6 and the limit of the integration, the base scattering can be assumed to be zero. From Figure 5.7, the values of  $K$  at different  $k$  are in the range of 1.0-1.2 which the value is close to 1.0 and in this thesis the values of  $K$  are assumed to be equal to 1.0.



**Figure 5.7** Nomogram of  $K$  values as a function of  $k$  and  $s_p$  calculated for the chemical composition  $(\text{CH}_2)_n$  and  $s_0 = 0.1$  [61].

X-ray diffraction pattern of each pure polymers, SPS blends and its blends with additives at various composition were shown in Figure 5.8-5.13.

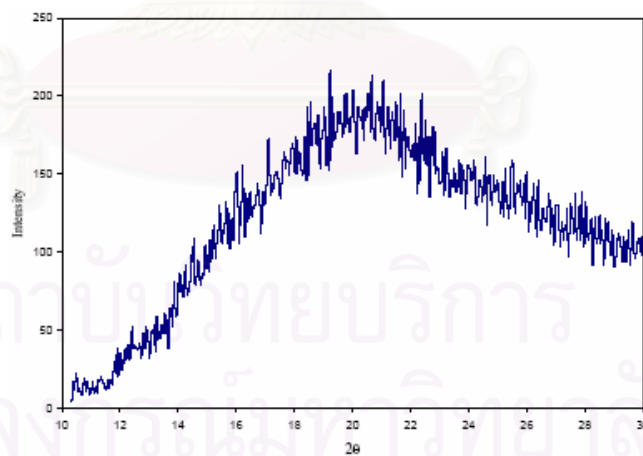
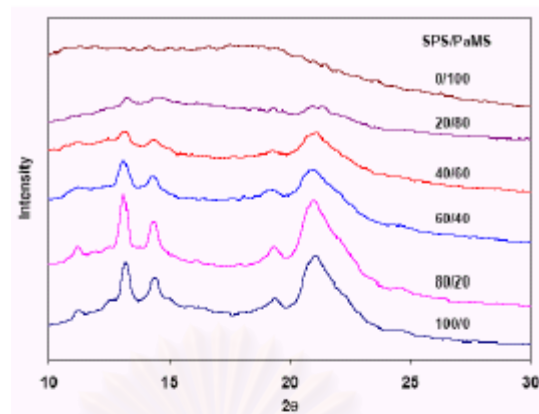
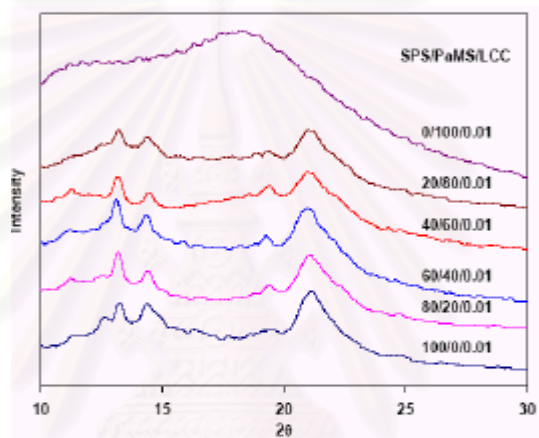


**Figure 5.8** X-ray diffraction pattern of amorphous SPS

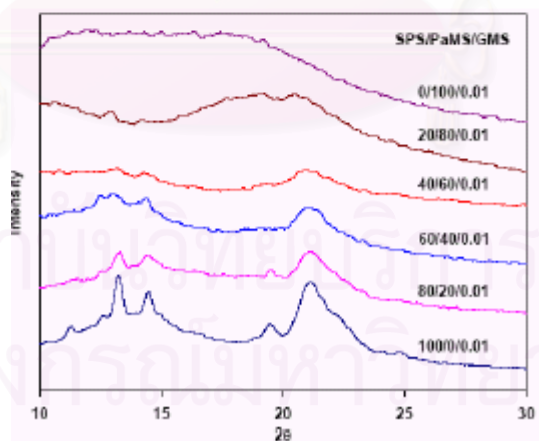




(a)

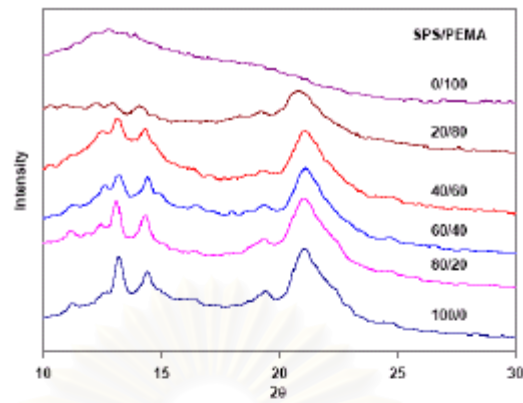


(b)

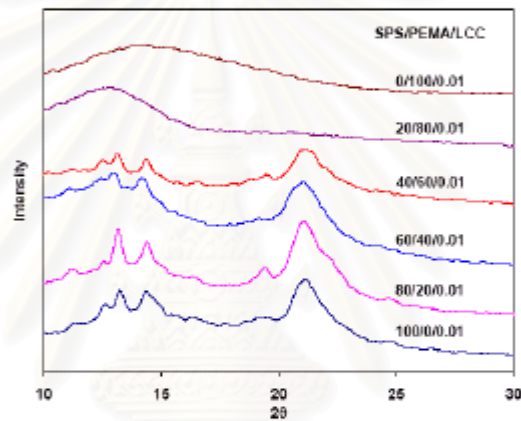


(c)

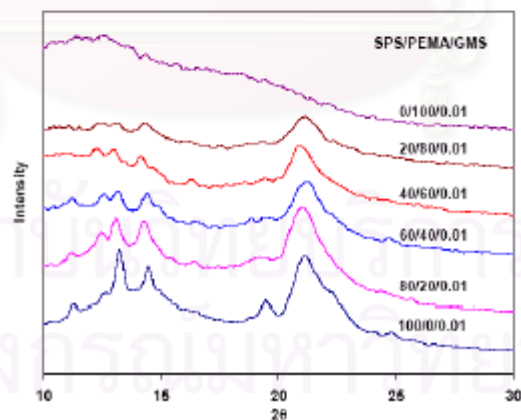
**Figure 5.9** The X-ray diffraction patterns for SPS/PaMS blends and their blend with additives at various compositions: (a) SPS/PaMS blends; (b) SPS/PaMS/LCC blends and (c) SPS/PaMS/GMS blends



(a)

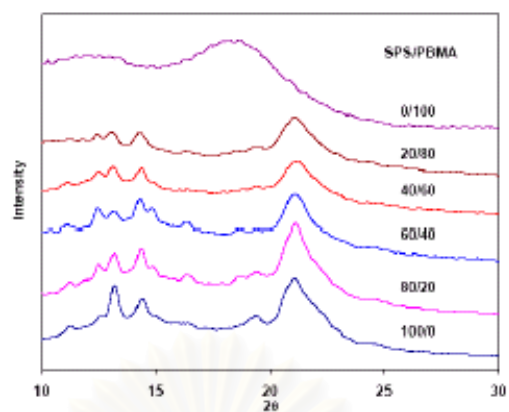


(b)

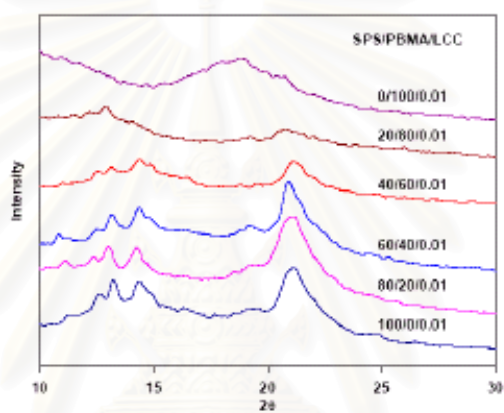


(c)

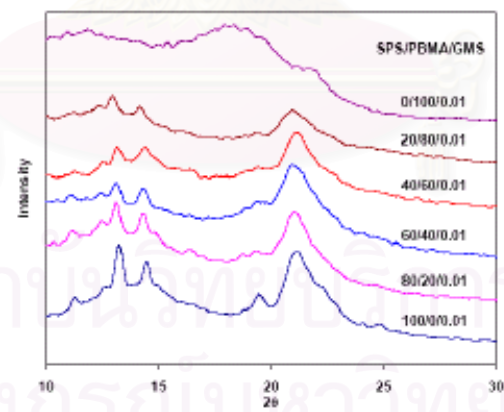
**Figure 5.10** The X-ray diffraction patterns for SPS/PEMA blends and their blend with additives at various compositions: (a) SPS/PEMA blends; (b) SPS/PEMA/LCC blends and (c) SPS/PEMA/GMS blends



(a)

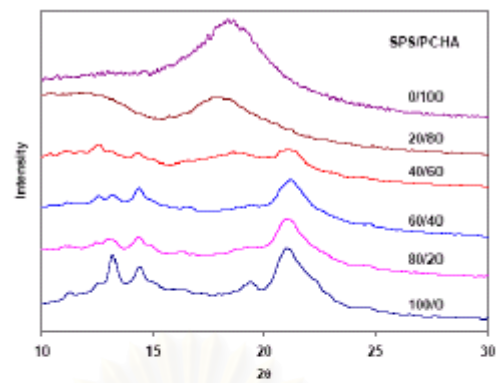


(b)

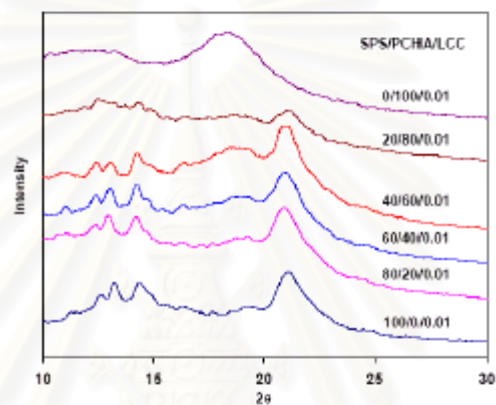


(c)

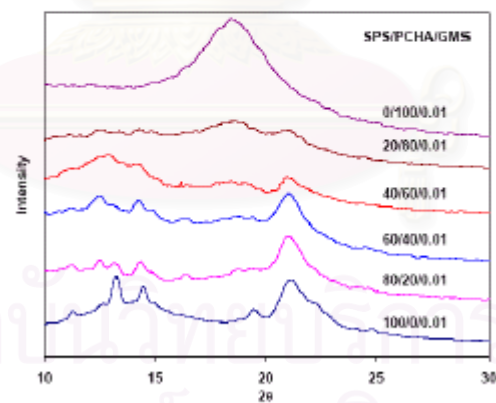
**Figure 5.11** The X-ray diffraction patterns for SPS/PBMA blends and their blend with additives at various compositions: (a) SPS/PBMA blends; (b) SPS/PBMA/LCC blends and (c) SPS/PBMA/GMS blends



(a)

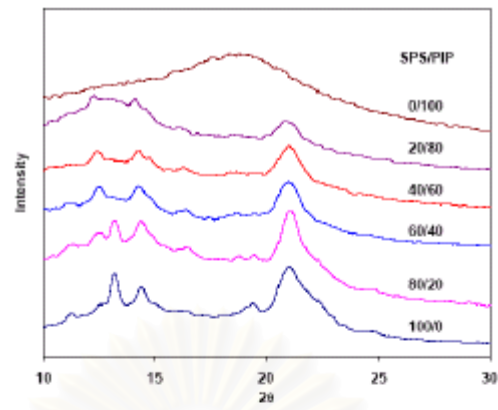


(b)

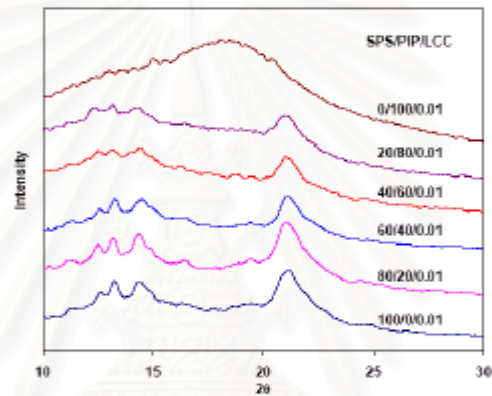


(c)

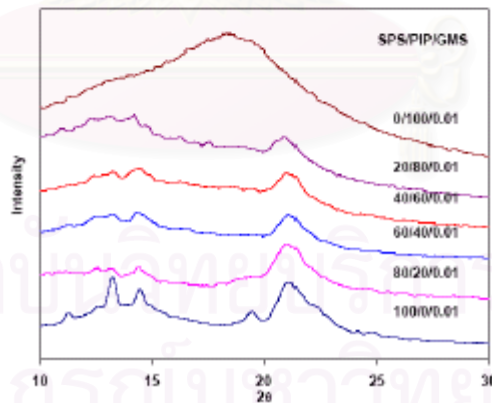
**Figure 5.12** The X-ray diffraction patterns for SPS/PCHA blends and their blend with additives at various compositions: (a) SPS/PCHA blends; (b) SPS/PCHA/LCC blends and (c) SPS/PCHA/GMS blends



(a)



(b)



(c)

**Figure 5.13** The X-ray diffraction patterns for SPS/PIP blends and their blend with additives at various compositions: (a) SPS/PIP blends; (b) SPS/PIP/LCC blends and (c) SPS/PIP/GMS blends

The percent crystallinity from Table 5.20-5.24 come from the XRD data of the blend and the pure component and were calculated according to the method that explain above.

**Table 5.20** %Crystallinity of SPS/PaMS, SPS/PaMS/GMS and SPS/PaMS/LCC blends at various compositions

% SPS	% Crystallinity		
	SPS/PaMS	SPS/PaMS/GMS	SPS/PaMS/LCC
40	19.37	38.54	20.00
60	23.93	27.27	23.49
80	38.42	27.23	28.98
100	57.26	49.59	51.63

Crystallinity measurements offer a useful way to ascertain the influence of PaMS on the crystallization behaviour of SPS/PaMS blends. Table 5.20 shows percent crystallinity of SPS/PaMS, SPS/PaMS/GMS and SPS/PaMS/LCC blends at various compositions. As the PaMS content increases, percent crystallinity decrease and there is a noticeable enhancement of the diffuse amorphous scattering. Comparison of two analytically characteristic results between DSC and XRD, the results of percent crystallinity correspond to the melting enthalpy results (Table 5.2-5.4).

When LCC and GMS were added into the pure SPS, percent crystallinity decreased about 6-7 %. But additives have no tendency to change percent crystallinity of SPS/PaMS blends. In other words, the pure SPS will decrease the percent of crystallinity when added the LCC or GMS, but in the blend of SPS and PaMS, the percent crystallinities of the blend were not affected from the additive.



**Table 5.21** %Crystallinity of SPS/PEMA, SPS/PEMA/GMS and SPS/PEMA/LCC blends at various compositions

% SPS	% Crystallinity		
	SPS/PEMA	SPS/PEMA/GMS	SPS/PEMA/LCC
40	27.00	29.33	31.58
60	37.25	35.38	41.07
80	41.43	44.75	44.41
100	57.26	49.59	51.63

From Table 5.21 shown percent of SPS/PEMA, SPS/PEMA/GMS and SPS/PEMA/LCC blends at various compositions. As the PEMA content increases, percent of the crystallinity decreases and there is a noticeable enhancement of the diffuse amorphous scattering. Moreover, LCC and GMS have no tendency to change percent of crystallinity of SPS/PEMA blends as same as SPS/PaMS blends.

**Table 5.22** %Crystallinity of SPS/PBMA, SPS/PBMA/GMS and SPS/PBMA/LCC blends at various compositions

% SPS	% Crystallinity		
	SPS/PBMA	SPS/PBMA/GMS	SPS/PBMA/LCC
40	39.57	36.95	34.79
60	36.65	34.12	30.58
80	37.79	38.12	41.94
100	57.26	49.59	51.63

Table 5.22 shown percent of SPS/PBMA, SPS/PBMA/GMS and SPS/PBMA/LCC blends at various compositions. As the PBMA content increases, percent of the crystallinity decreases and there is a noticeable enhancement of the diffuse amorphous scattering. For the effects of addition LCC and GMS, no effect in reduction of percent crystallinity of SPS/PBMA blends has occurred as well as SPS/PaMS blends.

**Table 5.23** %Crystallinity of SPS/PCHA, SPS/PCHA/GMS and SPS/PCHA/LCC blends at various compositions

% SPS	% Crystallinity		
	SPS/PCHA	SPS/PCHA/GMS	SPS/PCHA/LCC
40	34.80	37.00	28.93
60	46.77	36.50	28.38
80	43.68	40.34	29.49
100	57.26	49.59	51.63

From Table 5.23 shown percent of SPS/PCHA, SPS/PCHA/GMS and SPS/PCHA/LCC blends at various compositions. As the PCHA content increases, percent of crystallinity decreases and there is a noticeable enhancement of the diffuse amorphous scattering. For the effect of addition GMS, percent crystallinity of SPS/PCHA blends will slightly decrease and LCC have more pronounce effects than GMS.

**Table 5.24** %Crystallinity of SPS/PIP, SPS/PIP/GMS and SPS/PIP/LCC blends at various compositions

% SPS	% Crystallinity		
	SPS/PIP	SPS/PIP/GMS	SPS/PIP/LCC
40	23.37	21.58	24.45
60	27.76	29.70	31.13
80	32.62	43.00	31.34
100	57.26	49.59	51.63

Table 5.24 shown percent of SPS/PIP, SPS/PIP/GMS and SPS/PIP/LCC blends at various compositions. As the PIP content increased percent of crystallinity decreased and there is a noticeable enhancement of the diffuse amorphous scattering. For the effect of addition LCC and GMS no reduction in percent crystallinity of SPS/PIP blends were found.

From these results, the addition of GMS or LCC affects the percent crystallinity of the pure SPS. However when compare the additive less blend with the blend with LCC or GMS, no distinct change in the percent crystallinities were clearly found.

### **5.6 Effect of Blend on Crystal Formation**

From percent of crystallinity in Table 5.20-5.24, it is expected that when decrease the percent of SPS in the blend, the percent crystallinities were decreased. However, in the first reduction of SPS to 80%wt, the percent of the crystallinity dramatically decrease compare to other concentrations. This results correspond to the DSC result that detect the dramatically decrease in  $T_g$  in 80%wt SPS samples. Compare to other concentration, both XRD and DSC results show the slightly decrease the  $T_g$  when added the SPS but in the small amount compare to 80%wt samples.

With the same phenomenon found in various systems when the percent crystallinity drop down in the first addition of polymer pair at the low percent of the polymer pair (90%wt SPS), the characters of the SPS system can be predicted. However, the decrease in the percent crystallinity of the blend at different composition of polymer pair are less significant which may results from the lower amount of SPS in the blend, therefore less crystals are affected.

## CHAPTER VI

### CONCLUSIONS AND SUGGESTIONS

#### 6.1 Conclusions

In this research, the miscibility of SPS blends were investigated. The SPS which synthesized by using metallocene catalyst, with several polymers such as poly( $\alpha$ -methyl styrene), poly(ethyl methacrylate), poly(*n*-butyl methacrylate), poly(cyclohexyl acrylate), poly(*cis*-isoprene) and poly(vinyl methyl ether). Moreover, effects of addition additives to crystallinity of their blends were also studied. The conclusion of this research can be summarized as follow:

1. From DSC, it was found that the SPS have tendency to miscible with poly( $\alpha$ -methyl styrene), poly(ethyl methacrylate), poly(*n*-butyl methacrylate), poly(cyclohexyl acrylate) and poly(*cis*-isoprene) by melt mixing method, but the phase separation were found in the systems of poly(vinyl methyl ether) blends.
2. The glass transition temperatures of all the blends with additives do not significantly change from no additive binary blends. This phenomenon proves that additives do not have direct plasticizing effects on glass transition temperature of pure binary blends.
3. The CBC-33 and GMS slightly decrease crystalline melting temperature of their blends. Because CBC-33 and GMS reduce melt viscosity of the blends, crystal of the blends will melt easier. In other words, the  $T_m$  tend to decrease when added with GMS or LCC which are affected from the mobility of the molecules.
4. Both LCC and GMS slightly decrease  $T_c$  of polymer blends. Because LCC and GMS reduce melt viscosity of the blends, the molecule could move or separate

easily, therefore crystals difficult form to crystalline. Therefore when mobile melt molecule tend to form the crystal, it will hardly form the crystal in case of GMS and LCC addition in the blend. In other words,  $T_c$  will be decrease in the case of adding GMS or LCC because the high mobility of the polymer molecules.

5. This research show the effects of the blend preparation that is the melt mixing method and the solution casting methods. In the small size samples, the melted mixing method cannot produce the truly homogeneous sample when compare with the solvent casting method. The results from melt mixing show the high concentration of SPS while the solution casting results show the different trend. Moreover, the Flory-Fox equation of  $T_g$  can not well predict the blends  $T_g$  both in the melted mixing and the solvent casting method.
6. From XRD results, the percent crystallinity of the blend will be decrease when decrease the percent of SPS in the blend. These may be resulted from the larger amorphous phase in the case of low concentration of SPS.
7. From XRD results, the addition of GMS or LCC affect the percent crystallinity of the pure SPS. However when compare the pure blend with the blend with LCC or GMS, no distinct change in the percent crystallinities were clearly found.

## 6.2 Suggestions

The recommendations for further research may be given as follows:

1. Other pairs between semicrystalline polymer and amorphous polymer should be chosen for studying in order to found the pronounce effects of the addition of GMS or LCC.
2. Choose other models for predict  $T_g$  of polymer blends such as Gordon-Taylor equation.
3. This research can be extended to the study of the mechanism of additive for the decreasing the % crystallinity of the blends.
4. It should be interesting to study mechanical properties of polymer blends.



สถาบันวิทยบริการ  
จุฬาลงกรณ์มหาวิทยาลัย



## REFERENCES

1. Ishihara N, Kuramoto M, Uoi M. **Macromolecules** 1998; 21:3356.
2. Guerra G, Vitagliano VM, De Rosa C, Petraccone V, Corradini P. **Macromolecules** 1990; 23:1539.
3. Lee D-H, Yoon K-B, Lee E-H, Noh S-K. **Polymer (Korea)** 1995; 19:700.
4. Grassi A, Longo P, Guerra G. **Makromol. Chem. Rapid Commun.** 1989; 10:687.
5. Sun Z, Morgan RJ, Lewis DN. **Polymer** 1992; 33:660.
6. Min K-E, Hong S, Lee D-H. **Polymer (Korea)** 1996; 20:601.
7. Yee AF. **Polym. Eng. Sci.** 1977; 17:213.
8. Candi FD, Romano G, Russo R, Vittoria V. **Colloid Polym. Sci.** 1990; 268:720.
9. Cimmino S, Di Pace E, Martuscelli E, Silvestre C. **Polymer** 1991; 32:1080.
10. Utracki L.A., **Polymer Blends Handbook**, volume 1, London, 2002.
11. Lutz, John. T. Jr. and Grossman, Richard. F., **Polymer Modifiers and Additives**, New York, Marcel Dekker, 2001.
12. Patwardhan A.A. and Belfiore L.A. **Polym. Eng. Sci.** 1988; 28:916.
13. Ishihara N, Seimiya T, Kuramoto M and Uoi M. **Macromolecules** 1986; 19:2464.
14. Kobayashi M, Nakaoki T, and Ishihara N. **Macromolecules** 1989; 22:4377.
15. Zambelli A, Oliva L and Pellecchia C. **Macromolecules** 1989; 22:2129.
16. Kaminsky W. **Macromolecules** 1997; 30:7647.
17. Ready T.E., Day R.O., Chien J.C.W. and Rausch M.D. **Macromolecules** 1993; 26:5822.
18. Tomotsu N, Kuramoto M, Takeuchi M and Maezawa H. **Metallocenes** 1996; 96:211.
19. Chien J.C.W. **Metallocenes** 1996; 96:223.
20. Tomotsu N, Ishihara N, Newman T.H. and Malanga M.T. **J. Mole. Cat. A.** 1998; 128:167.
21. Yang M, Cha C and Shen Z. **Polym. J.** 1990; 22:919.
22. Miyashita A, Nabika M and Suzuki T. **40<sup>th</sup> Japanese Symposium on Organometallic Chemistry, abstract**, 1993, p. 46.
23. Utraki L.A. **Polym. Eng. Sci.** 1982; 22:1165.

24. Allcock H.R. and Lampe F.W. **Contemporary Polymer Chemistry**, 2<sup>nd</sup> ed., Prentice Hall Inc, New Jersey, 1990.
25. Widmaier J.M. and Mignard G. **Eur. Polym. J.** 1987; 23:989.
26. Cimmino S, Di Pace E, Martuscelli E and Silvestre C. **Polymer** 1993; 34:2799.
27. Cimmino S, Di Pace E, Martuscelli E, Silvestre C, Rice D.M. and Karasz F.E. **Polymer** 1993; 34:214.
28. Mendal T.K. and Woo E.M. **Polymer** 1999; 40:2813.
29. Guerra G, Vitagliano VM, De Rosa C, Petraccone V, Corradini P. **J. Polym. Sci. Part. B: Polym. Phys.** 1991; 29:265.
30. Choi S.H., Cho I and Kim K.U. **Polym. J.** 1999; 31:828.
31. Li H, Li G, Yang W and Shen J. **Polym. Prepr. Am. Chem. Soc. Div. Polym. Chem.** 1998; 39:689.
32. Hong B.K., Jo W.H., Lee S.C. and Kim J. **Polymer** 1998; 39:1793.
33. Bonnet M, Buhk M, Trogner G, Rogausch K.D. and Petermann J. **Acta. Polym.** 1998; 49:174.
34. Hong B.K., Jo W.H. and Kim J. **Polymer** 1998; 39:3753.
35. Buckley A., Conciatori A.B. and Calundann G.W. **U.S. Patent** 1984; 4,434,262.
36. Siegmann A., Dagan A. and Kenig S. **Polymer** 1985; 26:1325.
37. Tariq M.M., Pierre J.C. and Nathalie C. **Polym. Eng. Sci.** 1989; 29:600.
38. Lin Y.C., Lee H.W. and Winter H.H. **Polymer** 1994; 34:4703.
39. Anchana Chuenchaokit. **Effects of Thermotropic Liquid Crystal on Properties of Polycarbonates.** Master's Thesis, Department of Chemical Engineering, Graduate School, Chulalongkorn University, 1998.
40. Suraphan Powanusorn. **Application of Low Molar Mass Thermotropic Liquid Crystals as an Additive for Polymers.** Master's Thesis, Department of Chemical Engineering, Graduate School, Chulalongkorn University, 2000.
41. Noppawan Motong. **Effect of Mixing and Processing on the Viscosity of Polycarbonat blends with Low Molar Mass Liquid Crystal.** Master's Thesis, Department of Chemical Engineering, Graduate School, Chulalongkorn University, 2002.
42. Wacharawichananta S, Thongyai S, Tanodekaewb S, Higginsc J.S. and Clarke N. **Polymer** 2004; 45:2201.

43. Pinrat Pinweha. **Titanocene Catalysts with Boron Cocatalyst for Syndiotactic Polymerization of Styrene** Master's Thesis, Program of Petrochemistry and Polymer Science, Graduate School, Chulalongkorn University, 2000.
44. Wild F.R.W.P., Wasincioneck M., Huntner G. and Brintzinger H.H. **J. Organomet. Chem.** 1985; 63: 288.
45. Schellenberg J. and Tomotsu N. **Prog. Polym. Sci.** 2002; 27:1925.
46. Boleslawski M and Pasynkiewicz S. **J. Organomet. Chem.** 1972; 43:81.
47. Ueyama N, Araki T and Tani H. **Inorg. Chem.** 1973; 12:2218.
48. Mani R.and Burns C.M. **Polymer.** 1993; 34:1941.
49. Hervig J.and Kaminsky W. **Polym. Bull.** 1983; 9:464.
50. Huang J and Rampel G.L. **Prog. Polym. Sci.** 1995; 20:459.
51. Scheirs J.and Priddy D.B. **Modern Styrenic Polymers: Polystyrene and Styrenic Copolymers**, England, John Wiley & Son (2003).
52. Sperling L.H. **Introduction to Physical Polymer Science**, 3<sup>rd</sup> Ed., John Wiley & Sons, Inc., 2001.
53. Netfirms. **Introduction to Liquid Crystals**, Available from <http://adminnet.eng.ox.ac.uk/lc.research/introf.html>.
54. Netfirms. **Polymer Liquid Crystals**, Available from <http://plc.cwru.edu/tutorial/enhanced/files/lindex.html>.
55. Gray G.W. **Molecular Structure and the Properties of Liquid Crystals**, London,Academic Press, 1962.
56. Demus D, Goodby J, Gray G.W., Spiess H.W. and Vill V. **Handbook of Liquid Crystals**, Vol. 2A: Low Molecular Weight Liquid Crystals I, New York, Wiley-VCH, 1998.
57. Cifferri A., Krigbaum W.R. and Meyer R.B. **Polymer Liquid Crystal**, London, Academic Press, 1982.
58. Achanai Buasri. **Effects of Low Molar Mass Liquid Crystal Addition on Crystal Structure of Syndiotactic Polystyrene**, Master's Thesis, Department of Chemical Engineering, Graduate School, Chulalongkorn University, 2003.
59. Brandrup J. and Immergut E.H. **Polymer Handbook**, 3<sup>rd</sup> ed., New York, John Wiley&Sons, 1989.

60. Ampaipun Sivavichchakij. **Effects of Molecular Weight of Syndiotactic Polystyrene on the Miscibility of the Polymer Blends**, Master's Thesis, Department of Chemical Engineering, Graduate School, Chulalongkorn University, 2004.
61. Alexander L.E., **X-ray Diffraction Methods in Polymer Science**, New York, John Wiley & Sons, 1969.



สถาบันวิทยบริการ  
จุฬาลงกรณ์มหาวิทยาลัย



**APPENDIX**

สถาบันวิทยบริการ  
จุฬาลงกรณ์มหาวิทยาลัย

Appendix A: The Data of DSC Characterization

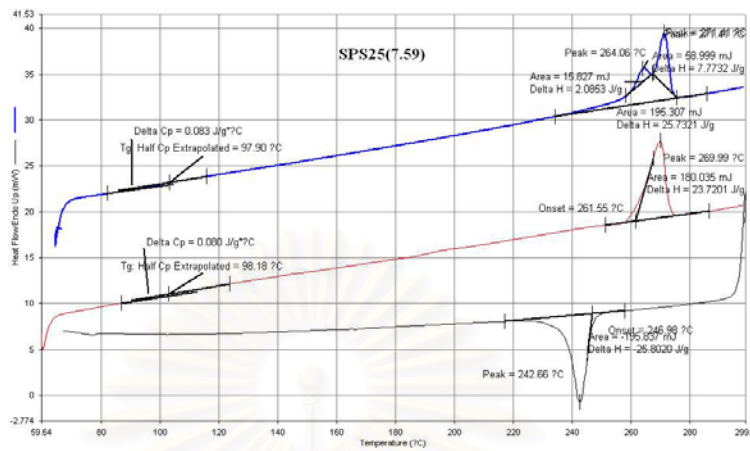


Figure A.1 DSC curve of SPS

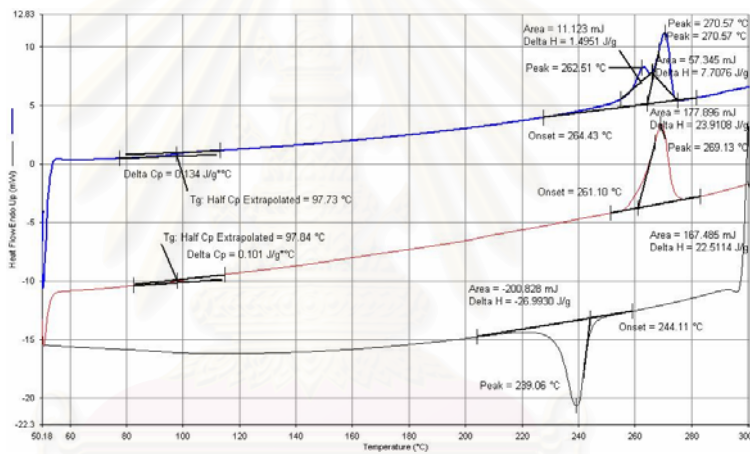


Figure A.2 DSC curve of SPS blended with LCC

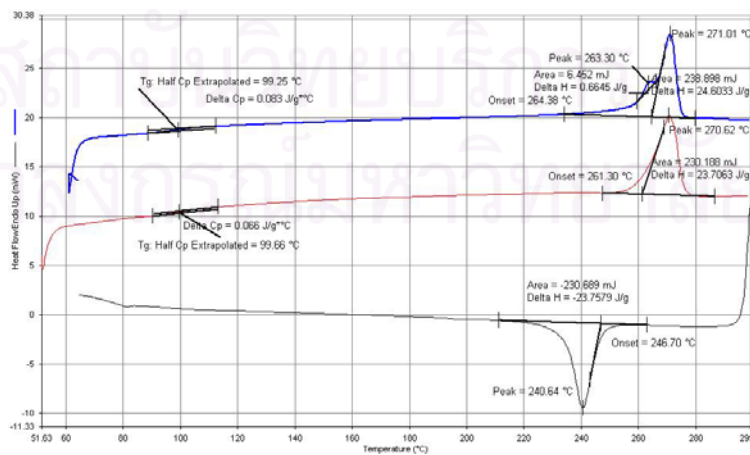
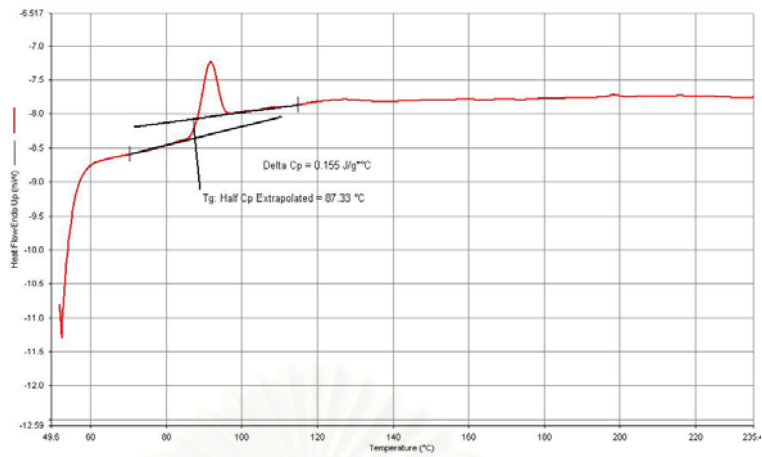
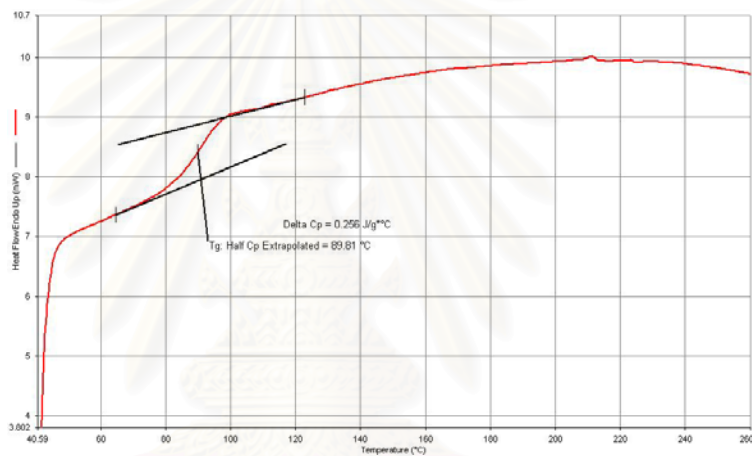


Figure A.3 DSC curve of SPS blended with GMS





**Figure A.4** DSC curve of PaMS



**Figure A.5** DSC curve of PaMS blended with LCC

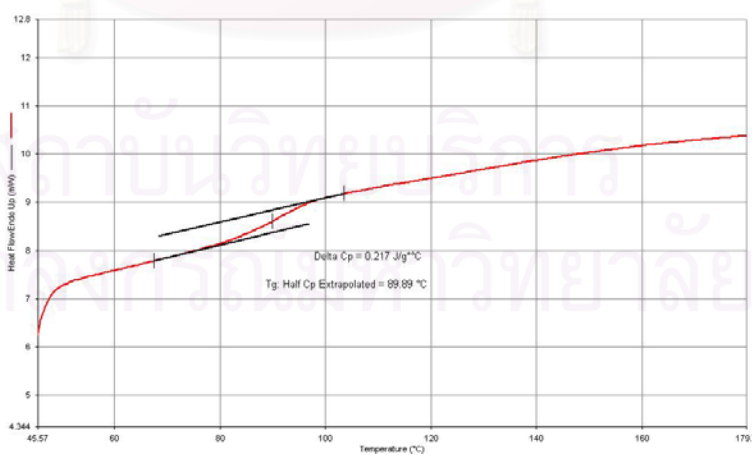


**Figure A.6** DSC curve of PaMS blended with GMS

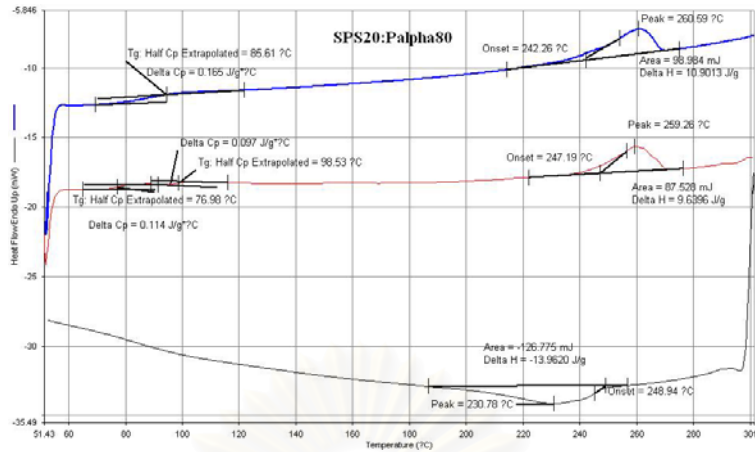


Figure A.7 DSC curve of SPS20/PaMS80 blends

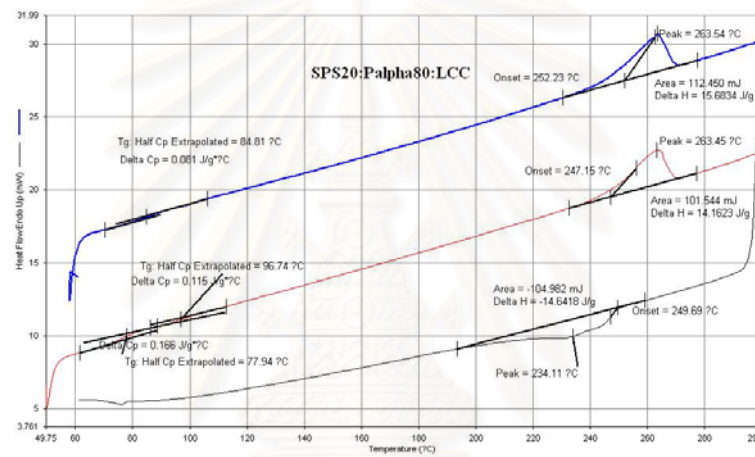


Figure A.8 DSC curve of SPS20/PaMS80/LCC blends

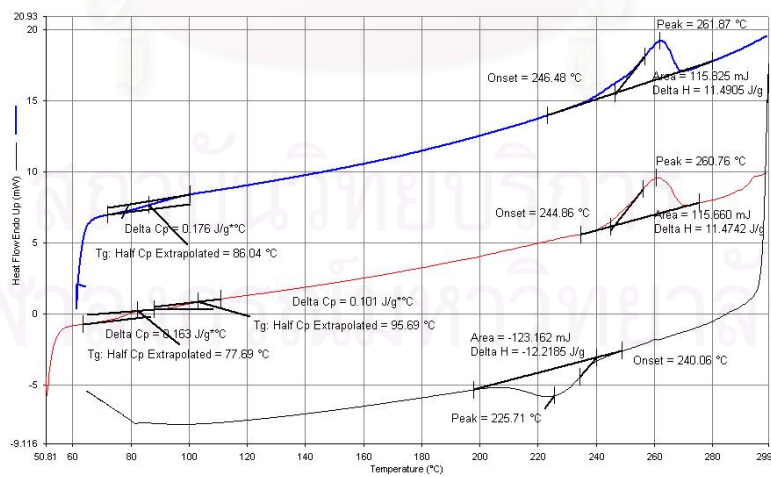


Figure A.9 DSC curve of SPS20/PaMS80/GMS blends

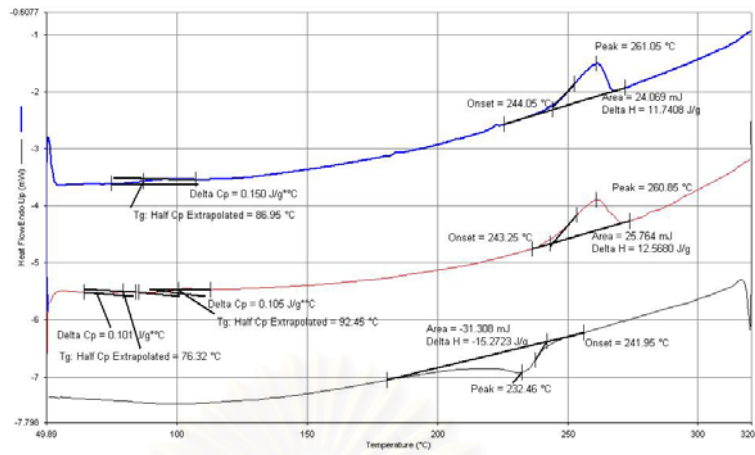


Figure A.10 DSC curve of SPS40/PaMS60 blends

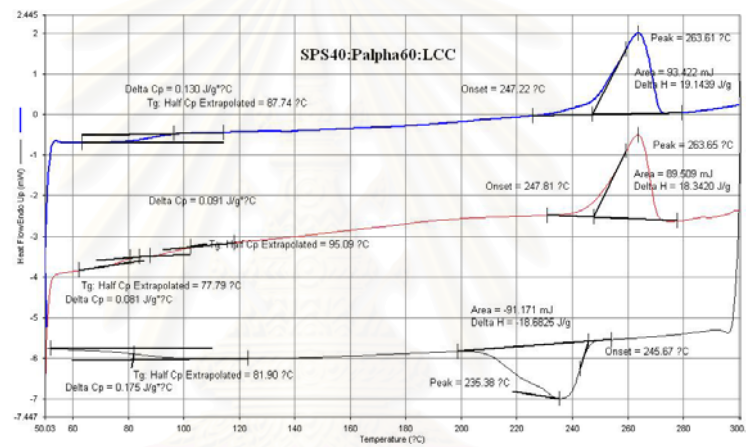


Figure A.11 DSC curve of SPS40/PaMS60/LCC blends

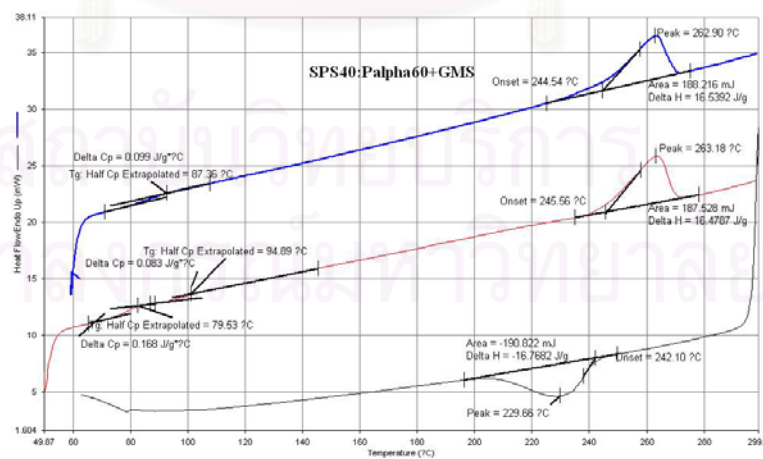


Figure A.12 DSC curve of SPS40/PaMS60/GMS blends

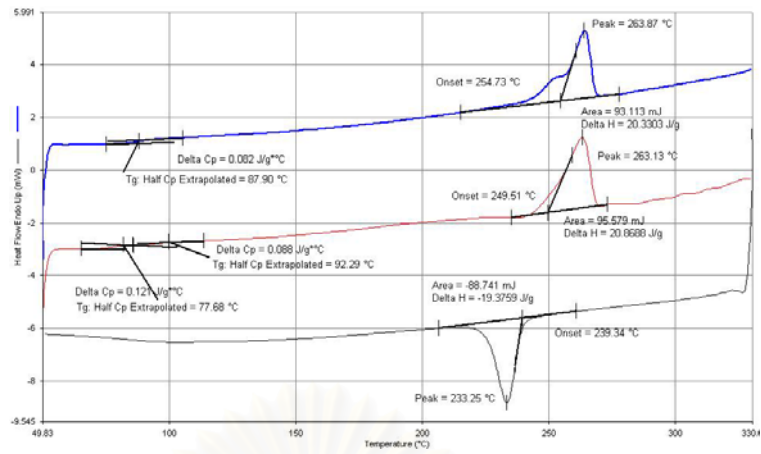


Figure A.13 DSC curve of SPS60/PaMS40 blends

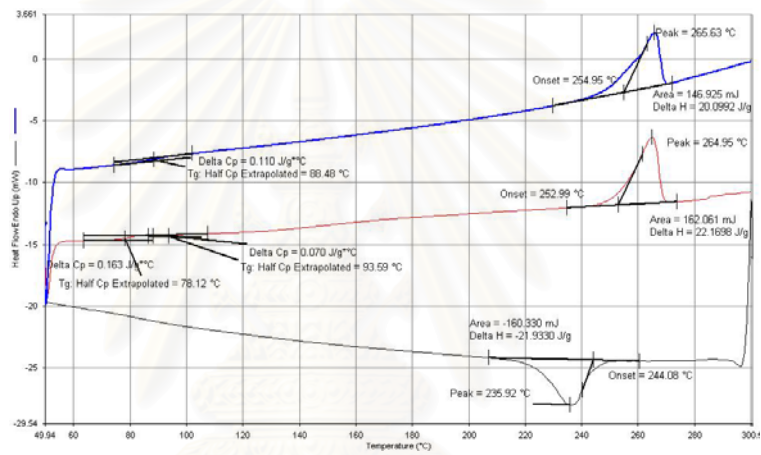


Figure A.14 DSC curve of SPS60/PaMS40/LCC blends

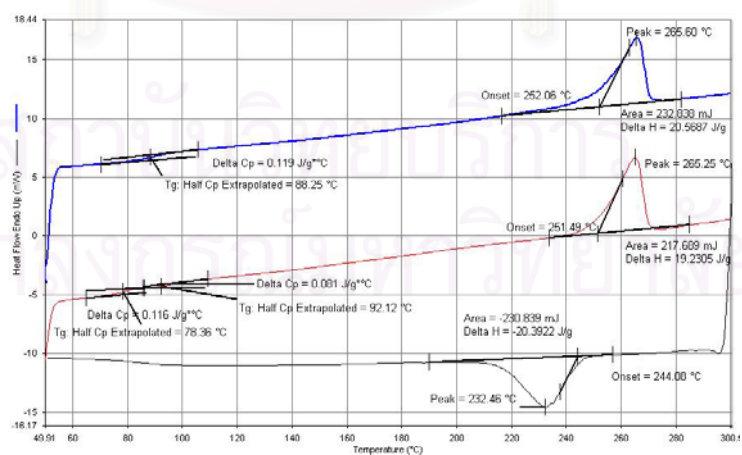


Figure A.15 DSC curve of SPS60/PaMS40/GMS blends

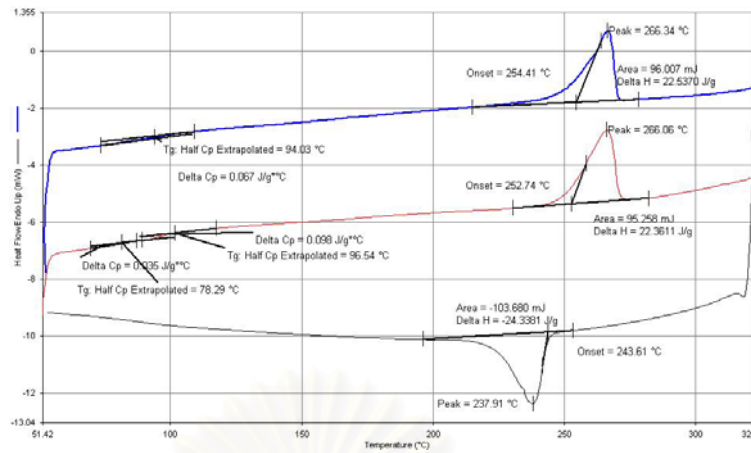


Figure A.16 DSC curve of SPS80/PaMS20 blends

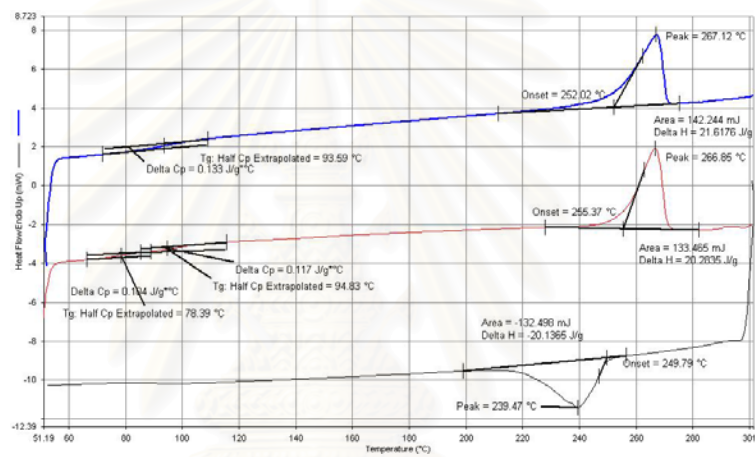


Figure A.17 DSC curve of SPS80/PaMS20/LCC blends

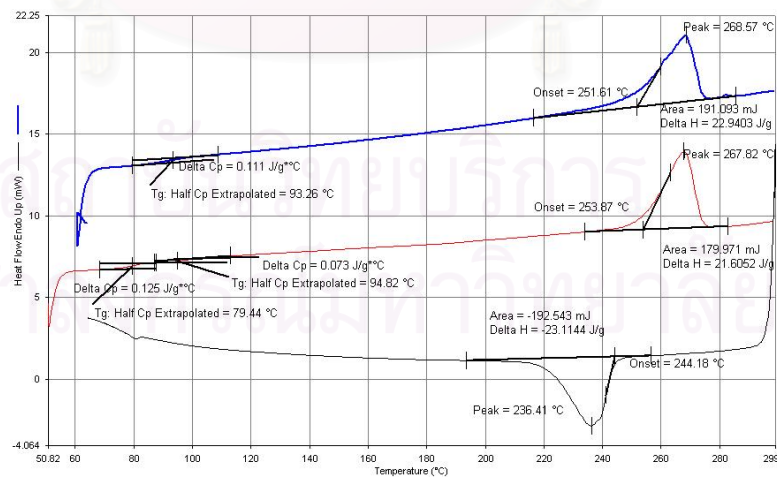
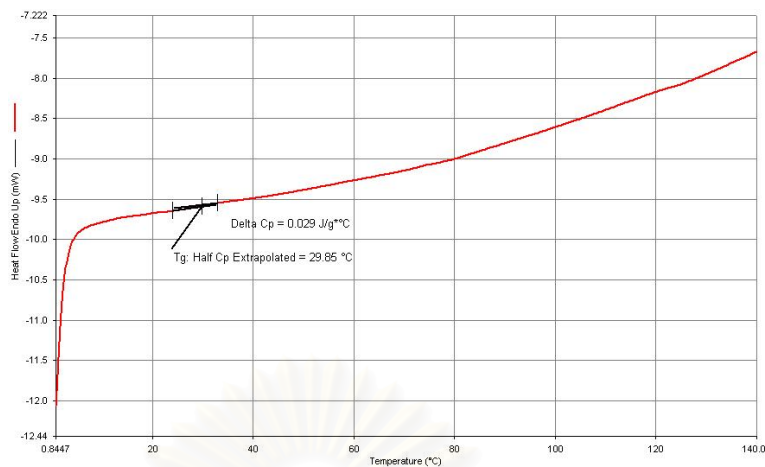
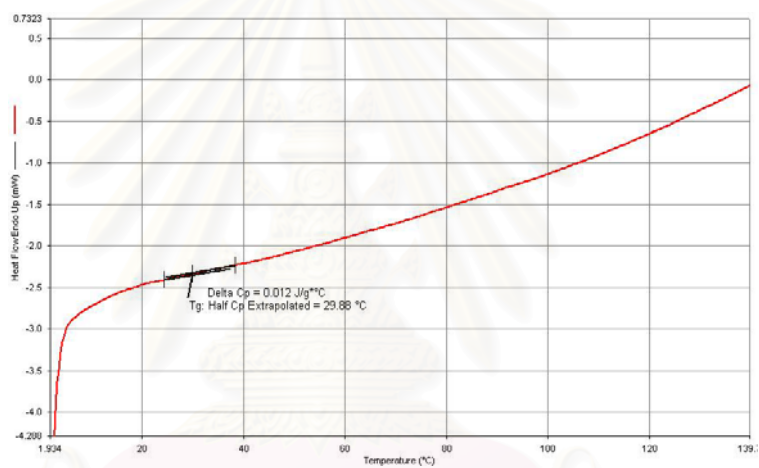


Figure A.18 DSC curve of SPS80/PaMS20/GMS blends



**Figure A.19** DSC curve of PBMA



**Figure A.20** DSC curve of PBMA blended with LCC

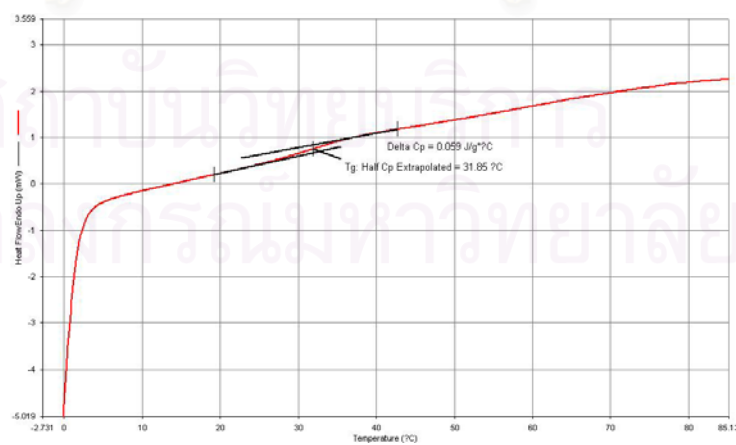


**Figure A.21** DSC curve of PBMA blended with GMS



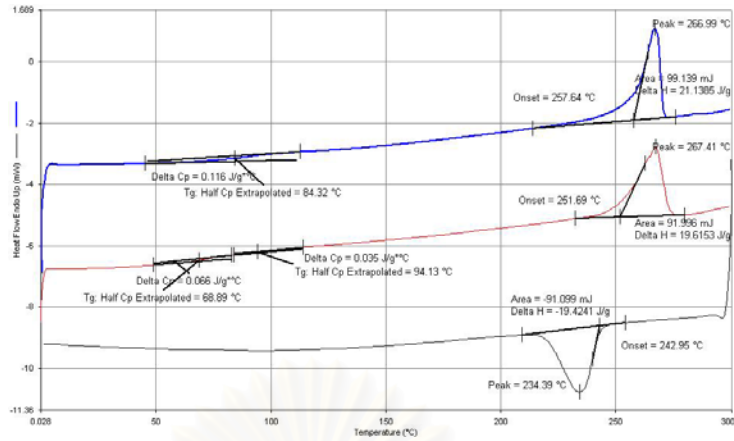


Figure A.22 DSC curve of SPS20/PBMA80 blends

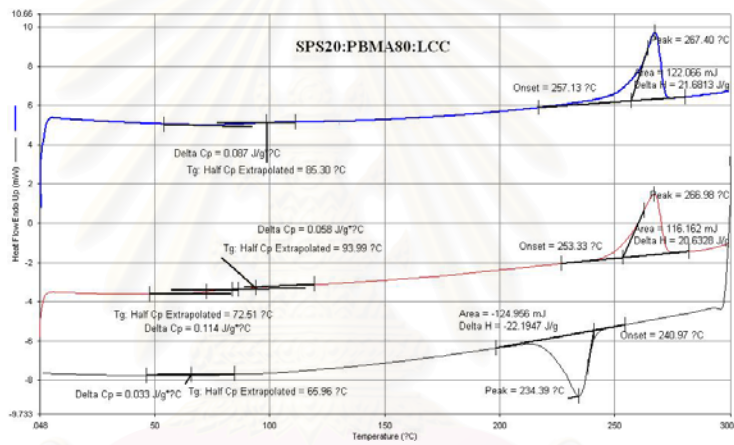


Figure A.23 DSC curve of SPS20/PBMA80/LCC blends

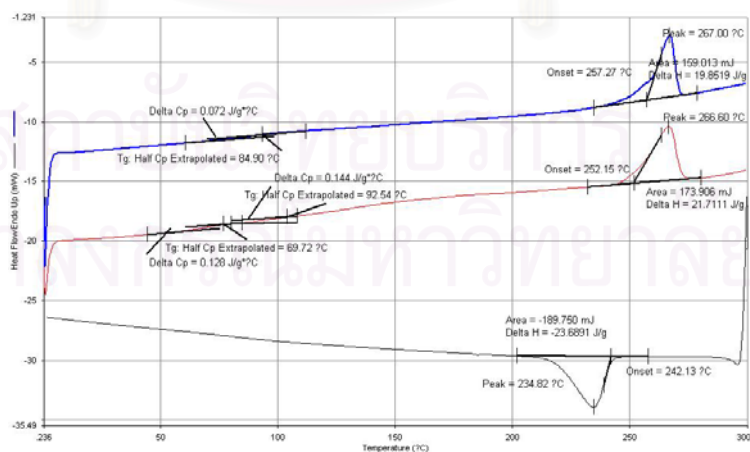


Figure A.24 DSC curve of SPS20/PBMA80/GMS blends

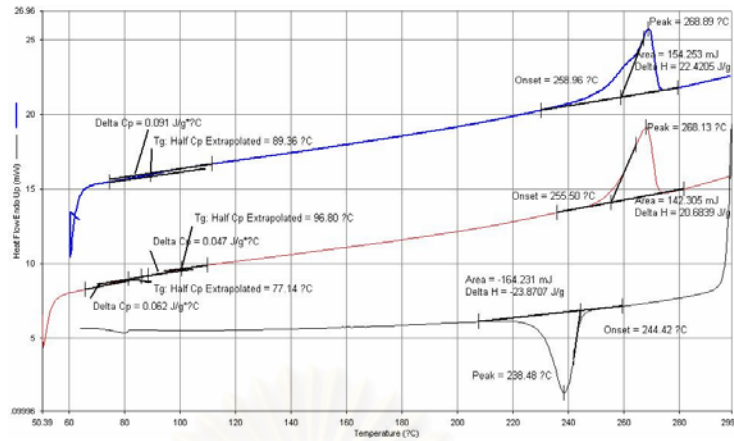


Figure A.25 DSC curve of SPS40/PBMA60 blends

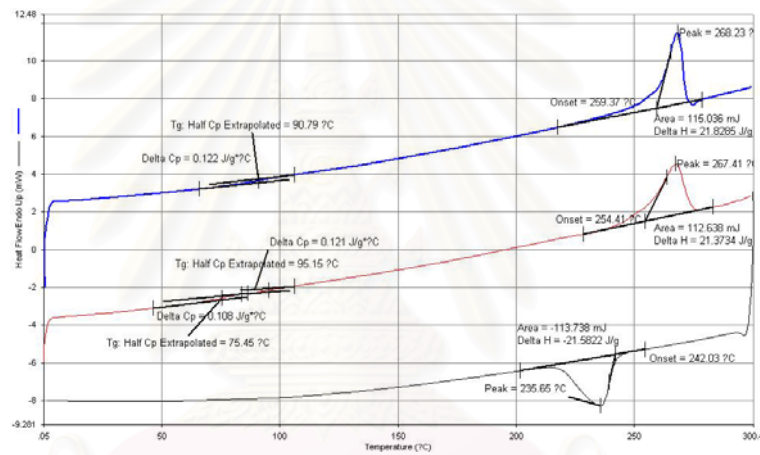


Figure A.26 DSC curve of SPS40/PBMA60/LCC blends

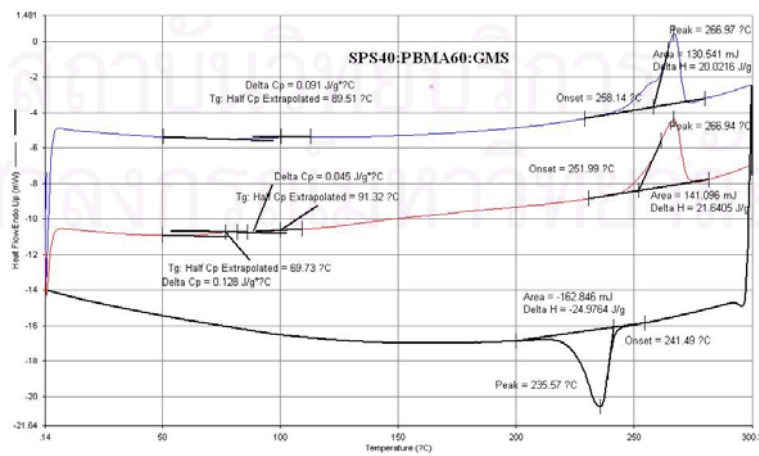


Figure A.27 DSC curve of SPS40/PBMA60/GMS blends

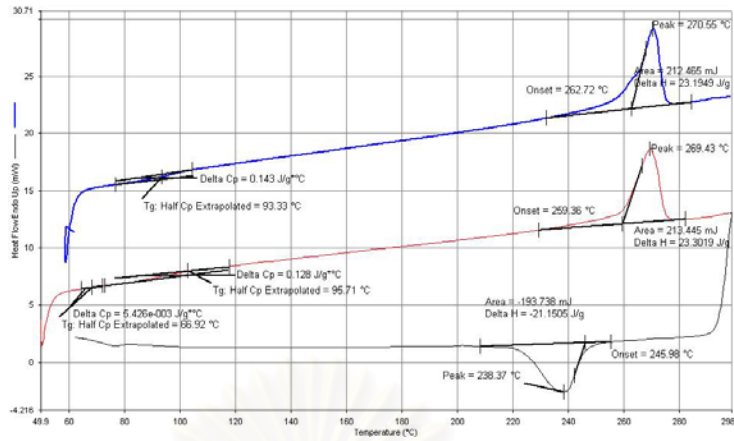


Figure A.28 DSC curve of SPS60/PBMA40 blends

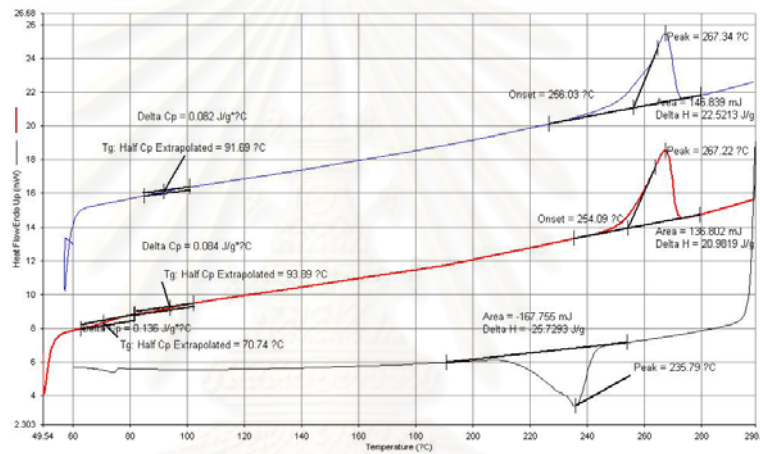


Figure A.29 DSC curve of SPS60/PBMA40/LCC blends

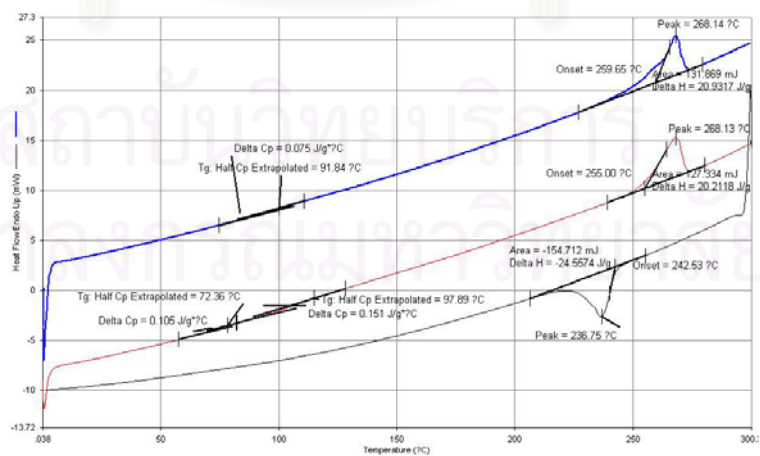


Figure A.30 DSC curve of SPS60/PBMA40/GMS blends

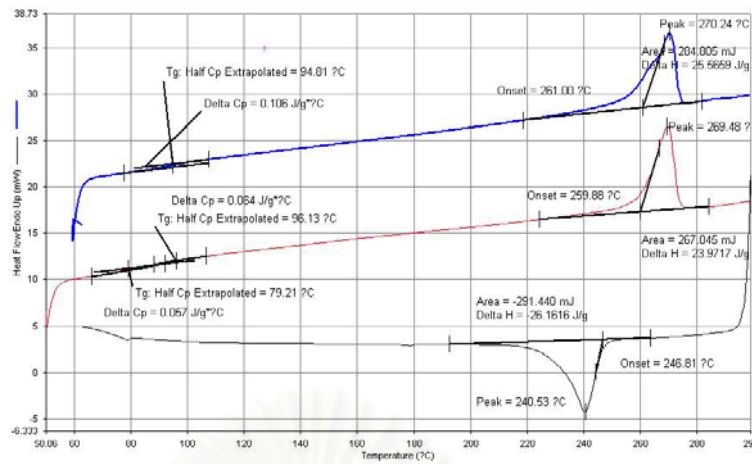


Figure A.31 DSC curve of SPS80/PBMA20 blends

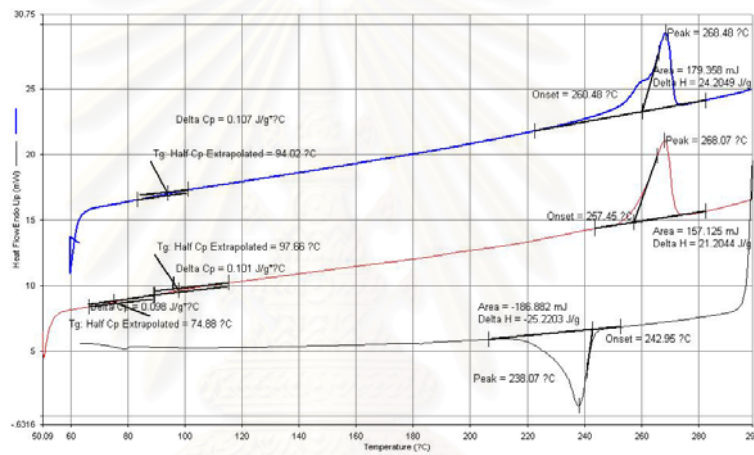


Figure A.32 DSC curve of SPS80/PBMA20/LCC blends

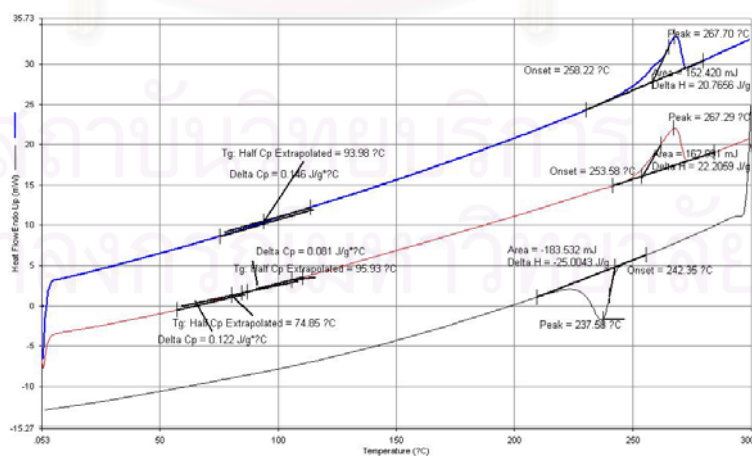
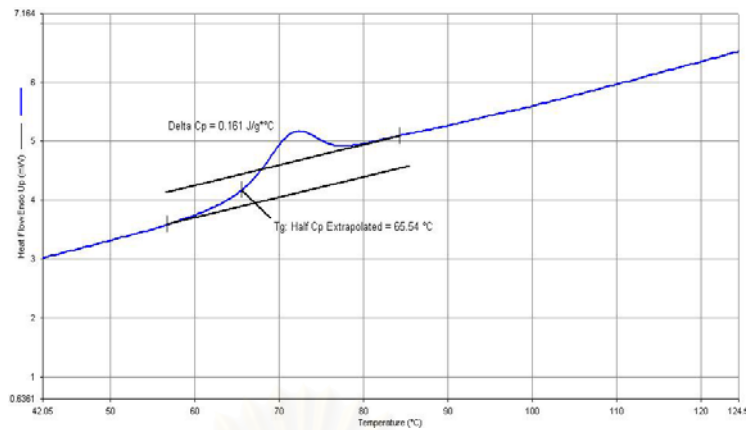
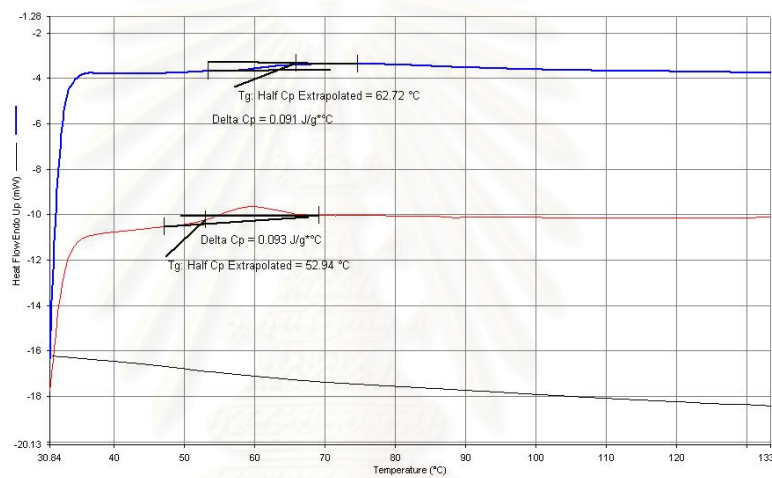


Figure A.33 DSC curve of SPS80/PBMA20/GMS blends



**Figure A.34** DSC curve of PEMA



**Figure A.35** DSC curve of PEMA blended with LCC

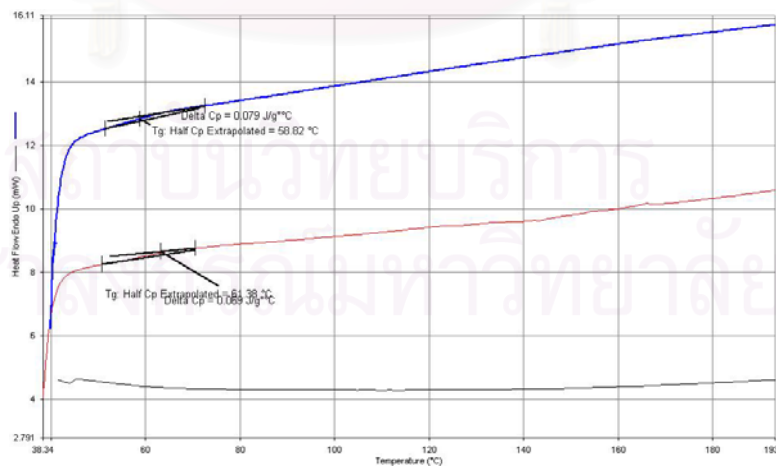


**Figure A.36** DSC curve of PEMA blended with GMS

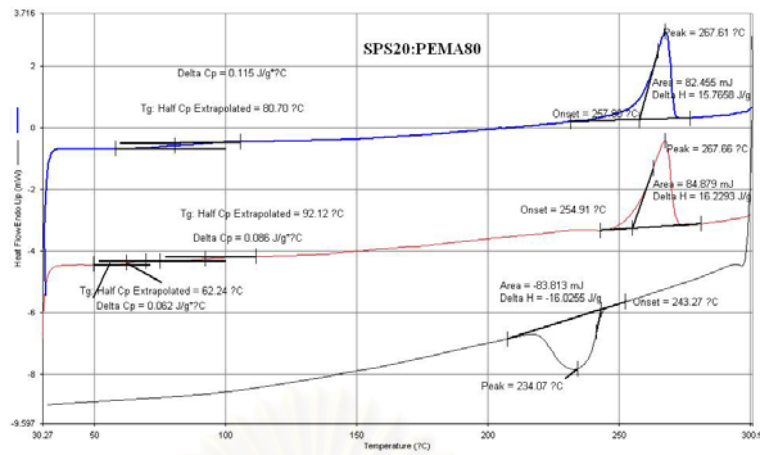


**Figure A.37** DSC curve of SPS20/PEMA80 blends

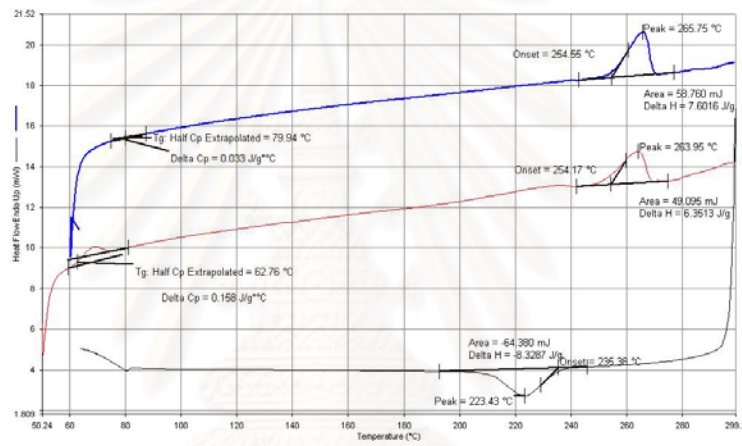


**Figure A.38** DSC curve of SPS20/PEMA80/LCC blends

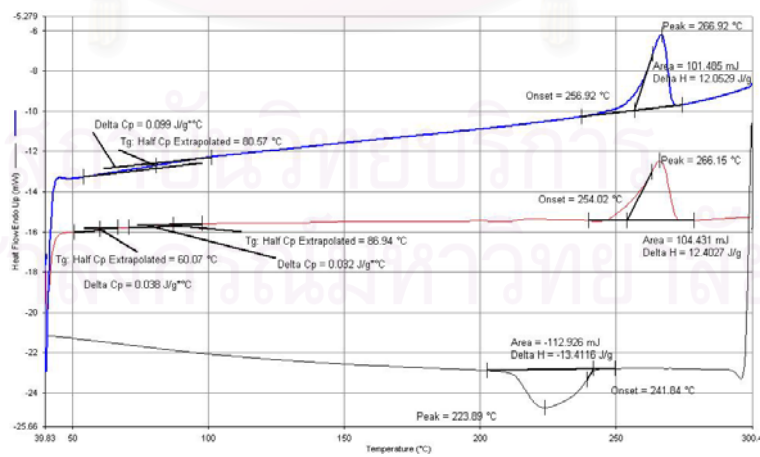


**Figure A.39** DSC curve of SPS20/PEMA80/GMS blends



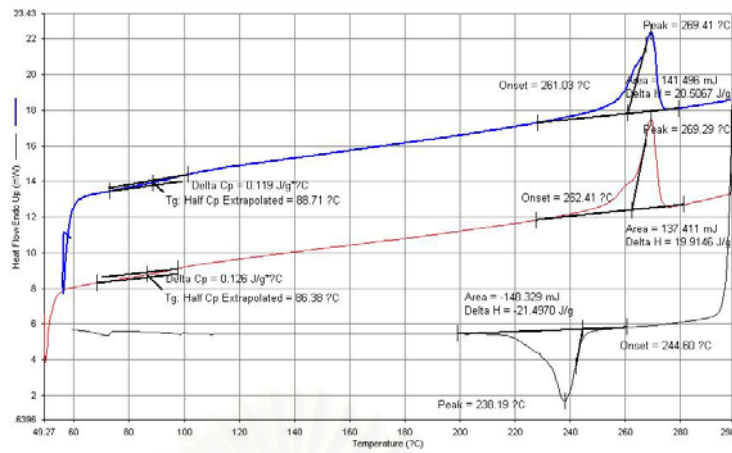


Figure A.40 DSC curve of SPS40/PEMA60 blends

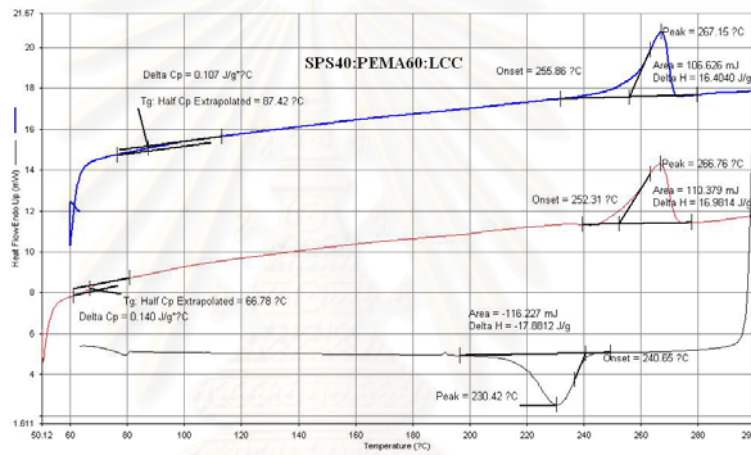


Figure A.41 DSC curve of SPS40/PEMA60/LCC blends

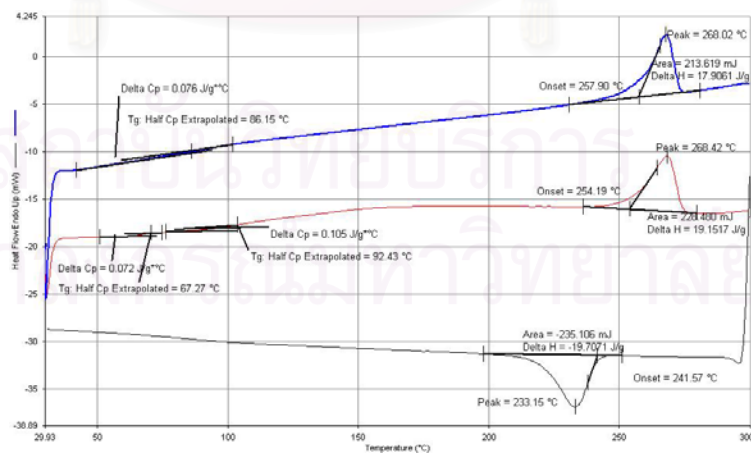
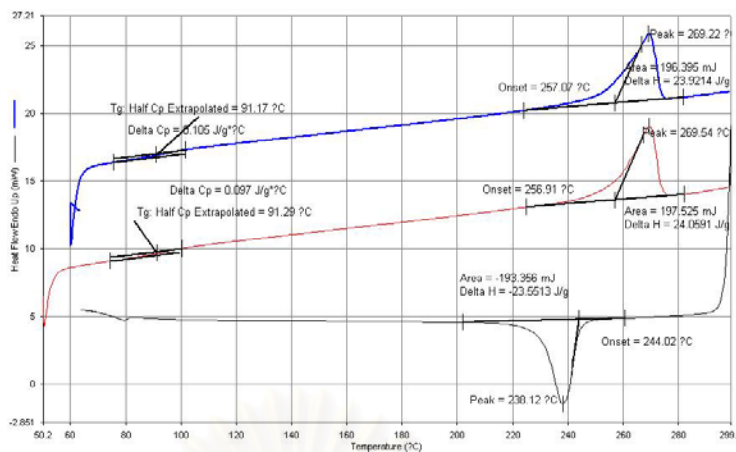
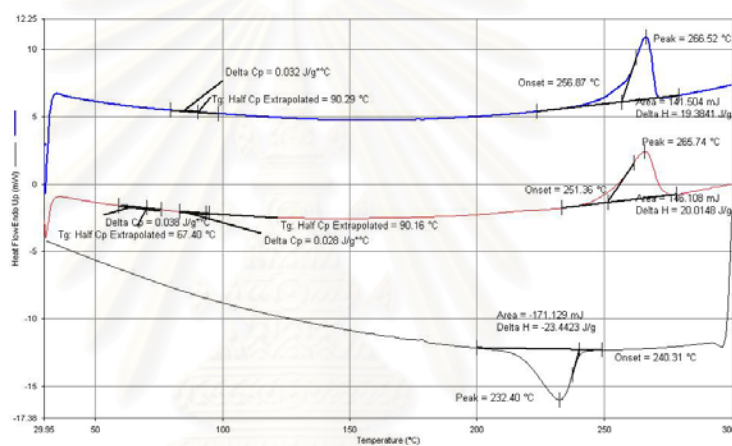


Figure A.42 DSC curve of SPS40/PEMA60/GMS blends



**Figure A.43** DSC curve of SPS60/PEMA40 blends



**Figure A.44** DSC curve of SPS60/PEMA40/LCC blends

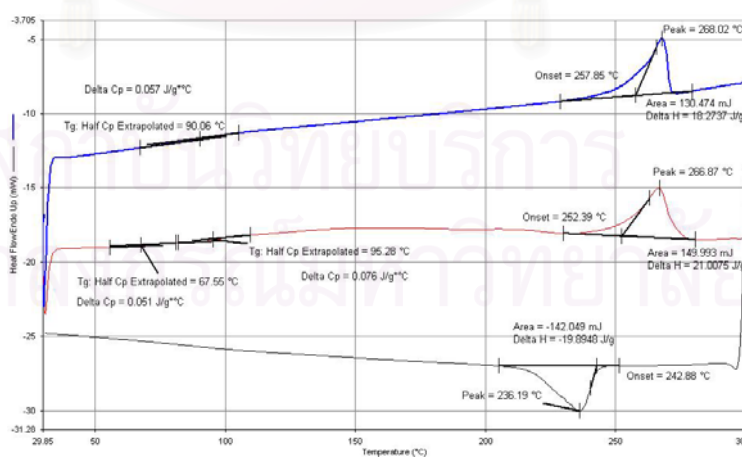


**Figure A.45** DSC curve of SPS60/PEMA40/GMS blends

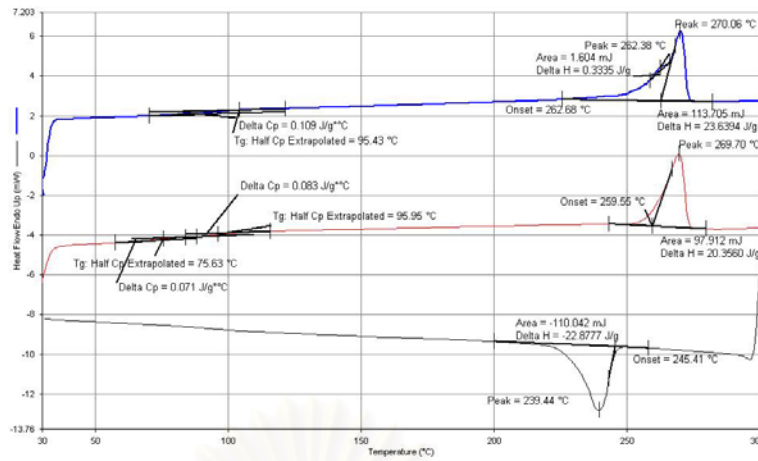


Figure A.46 DSC curve of SPS80/PEMA20 blends

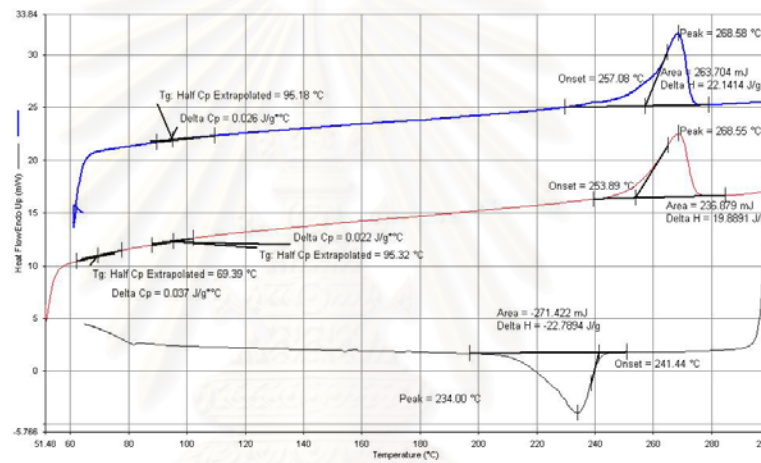


Figure A.47 DSC curve of SPS80/PEMA20/LCC blends

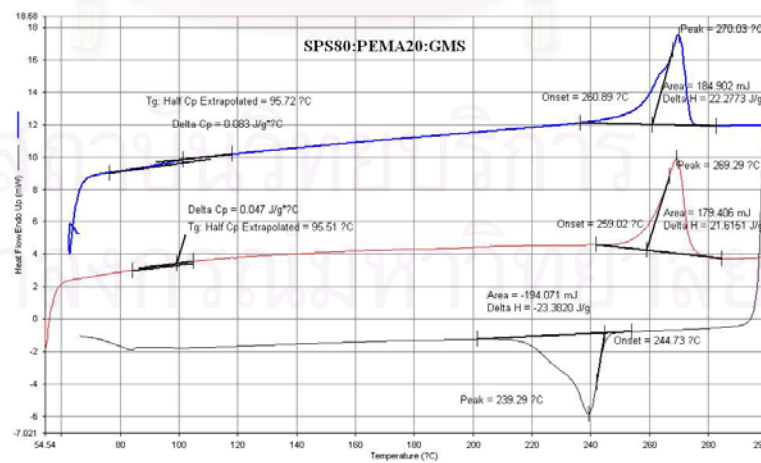
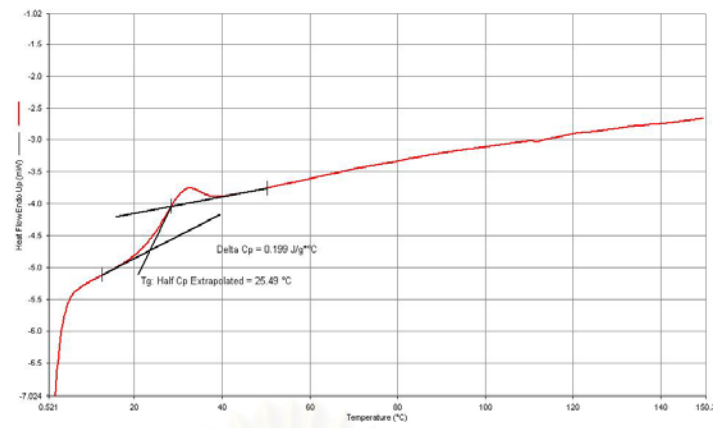
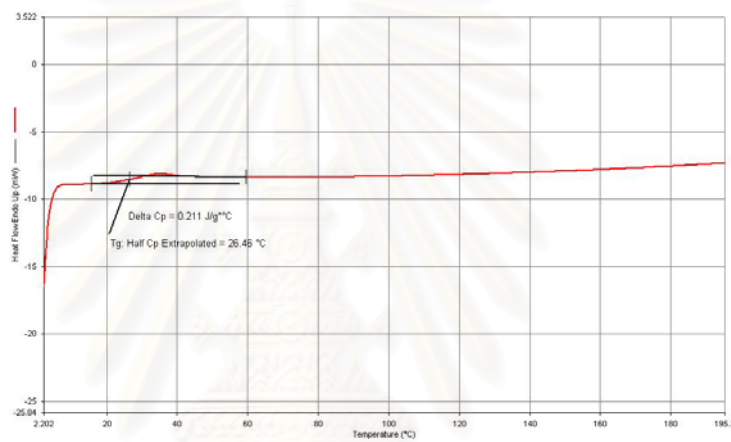


Figure A.48 DSC curve of SPS80/PEMA20/GMS blends



**Figure A.49** DSC curve of PCHA



**Figure A.50** DSC curve of PCHA blended with LCC

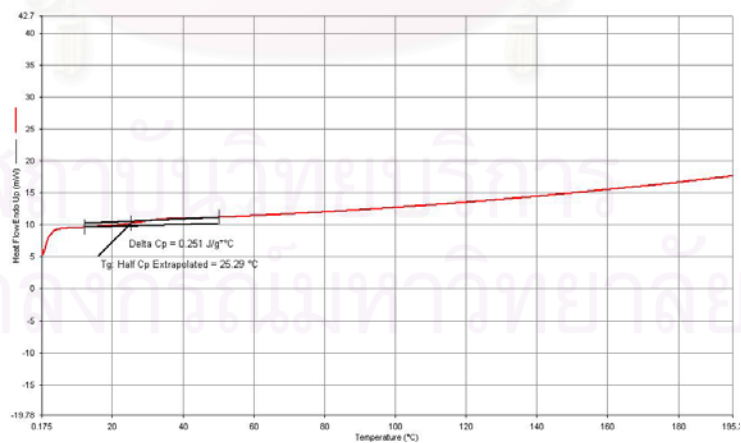


**Figure A.51** DSC curve of PCHA blended with GMS

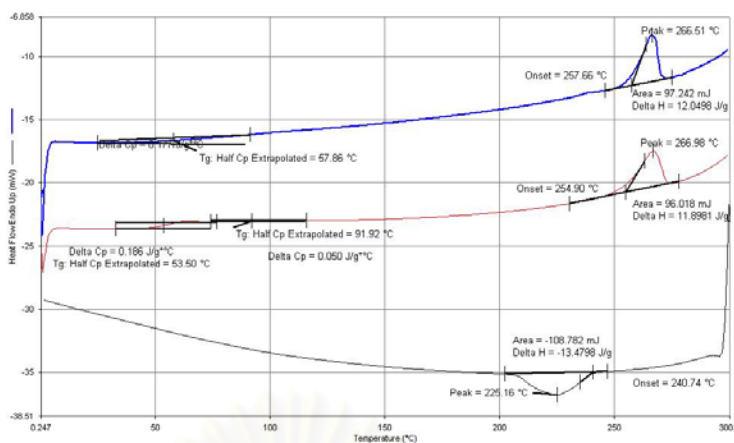


Figure A.52 DSC curve of SPS20/PCHA80 blends

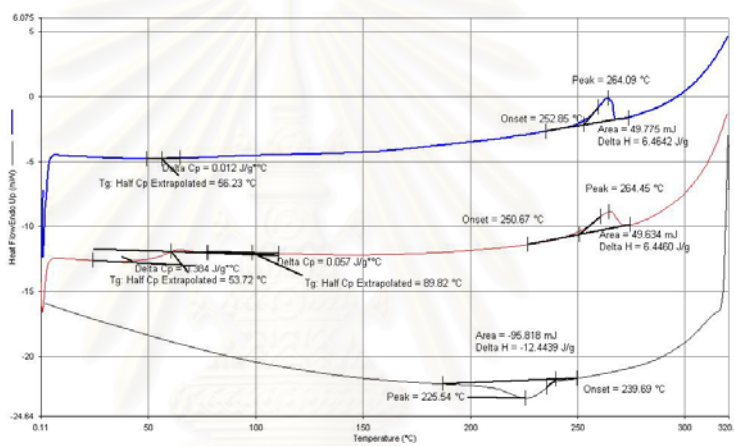


Figure A.53 DSC curve of SPS20/PCHA80/LCC blends

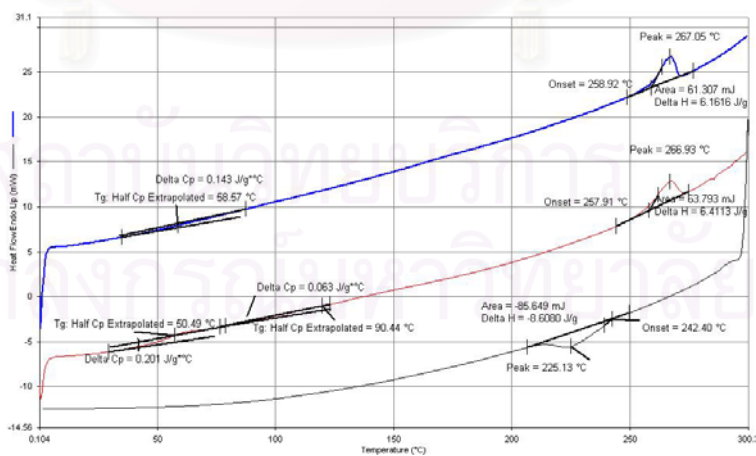


Figure A.54 DSC curve of SPS20/PCHA80/GMS blends

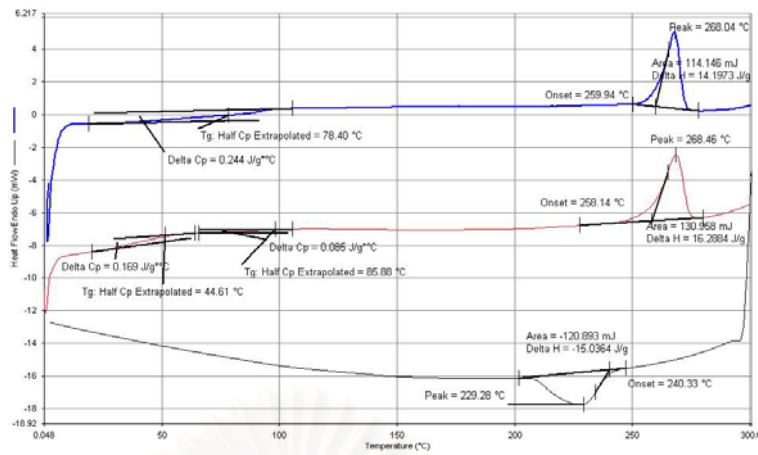


Figure A.55 DSC curve of SPS40/PCHA60 blends

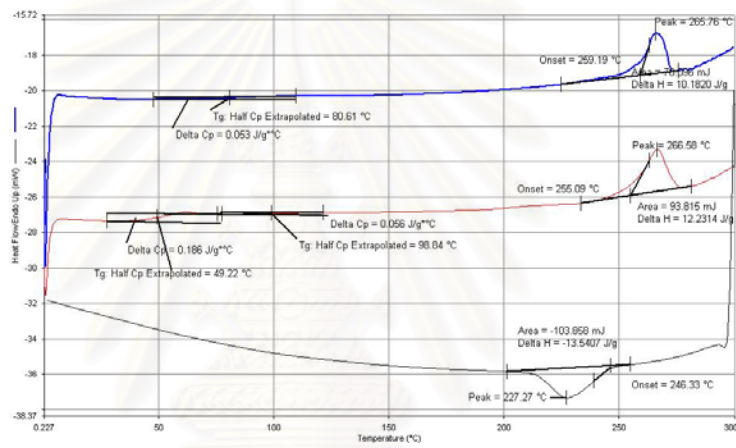


Figure A.56 DSC curve of SPS40/PCHA60/LCC blends

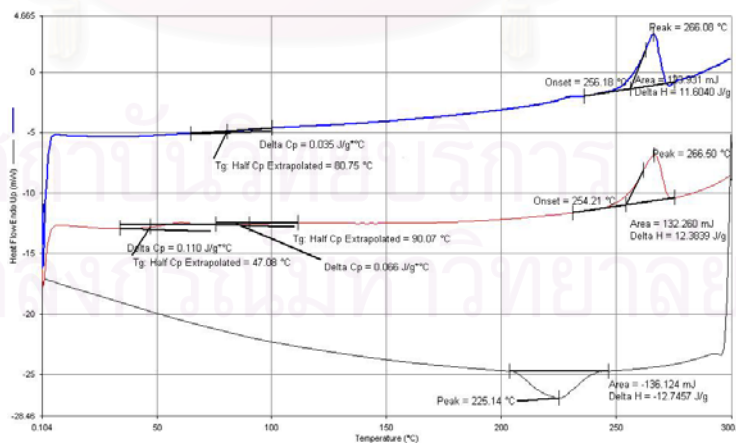


Figure A.57 DSC curve of SPS40/PCHA60/GMS blends



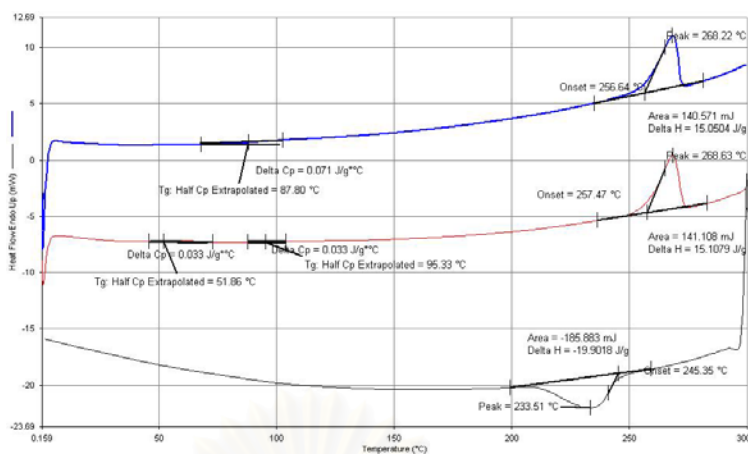


Figure A.58 DSC curve of SPS60/PCHA40 blends

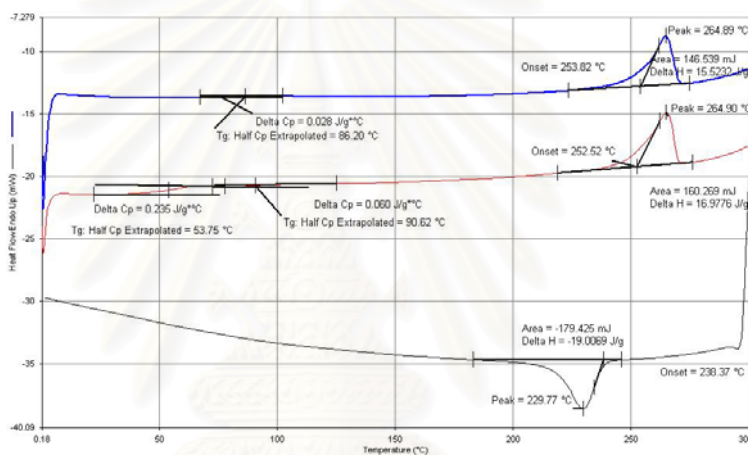


Figure A.59 DSC curve of SPS60/PCHA40/LCC blends

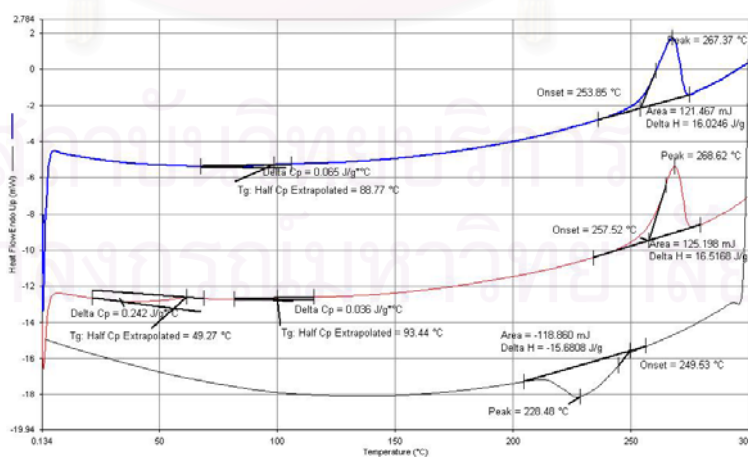


Figure A.60 DSC curve of SPS60/PCHA40/GMS blends

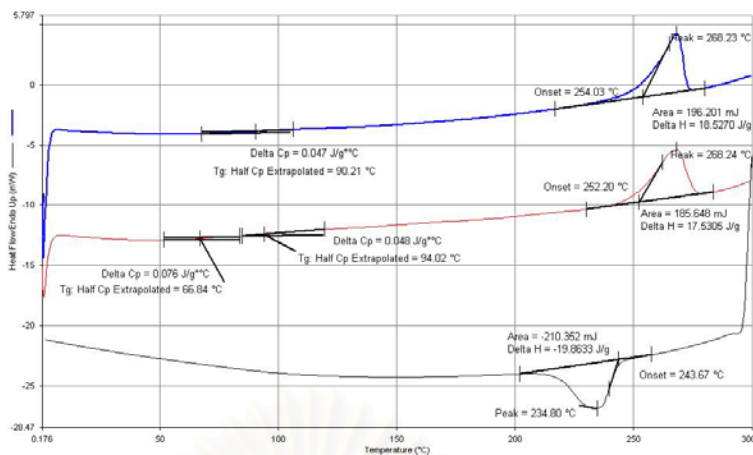


Figure A.61 DSC curve of SPS80/PCHA20 blends

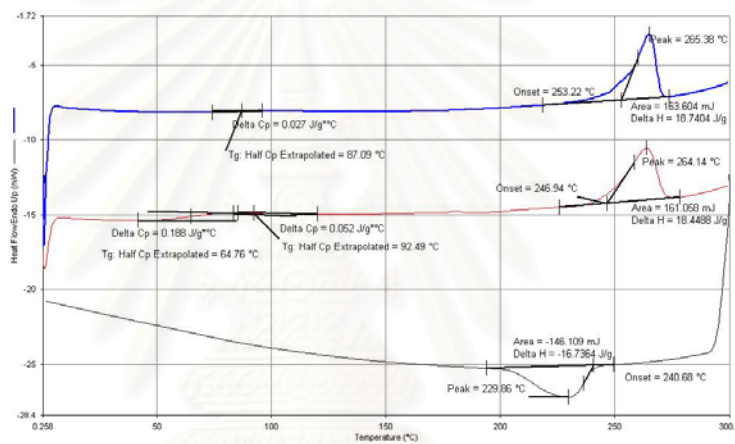


Figure A.62 DSC curve of SPS80/PCHA20/LCC blends

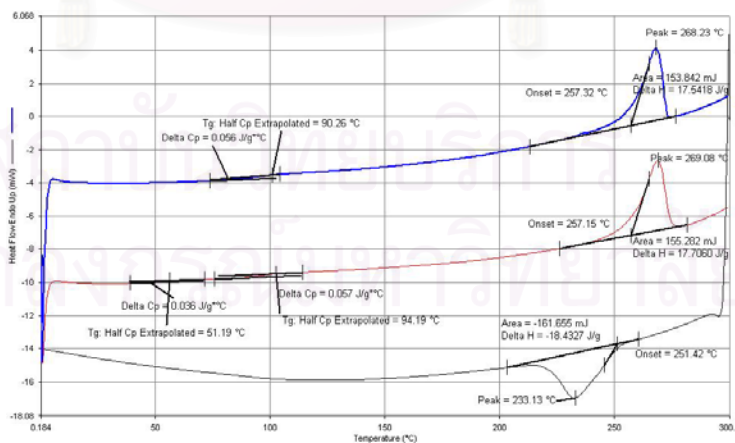
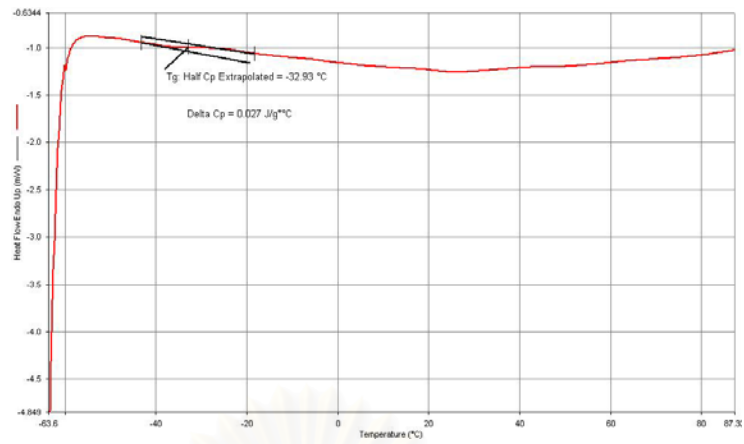
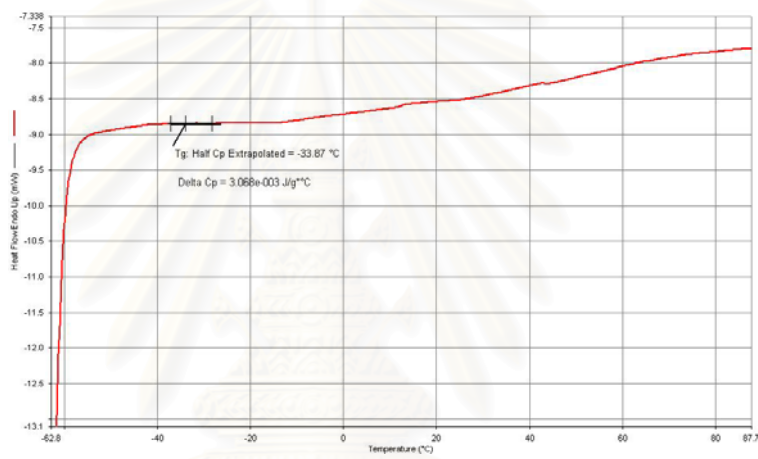


Figure A.63 DSC curve of SPS80/PCHA20/GMS blends



**Figure A.64** DSC curve of PIP



**Figure A.65** DSC curve of PIP blended with LCC

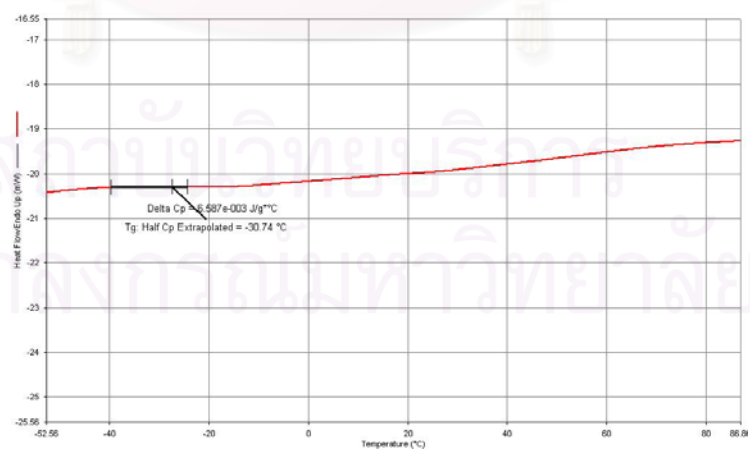


**Figure A.66** DSC curve of PIP blended with GMS

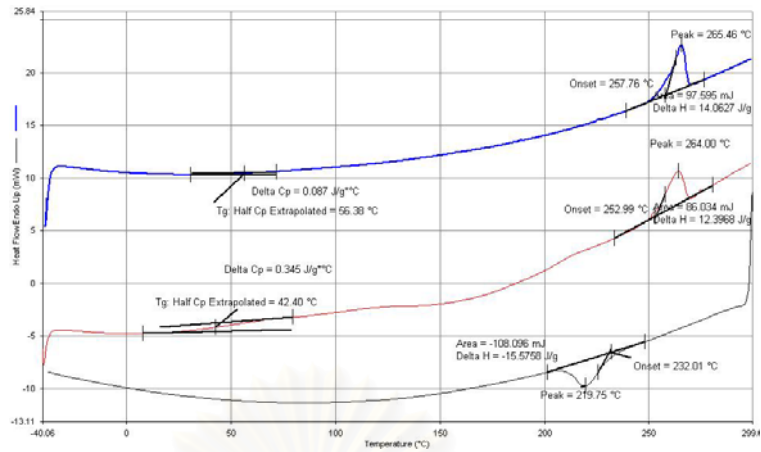


**Figure A.67** DSC curve of SPS20/PIP80 blends

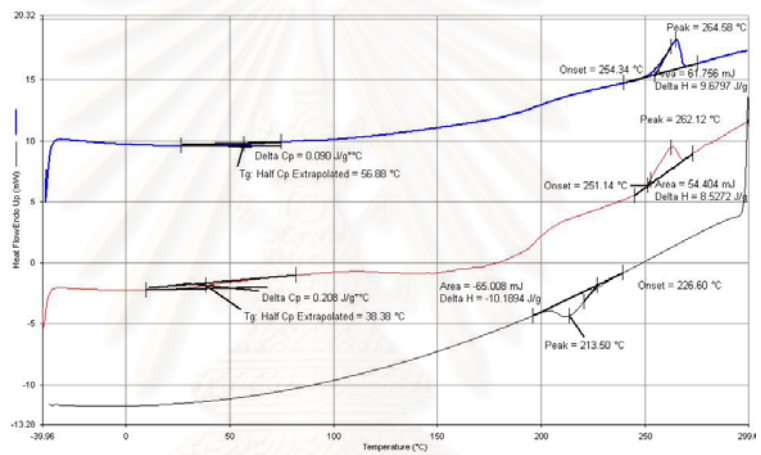


**Figure A.68** DSC curve of SPS20/PIP80/LCC blends

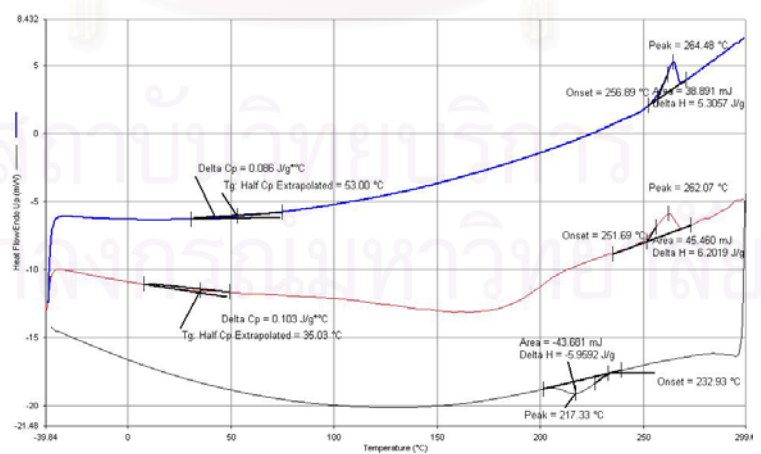


**Figure A.69** DSC curve of SPS20/PIP80/GMS blends

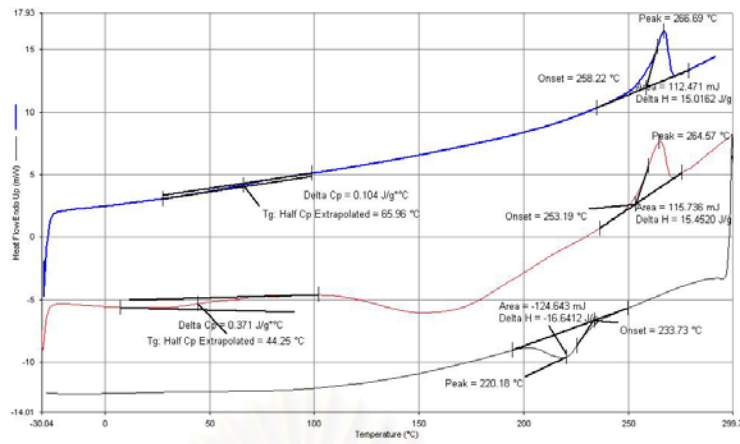


Figure A.70 DSC curve of SPS40/PIP60 blends

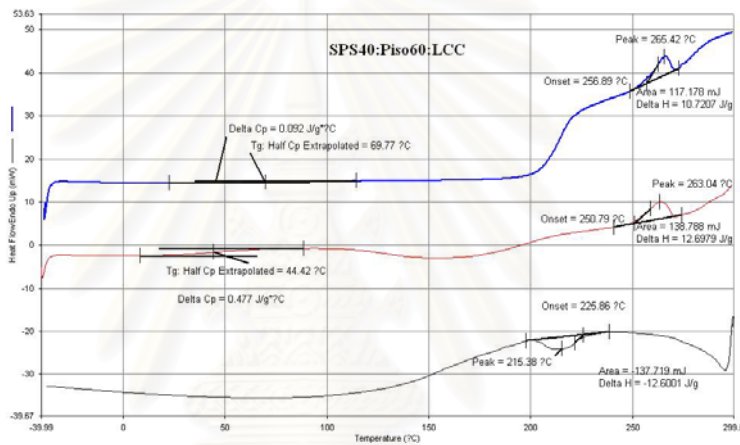


Figure A.71 DSC curve of SPS40/PIP60/LCC blends

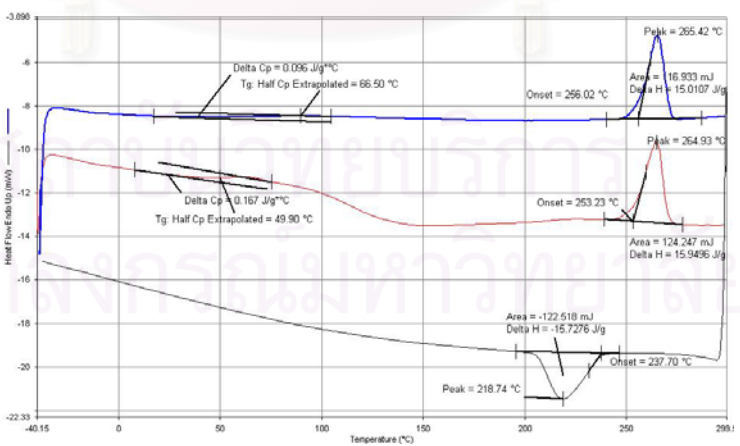


Figure A.72 DSC curve of SPS40/PIP60/GMS blends

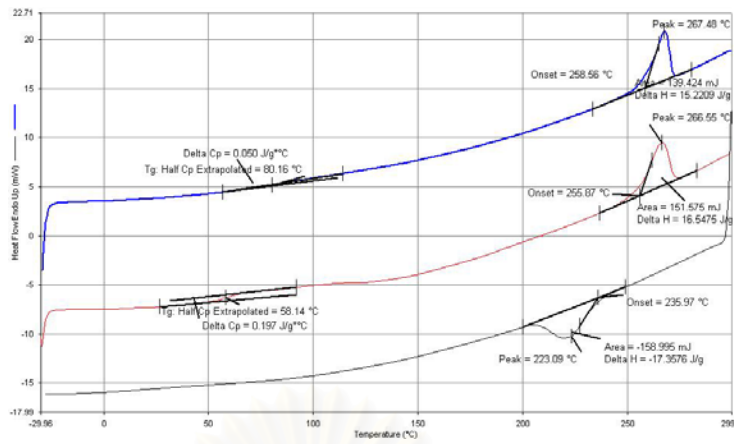


Figure A.73 DSC curve of SPS60/PIP40 blends

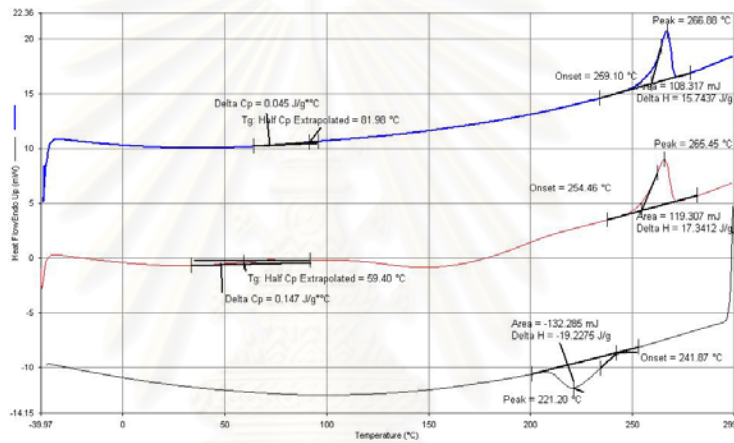


Figure A.74 DSC curve of SPS60/PIP40/LCC blends

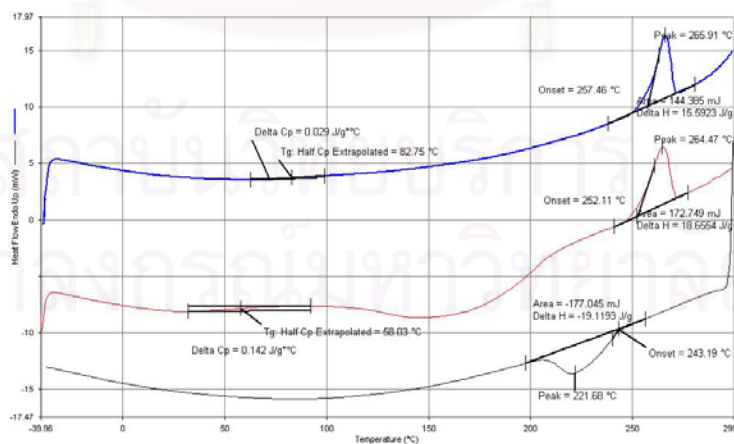


Figure A.75 DSC curve of SPS60/PIP40/GMS blends



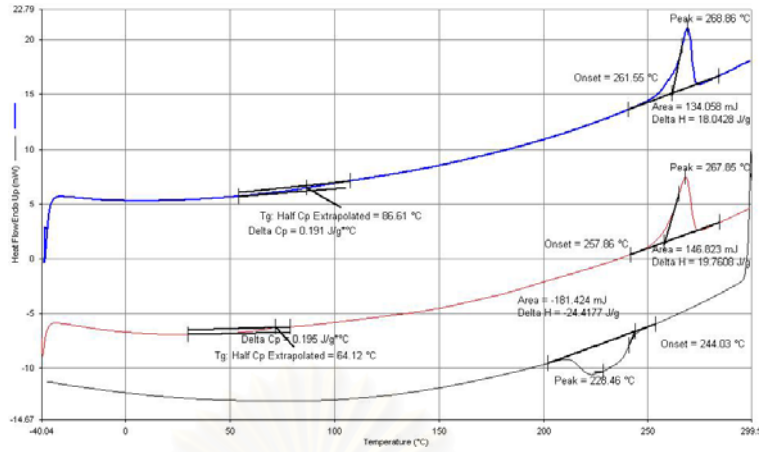


Figure A.76 DSC curve of SPS80/PIP20 blends

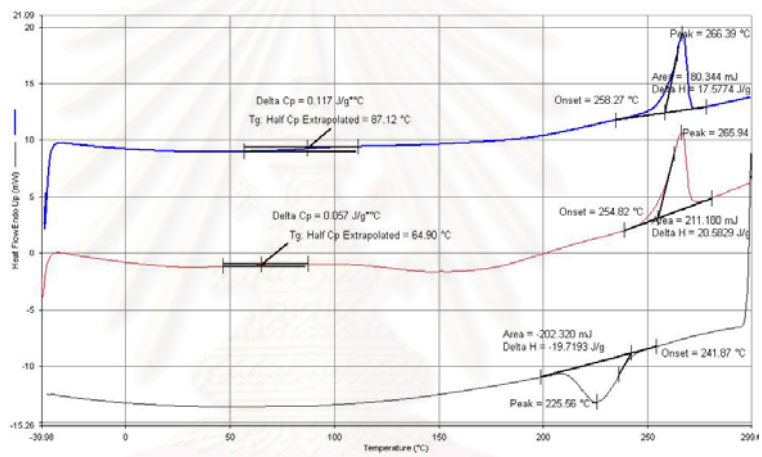


Figure A.77 DSC curve of SPS80/PIP20/LCC blends

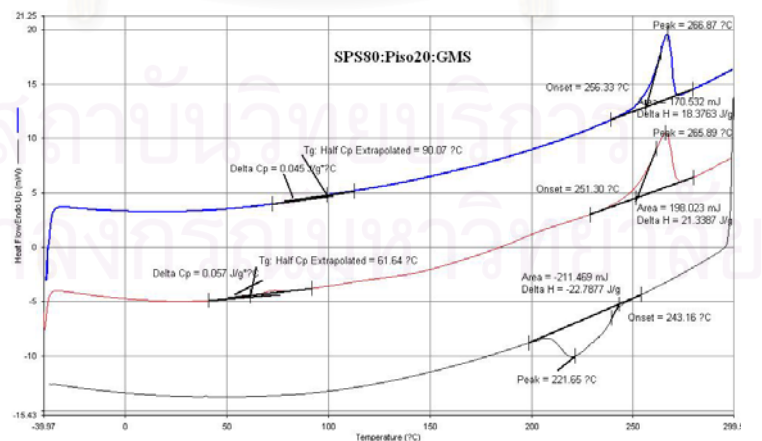
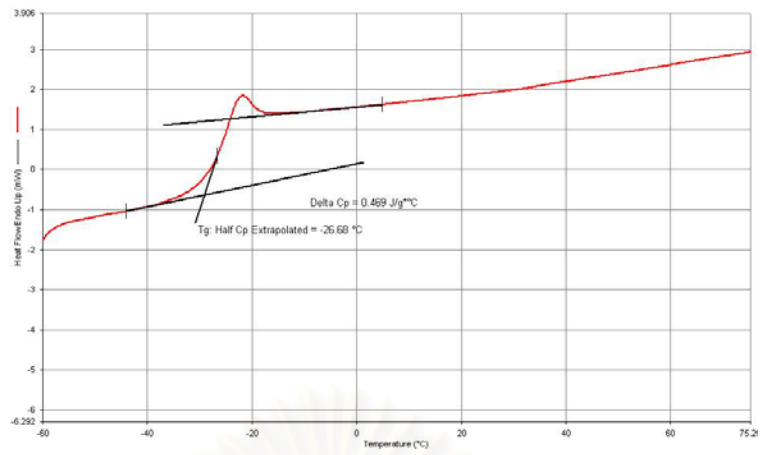
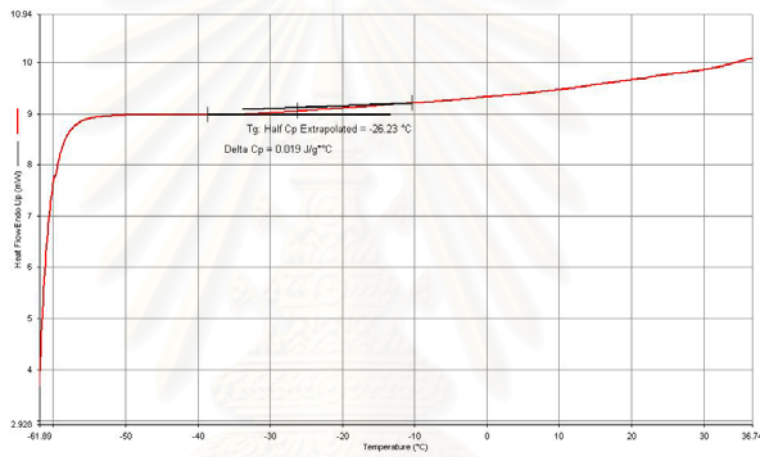


Figure A.78 DSC curve of SPS80/PIP20/GMS blends



**Figure A.79** DSC curve of PVME



**Figure A.80** DSC curve of PVME blended with LCC

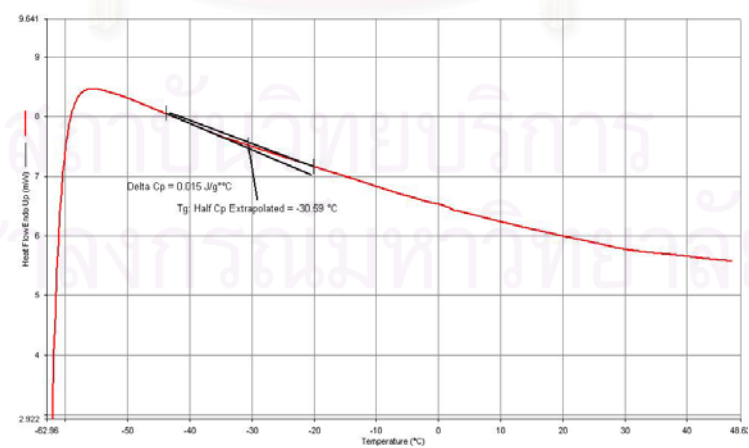


**Figure A.81** DSC curve of PVME blended with GMS

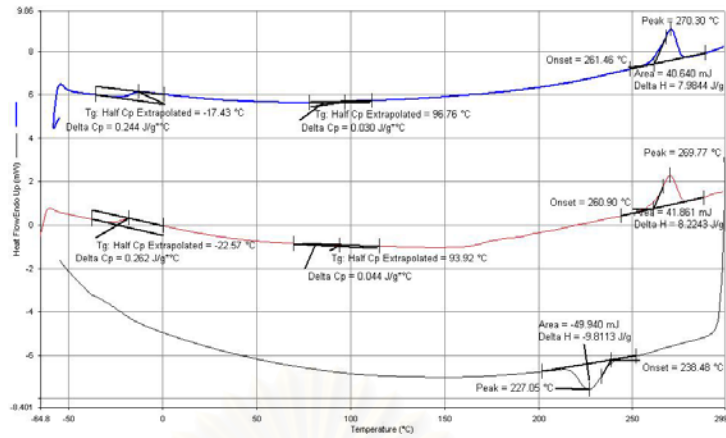


Figure A.82 DSC curve of SPS20/PVME80 blends

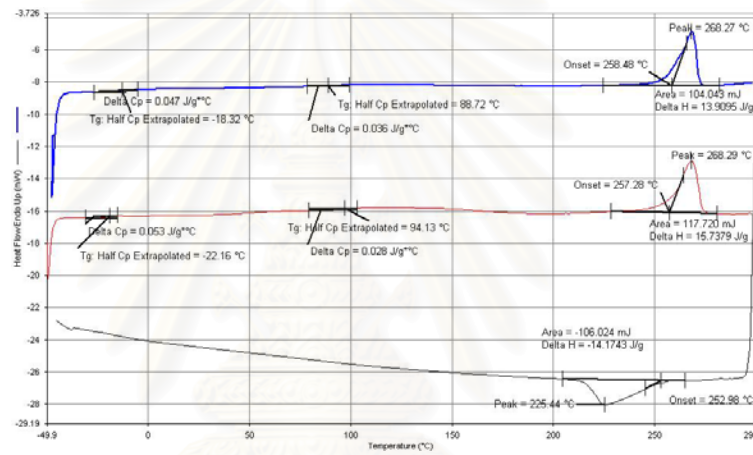


Figure A.83 DSC curve of SPS20/PVME80/LCC blends

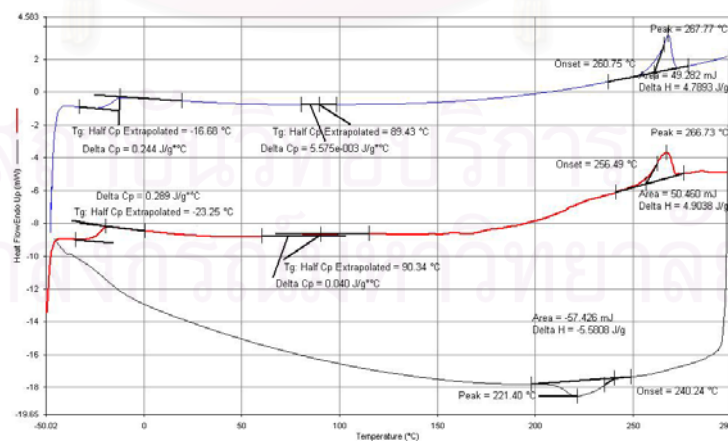


Figure A.84 DSC curve of SPS20/PVME80/GMS blends

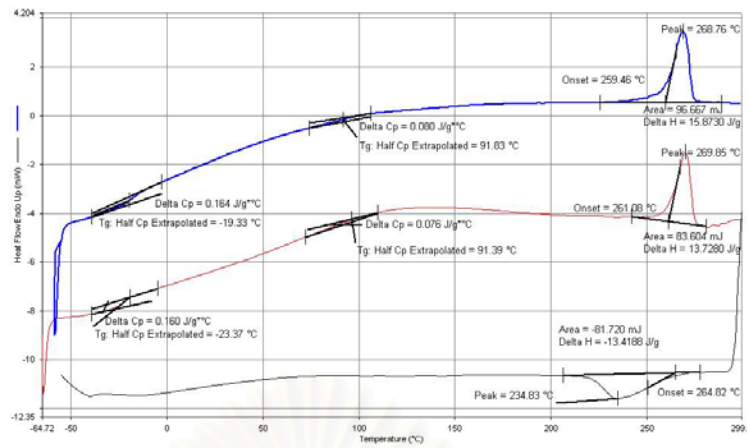


Figure A.85 DSC curve of SPS40/PVME60 blends

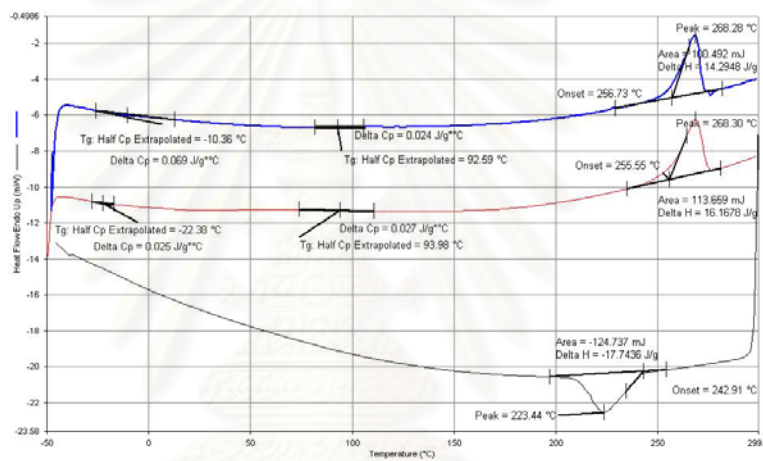


Figure A.86 DSC curve of SPS40/PVME60/LCC blends

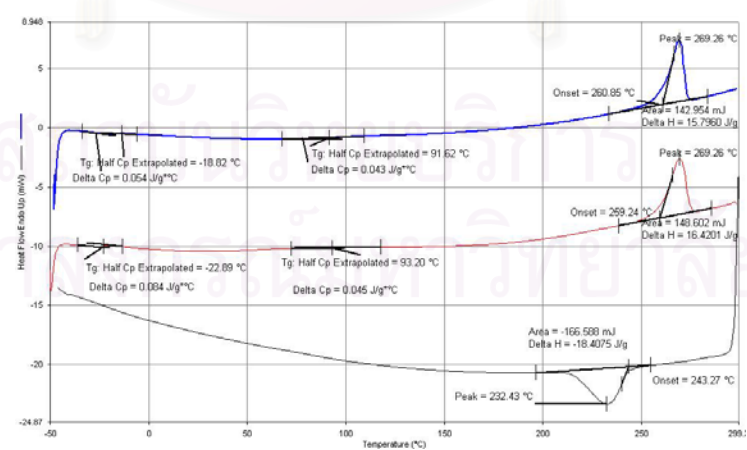


Figure A.87 DSC curve of SPS40/PVME60/GMS blends

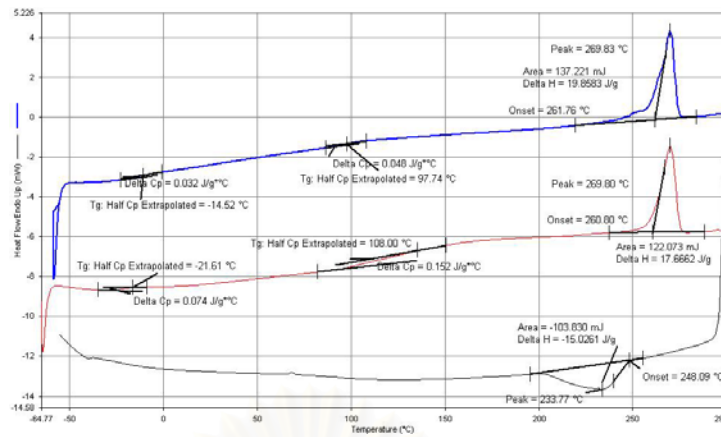


Figure A.88 DSC curve of SPS60/PVME40 blends

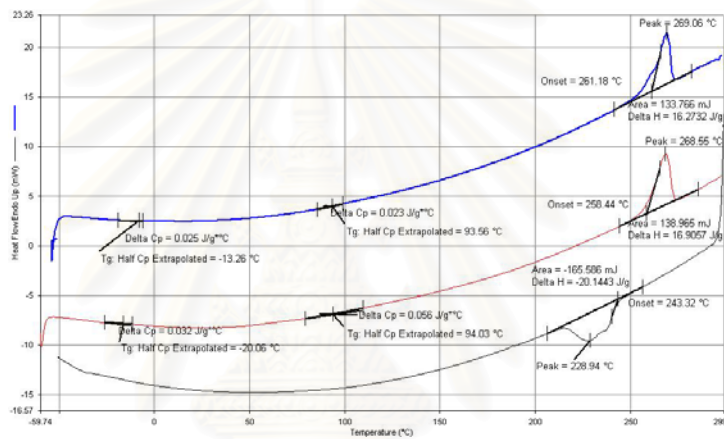


Figure A.89 DSC curve of SPS60/PVME40/LCC blends

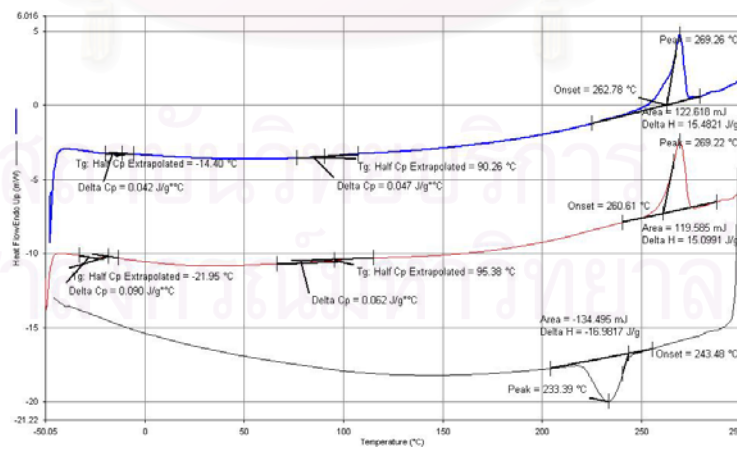


Figure A.90 DSC curve of SPS60/PVME40/GMS blends

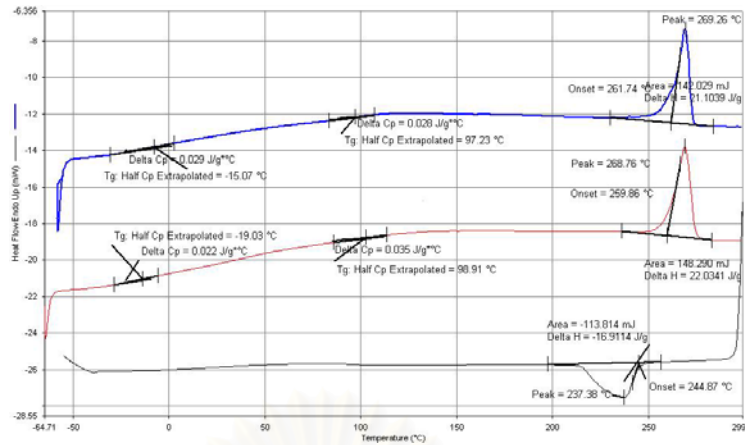


Figure A.91 DSC curve of SPS80/PVME20 blends

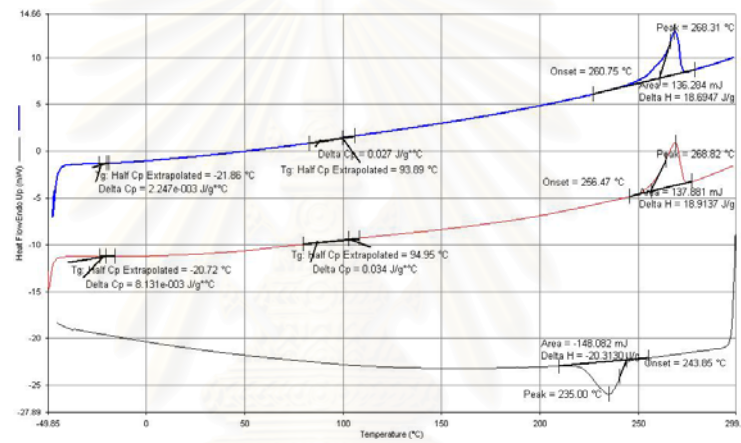


Figure A.92 DSC curve of SPS80/PVME20/LCC blends

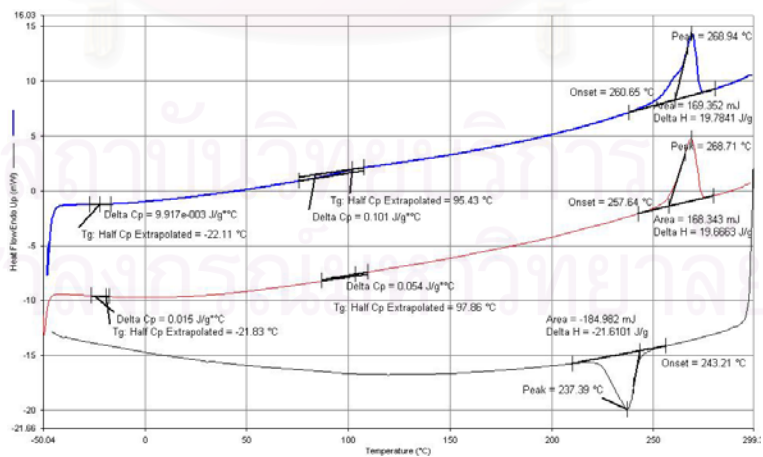


Figure A.93 DSC curve of SPS80/PVME20/GMS blends



## VITA

Mr. Pichet Pahupongsab was born on January 2, 1981 in Bangkok, Thailand. He received the Bachelor's Degree of Chemical Engineering from the Department of Chemical Engineering, Faculty of Engineering, Kasetsart University in April 2003, He continued his Master's study at Chulalongkorn University in June, 2003.



สถาบันวิทยบริการ  
จุฬาลงกรณ์มหาวิทยาลัย